

UNIVERSITY OF OKLAHOMA

GRADUATE COLLEGE

TESTING OF NOVEL ENZYME PRODRUG AND PHOTOTHERMAL
THERAPEUTICS FOR THE TREATMENT OF BREAST CANCER

A DISSERTATION

SUBMITTED TO THE GRADUATE FACULTY

in partial fulfillment of the requirements for the

Degree of

DOCTOR OF PHILOSOPHY

By

BRENT VAN RITE

Norman, Oklahoma

2012

TESTING OF NOVEL ENZYME PRODRUG AND PHOTOTHERMAL
THERAPEUTICS FOR THE TREATMENT OF BREAST CANCER

A DISSERTATION APPROVED FOR THE
DEPARTMENT OF BIOENGINEERING

BY

Dr. Roger Harrison, Chair

Dr. Matthias Nollert

Dr. Vassilios Sikavitsas

Dr. Ann West

Dr. Rajagopal Ramesh

ACKNOWLEDGEMENTS

I am eternally grateful for commitment of my advisor Dr. Roger G. Harrison. He has been a constant source of knowledge, inspiration, and limitless folders of research papers. For four years, he has provided valuable insight from experience in research methods and techniques; Friday 5 pm meetings will never be forgotten. A sincere thank you to my advisory committee members Dr. Vassilios Sikavitsas, Dr. Matthias Nollert, and Dr. Rajagopal Ramesh for advice on research strategies and use of their labs when necessary and a special thank you to Dr. Ann West for her willingness to participate at the last minute.

I would like to thank my colleagues in the Harrison lab, especially Whitney Woodson, John Kraus and Antonietta Restuccia for additional hands they provided throughout my time. Whitney was an excellent friend and researcher. Antonietta has been a quick learner and great friend. John has provided daily help for the entire year we have worked together and is a great friend outside the lab. A sincere appreciation for the help from Samuel Van Gordon and Brandon Engebretson from Dr. Sikavitsas' lab for instrument training and techniques. To all the staff in the School of Chemical, Biological, and Materials Engineering office, I thank you for always providing smiling faces and conversations that got my mind off research.

Most importantly, I am forever indebted to my parents, Daniel and Jeanne Van Rite. Without them, I likely would not have the work ethic and drive to pursue and succeed in graduate school. They will always be the most important teachers that I have. To my sisters, Brittany Van Rite and Tiffany Schroeder, I appreciate your insight in life, our conversations, and the way you take my mind off work. With love, this dissertation is dedicated to you.

TABLE OF CONTENTS

ACKNOWLEDGEMENTS	<i>iv</i>
LIST OF FIGURES	<i>ix</i>
LIST OF TABLES	<i>xv</i>
ABSTRACT	<i>xvi</i>
1. INTRODUCTION	1
Overview of Directed Prodrug Therapy	4
Annexin V Binds Exposed Phosphatidylserine (PS) in Tumor Vasculature	7
Mechanism of Cell Death via Methioninase and Selenomethionine.....	8
Mechanism of Cell Death via Cytosine Deaminase and 5- Fluorocytosine	12
Hyperthermal Therapy using Single-Walled Carbon Nanotubes (SWNT)	14
F3 Peptide Binds Nucleolin Receptor Expressed on Proliferating Cells.....	17
Mechanism of Cell Death via Carbon Nanotube Heating	18
Overall Hypothesis and Experimental Plan.....	18
2. MATERIALS	23
Bacterial Plasmids, Stains, and Mutagenesis	23
DNA Manipulation and Protein Purification.....	23
Mammalian Cell Lines and Culture Media	25
<i>In Vitro</i> Binding, Binding Duration, and Cytotoxicity Assays	25
<i>In Vivo</i> Pharmacokinetics, Enzyme Prodrug, Phosphatidylserine Detection, Biodistribution, and Tumor Blood Flow Assays in Mice	26
<i>In vitro</i> Assays for Single-Walled Carbon Nanotubes with F3 Peptide	26
3. METHODS	28
Enzyme Prodrug Project	
Primer Design for PCR	28
Construction of Cytosine Deaminase-Annexin V Fusion Gene	29
Site-directed Mutagenesis of Methioninase-Annexin V Fusion Gene	33
Sequencing of Fusion Genes.....	35
Fusion Protein Expression, Purification, Analysis, and Storage	35
Binding of Fusion Proteins to Exposed PS on Endothelial and Cancer Cells	38
Cytotoxicity of Enzyme Prodrugs to Endothelial and Cancer Cells.....	41
ELISA for Methioninase-Annexin V Detection in Mice Serum.....	42
Dose Safety Injections of Selenomethionine	43
Development of MDA-MB-231 Tumor Xenografts in Mice.....	43
Detection of Externally Positioned PS in MDA-MB-231 Tumor Vasculature	44

Biodistribution of Methioninase-Annexin V in Mice	45
Treatment of MDA-MB-231 Breast Tumors in Mice.....	45
Determination of Blood Flow Through MDA-MB-231 Tumors.....	46
Carbon Nanotube Project	
Conjugation of F3 Peptide to SWNTs with a Phospholipid Linker.....	47
SWNT-F3 Cell Binding Using Fluorescence and Confocal Microscopy	48
Cytotoxicity of Varying Length SWNT-F3 Conjugates with NIR Light.....	49
4. RESULTS AND DISCUSSION.....	50
Enzyme Prodrug Project	
Construction of Cytosine Deaminase-Annexin V Fusion Gene	50
Site-Directed Mutagenesis of Methioninase-Annexin V	52
Fusion Protein Expression, Purification, Analysis, and Storage	53
Specific Fusion Protein Binding to Endothelial and Cancer Cells <i>In Vitro</i>	57
Cytotoxicity of Methioninase-Annexin V + Selenomethionine <i>In</i> <i>Vitro</i>	62
Cytotoxicity of Cytosine Deaminase-Annexin V + 5- Fluorocytosine <i>In Vitro</i>	70
Pharmacokinetics of Methioninase-Annexin V in Mice.....	72
Selenomethionine Toxicity in Mice.....	75
Detection of Exposed Phosphatidylserine in Tumor Vasculature of Mice	75
Biodistribution of Methioninase-Annexin V in Mice.....	77
MDA-MB-231 Tumor Treatment with Methioninase-Annexin V + Selenomethionine in Mice	79
Tumor Blood Flow After Methioninase-Annexin V + Selenomethionine Treatment	89
Carbon Nanotube Project	
SWNT-F3 Internalization Confirmed by Microscopy	91
Killing of Proliferating Cells Using SWNT-F3 + NIR Light	92
5. CONCLUSIONS AND FUTURE DIRECTIONS.....	97
BIBLIOGRAPHY.....	101
APPENDIX A.....	109
Enzyme Prodrug Project	
Cytosine Deaminase-Annexin V Fusion Gene Sequence	109
Methioninase-Annexin V Sequence after Site-Directed Mutagenesis	112
BCA Protein Assay Standard Curve	114
Bradford Protein Assay Standard Curve.....	114
Bradford Protein Microassay Standard Curve	115
L-Methioninase Enzymatic Activity Assay Standard Curve	115
Chromatograph from Purification of Methioninase-Annexin V.....	116

Determination of dissociation constant for methioninase-annexin V binding to human endothelial cells.	
Binding Stability of Cytosine Deaminase-Annexin V	116
Pathology Report of Treated MDA-MB-231 Breast Tumors in Mice	117
Carbon Nanotube Project	
SWNT Standard Curve	123
Conjugation History of F3 Peptide to Carbon Nanotubes	124
Carbon Nanotube Absorption Spectra	125
APPENDIX B - Protocols	126
Enzyme Prodrug Project	
Construction of Cytosine Deaminase-Annexin V Fusion Gene	126
QIAquick PCR Purification Kit Protocol	131
QIAquick Gel Extraction Kit Protocol	132
QIAprep Spin Mini-prep Kit Protocol	134
Agarose Gel Electrophoresis.....	135
Transformation of NovaBlue GigaSingles Competent Cells.....	137
Transformation of <i>E. coli</i> BL21(DE3) Cells.....	137
Transformation of XL-10 Gold Ultracompetent Cells	138
Site-directed Mutagenesis of L-Methioninase-Annexin V Fusion Gene	139
Fusion Protein Expression	141
Fusion Protein Purification	143
BCA Protein Assay	147
Bradford Protein Assay.....	148
Bradford Protein Microassay	149
SDS-PAGE Analysis of Proteins.....	149
L-Methioninase Activity Assay	152
Cytosine Deaminase Activity Assay.....	152
QCL-1000 Endpoint Chromogenic Limulus Amebocyte Lysate Endotoxin Assay	153
Biotinylation of Fusion Proteins	155
FITC Labeling of Fusion Proteins	156
DyLight 680 Labeling of L-Methioninase-Annexin V	157
Binding of Fusion Proteins to Exposed PS on Endothelial and Cancer Cells	158
Visualization of Fusion Proteins on the Surface of Cells	160
Binding Stability of Fusion Proteins on the Surface of Cells	160
Cytotoxicity of L-Methioninase-Annexin V + Selenomethionine.....	162
Cytotoxicity of Cytosine Deaminase-Annexin V + 5-Fluorocytosine.....	164
ELISA of L-Methioninase-Annexin V in Mouse Serum.....	166
Injection of MDA-MB-231/GFP Cancer Cells in Flank of Mice	167
Detection of Exposed Phosphatidylserine in Mice Tumors.....	169
Biodistribution of L-Methioninase in SCID Mice	171
Enzyme Prodrug Treatment of SCID Mice	172

Determination of Blood Flow Through Tumor Vasculature	173
Carbon Nanotube Project	
SWNT Standard Curve	175
Conjugation of F3 Peptide to SWNTs via Phospholipid Linker.....	175
Cell Binding and Visualization Using Fluorescence and Confocal Microscopy	176
NIR Laser Setup and Configuration.....	176
SWNT-F3 + NIR Laser Test Protocol	178

LIST OF FIGURES

Figure 1.1. Schematic of the complex metastatic process. Epithelial–mesenchymal transition (EMT) alters the cell phenotype to allow intravasation into the systemic circulation. Mesenchymal–epithelial transition (MET) occurs at the site of distant metastases	2
Figure 1.2. Selective cancer therapy using antibody-directed enzyme prodrug therapy.....	5
Figure 1.3. Structure of human annexin V protein	9
Figure 1.4. Structure of L-methioninase from <i>Pseudomonas putida</i>. Each monomer making up the homotetramer is shown in a different color.....	10
Figure 1.5. Structure of cytosine deaminase from <i>Saccharomyces cerevisiae</i>. Each monomer making up the homodimer is shown	13
Figure 2.1. pET-30 Ek/LIC vector map. A general layout of the features within the vector and the ligation independent cloning sequence (Novagen, 2012).....	24
Figure 4.1. Agarose gels of cytosine deaminase-annexin V fusion gene construction. A) Annexin V and cytosine deaminase amplification. B) Ligation of cytosine deaminase to annexin V.	51
Figure 4.2. SDS-PAGE of methioninase-annexin V. Coomassie blue was used to stain the gel. Lane 1, total soluble cells lysate; lane 2, unwanted flow-through; lane 3, eluted methioninase-annexin V; lane 4, methioninase-annexin V with the (His) ₆ tag removed.	56
Figure 4.3. SDS-PAGE of cytosine deaminase-annexin V. Coomassie blue was used to stain the gel. Lane 1, total soluble cells lysate; lane 2, unwanted flow-through; lane 3, eluted cytosine deaminase-annexin V; lane 4, cytosine deaminase V with the (His) ₆ tag removed.	56

Figure 4.4. Determination of dissociation constant for methioninase-annexin V binding to human endothelial cells. Methioninase-annexin V was biotinylated and streptavidin-HRP was used to quantify the binding. Total binding was obtained using 2 mM Ca^{2+} in the binding buffer. Non-specific binding was obtained by removing the Ca^{2+} from the binding buffer and replacing it with 5 mM of EDTA to chelate Ca^{2+} . Specific binding was obtained by subtracting the non-specific binding from the total binding. GraphPad Prism 5 software determined the specific binding to have a $K_d = 0.5 \pm 0.2$ nM. Data are presented as mean \pm SE (n = 3).....58

Figure 4.5. Visualization of fluorescent cytosine deaminase-annexin V binding to MDA-MB-231 breast cancer cells. Cells were seeded onto a cover glass and allowed to adhere. Cytosine deaminase-annexin V labeled with FITC was added, allowed to bind for 2 h, and washed to remove unbound fusion protein. Corresponding light (left) and fluorescence (right) images were acquired with a 40X objective to verify binding to the cell surface. The bar represents 100 μm61

Figure 4.6. Methioninase-annexin V fusion protein binding stability. The Alamar Blue assay for cell viability was performed each day, followed by the binding assay to determine the duration of binding of the fusion protein to exposed PS on the surface of each cell line. ABS/RFU is the absorbance at 450 nm, determined by the binding assay, divided by the relative fluorescence units at 590 nm, determined by the Alamar Blue assay. Data are presented as mean \pm SE (n = 3)63

Figure 4.7. Effect of selenomethionine conversion to methylselenol on HAAE-1 endothelial cells. Cells were grown in medium adjusted to 1000 μM of L-methionine. Cell viability was assessed using the Alamar Blue assay for cell viability and normalized to the control (i.e. no methioninase-annexin V and no selenomethionine). A one-way ANOVA was performed for statistical analysis. Cells treated with different selenomethionine concentrations but with no methioninase-annexin V were compared to the control on the same day, and statistical significance was denoted by # (p < 0.001). Cells treated with methioninase-annexin V were compared to cells with no methioninase-annexin V on the same day at the same selenomethionine concentration, and statistical significance was denoted by * (p < 0.001). Data are presented as mean \pm SE (n = 3).64

Figure 4.8. Effect of selenomethionine conversion to methylselenol on MCF-7 breast cancer cells. Cells were grown in medium adjusted to 1000 μM of L-methionine. Cell viability was assessed using the

Alamar Blue assay for cell viability and normalized to the control (i.e. no methioninase-annexin V and no selenomethionine). A one-way ANOVA was performed for statistical analysis. Cells treated with different selenomethionine concentrations but with no methioninase-annexin V were compared to the control on the same day, and statistical significance was denoted by # ($p < 0.001$). Cells treated with methioninase-annexin V were compared to cells with no methioninase-annexin V on the same day at the same selenomethionine concentration, and statistical significance was denoted by * ($p < 0.001$). Data are presented as mean \pm SE ($n = 3$)66

Figure 4.9. Effect of selenomethionine conversion to methylselenol on MDA-MB-231 breast cancer cells. Cells were grown in medium adjusted to 1000 μ M of L-methionine. Cell viability was assessed using the Alamar Blue assay for cell viability and normalized to the control (i.e. no methioninase-annexin V and no selenomethionine). A one-way ANOVA was performed for statistical analysis. Cells treated with different selenomethionine concentrations but with no methioninase-annexin V were compared to the control on the same day, and statistical significance was denoted by # ($p < 0.001$). Cells treated with methioninase-annexin V were compared to cells with no methioninase-annexin V on the same day at the same selenomethionine concentration, and statistical significance was denoted by * ($p < 0.001$). Data are presented as mean \pm SE ($n = 3$)67

Figure 4.10. Addition of methionine to eliminate MDA-MB-231 breast cancer cell death from methionine-depletion effects. Cells were grown in medium increasing amounts of L-methionine. Cell viability was assessed using the Alamar Blue assay for cell viability and normalized to the control (i.e. no methioninase-annexin V and no selenomethionine). A one-way ANOVA was performed for statistical analysis. Cells treated with extra methionine were compared to cells grown in Lebovitz's L-15 medium that received no fusion protein, and statistical significance was denoted by * ($p < 0.001$). Data are presented as mean \pm SE ($n = 3$)68

Figure 4.11. Effect of 5-fluorocytosine conversion to 5-fluorouracil on HAAE-1 endothelial cells. Cell viability was assessed using the Alamar Blue assay and normalized to the control (i.e. no cytosine deaminase-annexin V and no 5-fluorocytosine). A one-way ANOVA was performed for statistical analysis. Cells treated with cytosine deaminase-annexin V or cells treated with only 5-fluorouracil were compared to cells with no cytosine deaminase-annexin V on the same day at the same 5-fluorocytosine concentration, and statistical

significance was denoted by * ($p < 0.001$). Data are presented as mean \pm SE (n = 3)71

Figure 4.12. Effect of 5-fluorocytosine conversion to 5-fluorouracil on MCF-7 breast cancer cells. Cell viability was assessed using the Alamar Blue assay and normalized to the control (i.e. no cytosine deaminase-annexin V and no 5-fluorocytosine). A one-way ANOVA was performed for statistical analysis. Cells treated with cytosine deaminase-annexin V or cells treated with only 5-fluorouracil were compared to cells with no cytosine deaminase-annexin V on the same day at the same 5-fluorocytosine concentration, and statistical significance was denoted by * ($p < 0.001$). Data are presented as mean \pm SE (n = 3)73

Figure 4.13. Effect of 5-fluorocytosine conversion to 5-fluorouracil on MDA-MB-231 breast cancer cells. Cell viability was assessed using the Alamar Blue assay and normalized to the control (i.e. no cytosine deaminase-annexin V and no 5-fluorocytosine). A one-way ANOVA was performed for statistical analysis. Cells treated with cytosine deaminase-annexin V or cells treated with only 5-fluorouracil were compared to cells with no cytosine deaminase-annexin V on the same day at the same 5-fluorocytosine concentration, and statistical significance was denoted by * ($p < 0.001$). Data are presented as mean \pm SE (n = 3)74

Figure 4.14. Clearance time of methioninase-annexin V in the bloodstream of nude mice. Methioninase-annexin V was injected i.p. at 1 and 10 mg/kg. An ELISA was used to detect biotinylated methioninase-annexin V in mouse serum, followed by an antibody against annexin V. A secondary antibody IgG conjugated to peroxidase was with chromogenic substrate to develop the results. Data are presented as mean \pm SE (n = 4).....76

Figure 4.15. Detection of methioninase-annexin V bound to exposed PS on the surface of a tumor blood vessel in an MDA-MB-231 tumor grown in SCID mice. Biotinylated fusion protein was injection i.p.. Cryosections were stained using streptavidin-HRP and developed with DAB to prove methioninase-annexin V binding. Counterstaining was done with hematoxylin74

Figure 4.16. Biodistribution of methioninase-annexin V. Mice were injected with methioninase-annexin V labeled with DyLight 680

fluorescent dye. At 1 h (A), 12 h (B), and 24 h (C) post-injection, images were taken to detect the fusion protein. Red signal is DyLight 680 and green signal is GFP from the MDA-MB-231 cancer cells80

Figure 4.17. Treatment of MDA-MB-231 breast tumors in NU/J mice. Treatment consisted of three consecutive cycles, where each cycle was as follows: 10 mg/kg methioninase-annexin V injected on day 0 and 10 mg/kg selenomethionine injected on days 1, 2, and 3. Tumor volume data are presented as mean \pm SE (n = 7) with statistical significance compared to the control group denoted by * (p < 0.001).82

Figure 4.18. MDA-MB-231 tumor growth in various immunodeficient mouse models. A. Tumor volume data for NU/J, SCID, and NU/NU mice bearing MDA-MB-231 breast tumor xenografts. Data are presented as mean \pm SE (n = 3) with statistical significance denoted by * (p < 0.001). B. Fluorescence images of NU/J, SCID, and NU/NU mice taken with the IVIS Spectrum small imaging system showing GFP signal from MDA-MB-231 cells83

Figure 4.19. Enzyme prodrug treatment of MDA-MB-231 breast tumors in SCID mice. Treatment consisted of three consecutive cycles, where each cycle was as follows: 10 mg/kg methioninase-annexin V injected on day 0 and 10 mg/kg selenomethionine injected on days 1, 2, and 3. Tumor volume data are presented as mean \pm SE (n = 7) with statistical significance compared to the control group denoted by * (p < 0.001)85

Figure 4.20. Enzyme prodrug treatment of MDA-MB-231 breast tumors in SCID mice on a methionine-deficient diet. Treatment consisted of three consecutive cycles, where each cycle was as follows: 10 mg/kg methioninase-annexin V injected on day 0 and 5 mg/kg selenomethionine injected on days 1, 2, and 3. Tumor volume data are presented as mean \pm SE (n = 7) with statistical significance compared to the control group denoted by * (p < 0.001)88

Figure 4.21. Interruption of blood flow through tumor vasculature. Female SCID were injected with DyLight 680 red fluorescent dye the day after the completion of the three-cycle enzyme prodrug treatment with methioninase-annexin V and selenomethionine. The outline of the GFP signal showing the living tumor cell perimeter is in green. Mice were either untreated (A) or treated with methioninase-annexin V (B) to compromise tumor vasculature90

Figure 4.22. Internalization of SWNT-F3 by endothelial cells. Confocal image of dividing endothelial cells following 12 h of incubation with the SWNT-F3 conjugate. Cellular membranes are stained in red with CellMask Deep Red. The green fluorescence is from the SWNT-F3 conjugate (F3 tagged at the N-terminus with FITC).	93
Figure 4.23. Effect of SWNT-F3 with NIR laser 1 h post-irradiation. MCF-7 cells incubated for varying times with SWNT-F3 containing long (A), short (B), and very short (C) SWNTs were irradiated with NIR light at 980 nm. Cell viability was measured by the Alamar Blue assay with statistical significance was denoted by * ($p < 0.01$). Data are presented as mean \pm SE (n = 3)	94
Figure 4.24. Effect of SWNT-F3 with NIR laser 18 h post-irradiation. MCF-7 cells incubated for varying times with SWNT-F3 containing long (A), short (B), and very short (C) SWNTs were irradiated with NIR light at 980 nm. Cell viability was measured by the Alamar Blue assay with statistical significance was denoted by * ($p < 0.01$). Data are presented as mean \pm SE (n = 3)	95

LIST OF TABLES

Table 3.1. The polymerase chain reaction setup for cytosine deaminase and annexin V construction.....	30
Table 3.2. PCR thermocycling parameters	30
Table 3.3. Composition of the T4 DNA polymerase reaction	32
Table 3.4. Annealing of cytosine deaminase-annexin V to pET-30 Ek/LIC vector	32
Table 3.5. Site-directed mutagenesis polymerase chain reaction composition	34
Table 3.6. PCR thermocycling parameters for site-directed mutagenesis	34
Table 4.1. Summary of methioninase-annexin V purification.....	55

ABSTRACT

Primary cancer treatment often includes a combination of surgery, chemotherapy, or radiation. Chemotherapy and radiation have limited efficacy due to their negative side effects. Recent research has moved towards the development of therapies that are designed to specifically target malignant cells only. The majority of this work characterizes two novel enzyme prodrug therapies using fusion proteins containing annexin V to target only tumor vascular endothelial cells and cancer cells, reducing the burden of systemic toxicity in healthy tissue. Methioninase enzyme will convert inert selenomethionine to toxic methylselenol and also deplete the cancer cells of methionine necessary for protein synthesis and continued growth. Cytosine deaminase converts 5-fluorocytosine into the well-known cancer therapeutic 5-fluorouracil. Additionally, continued work using single-walled carbon nanotubes targeted to cancer cells by the F3 peptide was done.

Recombinant technology was used to express and purify methioninase-annexin V and cytosine deaminase-annexin V fusion proteins. *In vitro* testing of binding and cytotoxicity were completed. Studies of both fusion proteins binding to human endothelial cells and two breast cancer cell lines were done to obtain dissociation constants in the range of 0.6-6 nM, indicating relatively strong binding. Cytotoxicity studies revealed that methioninase-annexin V with selenomethionine can kill those same cell lines in only 3 days; cytosine deaminase-annexin V accomplished the same goal in 9 days using 5-fluorocytosine.

The remaining enzyme prodrug work involved testing the methioninase-annexin V system *in vivo*. Pharmacokinetic testing revealed complete clearance of

methioninase-annexin V from the bloodstream to occur within 8 hours following intraperitoneal injection. Selenomethionine levels up to 12 mg/kg were shown to cause no apparent toxicity, while higher levels were lethal. Tests were done with a maximum of 10 mg/kg. The enzyme prodrug system demonstrated a significant slowing of tumor growth compared to untreated mice or mice treated only with the prodrug or fusion protein. Using a fluorescent dye, it was shown that the blood flow through the treated tumor was significantly reduced. The results obtained *in vivo* with this enzyme prodrug treatment are promising.

F3-targeted single-walled carbon nanotubes were tested for their ability to bind to and become internalized by endothelial cells and breast cancer cells. Following incubation with SWNT-F3, cells were irradiated with a near-infrared laser 980 nm. The irradiation increased the cell death as determined by a cell viability assay. The photothermal therapy produced promising results *in vitro*, and tests with mice are recommended.

1. INTRODUCTION

Nearly every person knows someone that has been affected by cancer at some point in their life. Even though cancer death rates have been decreasing since ~1990, the Centers for Disease Control and Prevention statistics from 2009 indicate that nearly 570,000 deaths per year were the result of cancer, second only to heart disease [1]. According the American Cancer Society, males have a lifetime risk of 45% of acquiring some form of cancer and 23% risk of dying. Risks for females are 38% and 20% respectively. Prostate cancer for men is the highest risk of occurrence at 17% with one-sixth of those dying due to the disease. Breast cancer is the predominantly occurring disease for females with a 12% chance with one-quarter of those women dying [2].

The vast majority of cancer deaths are caused by metastatic lesions that occur as cancer progresses (**Figure 1.1**) [3]. There are several steps required for a primary tumor to become a malignant cancer. Within the primary tumor, cells must lose cell-cell contacts and gain the ability to migrate. Tumor cells must then breach the basement membrane using matrix proteases to enter blood or lymphatic vessels. Specific cancers circulate in vessels to reach particular tissue types where they have to adhere to the vessel wall and extravasate into the native tissue. For the metastatic legion to survive, the tumor cells must be able to recruit a blood and nutrient supply by forming new blood vessels in a process called angiogenesis. The process of angiogenesis has been reviewed by Carmeliet and Jain [4].

Contrary to highly ordered healthy tissue containing mature blood vasculature [5], cancerous tissue exhibits structural abnormalities like irregular branching, vessel diameter, and increased vessel leakage [6]. Once cells become malignant, rapid

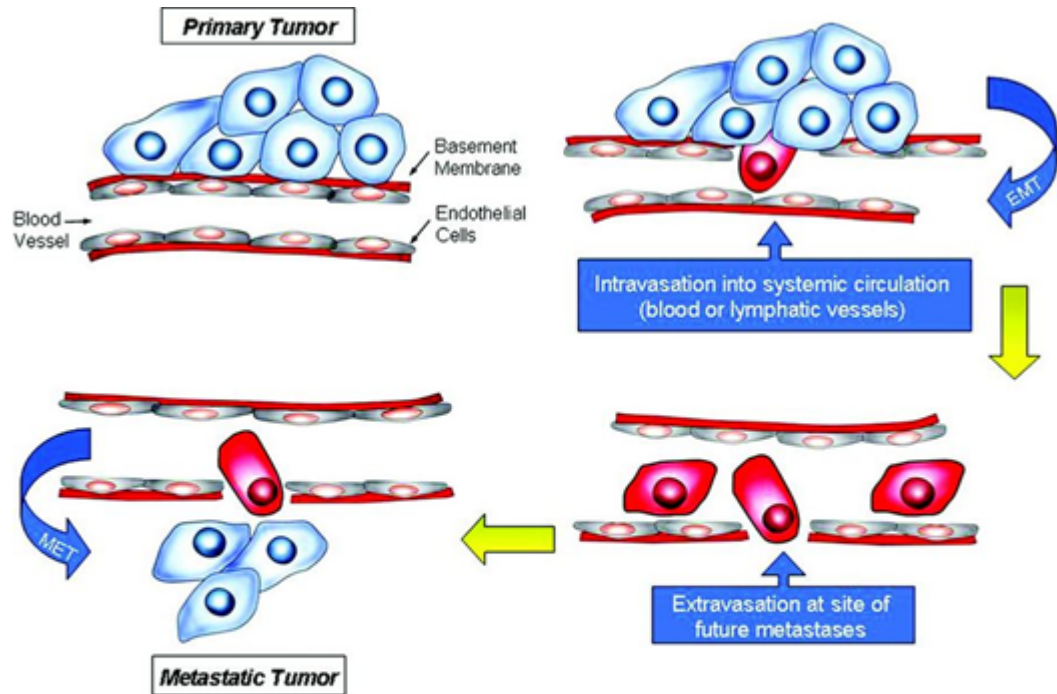


Figure 1.1. Schematic of the complex metastatic process. Epithelial-mesenchymal transition (EMT) alters the cell phenotype to allow intravasation into the systemic circulation. Mesenchymal-epithelial transition (MET) occurs at the site of distinct metastases (produced from Dotan et al.).

angiogenesis is essential to supply nutrients and oxygen for tumor growth and results in variable vessel structure with increased distance between tumor blood vessels, which leads to regions of hypoxia within the tumor [7, 8]. The limited diffusion of oxygen into these areas tends to inhibit cytotoxicity of chemotherapeutic agents because the cells are not rapidly dividing [9].

Standard clinical treatments of cancer include a combination of surgery, chemotherapy, and radiation. Systemically-administered chemotherapy drugs reach rapidly dividing tumor cells by the well-known enhanced permeability and retention effect [10]. Similarly, areas of rapidly dividing healthy cells such as cells of the bone marrow and intestinal epithelial cells are also affected, resulting in common severe side effects including hair loss, suppression of blood cell production, and inflammation of the intestines, among numerous other symptoms. The lack of specific targeting results in little drug accumulation in the tumor tissue and can be one of the many causes of drug resistance in tumor cells [11], making the cancer cells even difficult to kill [12].

The next sections will focus on directed prodrug therapies and how they are used to produce therapeutic drug levels without the inherent toxicity of typical chemotherapeutics. Exposure of phosphatidylserine to the bloodstream will then be described as a way to target enzymes to specific cancer tissue. The mechanisms employed by two specific enzyme prodrug systems, L-methioninase with selenomethionine and cytosine deaminase with 5-fluorocytosine, and how cell killing is expected to occur with each system will be discussed. A discussion of a different approach to treating cancer, photothermal therapy using carbon nanotubes, is then given. The following section introduces the F3 peptide used to target the carbon

nanotubes to the nucleolin receptor known to be expressed by proliferating tumor endothelial cells. Finally, the experimental hypotheses to be tested are presented along with the experimental design for each section.

Overview of Directed Prodrug Therapy

Enzyme prodrug therapy for cancer was designed as a way to avoid the systemic toxicity of chemotherapy. A type of enzyme prodrug therapy known as antibody-directed prodrug therapy (ADEPT) was first proposed in the 1980s as a means to confine the action of cytotoxic drugs to the tumor. In ADEPT, an antibody that binds to the tumors is linked to a drug-activating enzyme, and the resulting fusion protein is administered systemically and preferentially accumulates in the tumor [13] (see **Figure 1.2**, reproduced from Tietze et al [14]). A non-toxic prodrug is administered systemically and is converted in the tumor to a toxic drug by the enzyme. The enzyme should not have a human homolog to avoid prodrug activation in normal tissues.

Gene-directed prodrug therapy (GDEPT) is a related therapy and uses a specific gene that codes for an enzyme of interest. The gene, usually part of a vector, is administered to the patient by some means, and the gene is internalized in cancer cells and becomes part of the cell's DNA, enabling the enzyme to be produced by the cell. With the enzyme expressed, the systemic administration of the prodrug is done as with ADEPT.

A large amount of prodrug is able to be converted to the corresponding drug in the tumor tissue by every enzyme molecule bound or expressed by the cells. Therefore, a high drug concentration can be achieved within the tumor environment, and tumor cells are able to be killed in an efficient manner. Due to the formation of these low

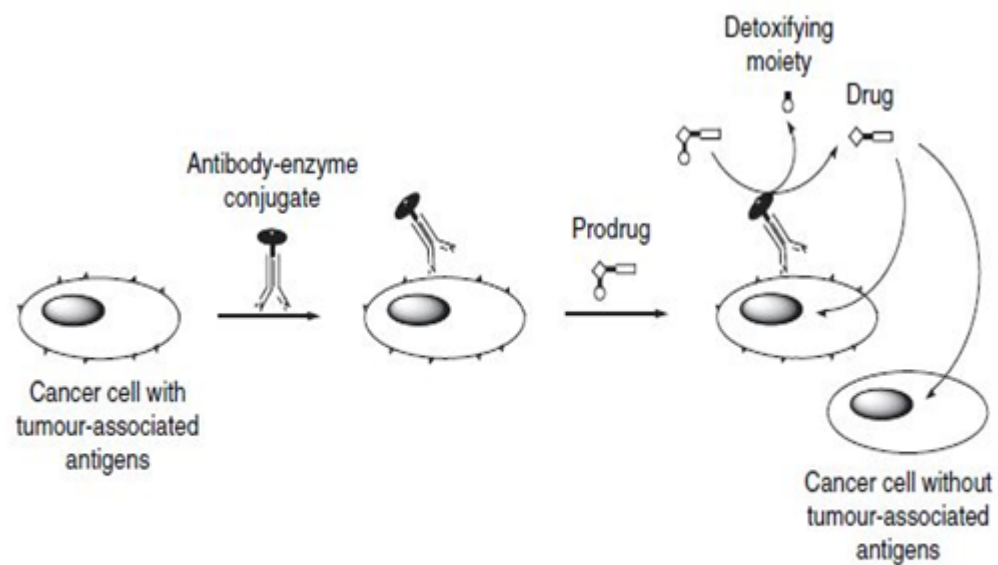


Figure 1.2. Selective cancer therapy using antibody-directed enzyme prodrug therapy (reproduced from Tietze, et al 2009).

molecular weight drugs in the extracellular environment, neighboring tumor cells that may not express the desired antigen can be killed by drug diffusion. This is known as a bystander effect and is a way to eliminate tumor cells that would not be susceptible to the treatment with traditional antibody–drug conjugates [15]. In order to have an effective therapy, a prodrug needs to maintain a low systemic toxicity and be soluble in aqueous solution. To prevent prodrug conversion throughout the body, the enzyme being employed should either be expressed at very low levels or not at all in healthy tissue and come from an exogenous source. The drug that results from the conversion of the prodrug should have low molecular weight, high cell uptake, and cytotoxicity. Furthermore, the enzyme complex needs to bind to only tumor-related cells and should have high enzymatic activity, should not be inactivated by the prodrug or the drug, and ideally should have low immunogenicity. A potential problem with the use of non-human enzymes in therapy is the possibility of an immune reaction. A way to reduce a protein's immunogenicity that has been well studied is the conjugation of polyethylene glycol (PEG) to the protein [16].

To accomplish the goal of developing a new cancer therapy that limits the inherent toxicity of standard chemotherapeutics, a specific target receptor and ligand must be identified. Much research has looked at antibodies or other proteins that bind overexpressed proteins on the surface of cells within tumors. However, the receptor is usually expressed in healthy tissue throughout the body as well. Every cell within a given tumor does not express the same receptors, making it difficult to target malignant cells in a tumor. For an enzyme prodrug system to be as effective as possible at

converting the prodrug to an active agent, the enzyme should be easily administered and accessible for rapid prodrug conversion.

Annexin V Binds Exposed Phosphatidylserine (PS) in Tumor Vasculature

In healthy mammalian cells, most all anionic phospholipids, including PS, are known to reside exclusively on the internal leaflet of the plasma cell membrane with the outer leaflet containing primarily cationic phospholipids [17, 18]. The asymmetry of the phospholipids is controlled by aminophospholipid translocase, an ATP-dependent enzyme that internalizes PS back to the cytoplasmic leaflet, and scramblase, a calcium-dependent transporter that flips PS to the external surface of the plasma membrane [19, 20]. Upon exposure to certain external stimuli, the PS gets translocated to the outer leaflet of the lipid bilayer in vascular endothelial cells, making it accessible to the bloodstream. Various conditions, both physiological and pathological--including platelet activation, cell aging, degranulation, apoptosis, necrosis, and malignancy--are responsible for the leaflet switching of the PS, which is controlled by two enzymes [21-24]. In malignant tissue, PS externalization can occur without these stimuli [19, 20], and several carcinoma cell lines have been shown to expose up to seven times more PS than healthy cells. Vascular endothelial cells are also known to expose PS which may be caused by acidity, hypoxia, inflammatory molecules, or oxygen species. These conditions can be stressful to endothelial homeostasis and result in calcium uptake and subsequent aminophospholipid translocase inactivation or scramblase activation [25, 26].

Work published in 2002 confirmed the translocation of anionic phospholipids including PS in mice bearing MDA-MB-231 tumors [25, 26]. A monoclonal antibody

that is reactive towards all anionic phospholipids was developed. The antibody and protein annexin V were biotinylated and then injected intravenously to the mice. Ex vivo staining proved that both proteins were bound to tumor vascular endothelial cells, tumor cells, and to necrotic regions of the tumor. Staining done on healthy tissue revealed no antibody or annexin V binding, thus indicating anionic phospholipids, including PS, were not externalized.

Annexin is a family of proteins that bind anionic phospholipids and contain 70-mer repeat sequences. Annexin V (36 kDa, monomer) has four repeat domains and is known to specifically bind to PS in a calcium-dependent manner (**Figure 1.3**). Each of the domains contains a calcium-binding site. As mentioned above, biotinylated annexin V was shown to be bound to vascular endothelial cells within a breast cancer tumor and to the tumor cells.

Mechanism of Cell Death via L-Methioninase and Selenomethionine

For the enzyme component, L-methionine gamma-lyase (accession #AAB03240) that exists as a homotetramer, also known as L-methioninase, from *Pseudomonas putida* was chosen (**Figure 1.4**). This enzyme catalyzes the alpha, gamma-elimination of L-methionine and is not found in human tissue [27]. L-methionine is converted to methanethiol, a-ketobutyrate, and ammonia. Methionine is an essential amino acid and has been shown to be very important for the continued survival and proliferation of cancer cells. Many tumor cell lines, such as those of brain, colon, kidney, lung and breast, have been shown to be methionine-dependent [28-30]. All healthy cells are considered to be methionine-independent because of their ability to manufacture methionine from the precursor homocysteine [28, 31, 32]. Homocysteine



Figure 1.3. Structure of human annexin V protein from RCSB Protein Data Bank (www.rcsb.org).

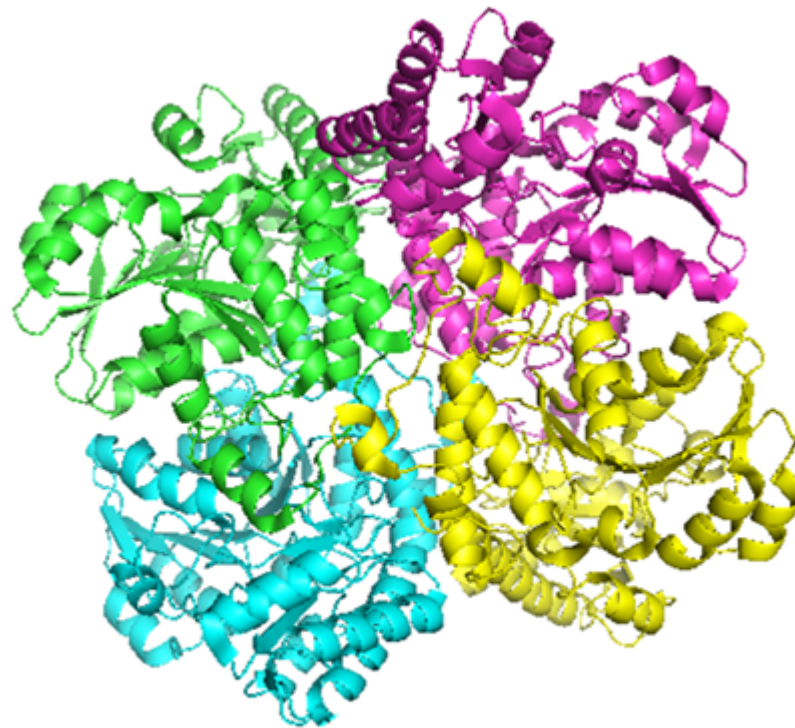


Figure 1.4. Structure of L-methioninase from *Pseudomonas putida* from RCSB Protein Data Bank (www.rcsb.org). Each monomer making up the homotetramer is shown in a different color.

lacks the methyl group that is attached to sulfur on the side chain. Below normal levels and activity of methionine synthase, one of the enzymes that methylates homocysteine to form methionine, have been shown for many methionine-dependent cancer cell lines [33, 34].

The prodrug selenomethionine is also cleaved by alpha, gamma-elimination into toxic methylselenol, a-ketobutyrate, and ammonia [35]. Methylselenol has been shown to be approximately 200-fold more cytotoxic to various human cancer cells than the prodrug [36] and is known to induce apoptosis in cancer cells [37, 38]. Gene array data produced by Zeng et al. [39] indicated that cell cycle arrest and apoptosis were found to be most common effects observed following fibrosarcoma tumor cell incubation with methylselenol. It is likely that cell cycle arrest and apoptosis play a key role in the inhibition of tumor cell invasion upon exposure to methylselenol. Other reports indicate methylselenol blocks cell cycle progression, induces apoptosis, and regulates gene expression in prostate and mammary cancer cells [40, 41].

Several mechanisms of action of the methioninase-annexin V/selenomethionine system are envisioned. The methylselenol generated at the surface of the endothelial cells in the tumor leads to destruction of these cells, which leads to clotting in the tumor vasculature and a cutoff of the supply of oxygen to the tumor. Thus, the primary tumor and distant metastases can be treated simultaneously. Methylselenol is also carried to the tumor cells by fluid permeating through the artery wall because of the pressure gradient across the artery wall. The destruction of the endothelial cells will release tumor antigens directly in the bloodstream, which can cause the immune system to mount a systemic attack on any remaining tumor cells anywhere in the body; this

immune response can be boosted by the administration of immunoadjuvants [42]. Finally, the L-methioninase will greatly reduce the supply of methionine in the tumor, which will weaken methionine-dependent cancer cells.

Mechanism of Cell Death via Cytosine Deaminase and 5-Fluorocytosine

The anti-metabolite 5-fluorouracil (5-FU) is widely used in the treatment of solid tumors, including those of the breast, gastrointestinal system, head and neck, and ovary [43]. It has been established that 5-FU is converted inside the cell to the active metabolites fluorodeoxyuridine monophosphate (FdUMP), fluorodeoxyuridine triphosphate (FdUTP), and fluorouridine triphosphate (FUTP) [44]. These metabolites misincorporate into RNA and DNA and inhibit the nucleotide synthesis enzyme thymidylate synthase. Unlike using a drug that rapidly disrupts the membrane, 5-FU requires DNA and RNA replication to induce toxicity. Cytotoxicity to non-cancerous tissues limits the dosage and frequency of drug administration. Common side effects of 5-FU are bone marrow suppression leading to neutropenia and infections, and gastrointestinal toxicities such as stomatitis, nausea, vomiting, and diarrhea [45].

To circumvent problems related to systemic administration, new delivery strategies have been studied to produce 5-FU at the site of the tumor using an inert prodrug. As part of an enzyme prodrug system, 5-fluorocytosine (5-FC), a common antimicrobial compound known to exhibit high bioavailability [46], has been used in combination with cytosine deaminase (CD, **Figure 1.5**) to produce biologically relevant levels of 5-FU locally. CD has been used in ADEPT by conjugating it to a single chain fragment variable (scFv) antibody [47, 48]. In ADEPT, however, the antibody-enzyme complex must diffuse across the vascular wall to reach the tumor cells. In a study of the

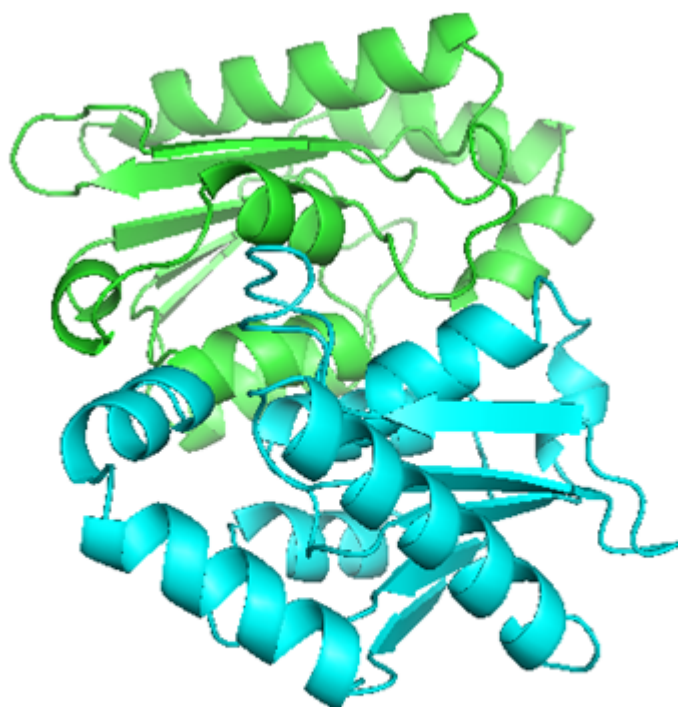


Figure 1.5. Structure of cytosine deaminase from *Saccharomyces cerevisiae* from RCSB Protein Data Bank (www.rcsb.org). Both monomers making up the homodimer are shown.

local distribution of a monoclonal antibody injected i.v. in patients with malignant melanoma, the antibody was found to be heterogeneously distributed through the tumor, which was not primarily due to heterogeneity of antigen expression but could have been a result of differences in capillary wall permeability [49]. Other studies have used CD-fusions for suicide GDEPT [50, 51] and viral-directed enzyme prodrug therapy (VDEPT) [52, 53]. Gene delivery is limited, however, by an inability to transfect large number of cells efficiently, while viral vectors have the potential of inducing severe immune responses and also suffer from a limited amount and size of plasmid DNA [54].

Hyperthermal Therapy using Single-Walled Carbon Nanotubes (SWNT)

Many reports have proven that inducing prolonged hyperthermia is an approach that has been successful *in vitro* and *in vivo* for killing tumor cells. The use of near-infrared (NIR) lasers [55, 56], magnetic thermal ablation [57], and RF and microwave ablation [58-61] have been reported to heat tissue. When occurring for a sufficient time, hyperthermia can cause severe tissue damage or complete necrosis. Dissipation of heat in healthy cells is critical when experiencing periods of elevated temperature. Healthy cells and tissue are known to withstand hyperthermia better than malignant cells [62]. Vascular adaptation within healthy tissue causes blood vessels to dilate, increasing blood flow to dissipate the heat. The lack of vasculature organization in tumors disrupts the adaption process and allows heat buildup inside the tumor [63]. An elevation in tumor cell temperature between 40-43°C for at least 5 minutes has been shown to induce protein coagulation, apoptosis, and necrosis [64]. However, temperatures reaching 54-60°C require less than 1 minute to induce apoptosis, necrosis, and lipid bilayer disruption [65].

Photothermal therapy is one method to induce hyperthermia and has been used in a number of clinical settings including cancer. In one type of photothermal therapy of cancer, nanoparticles are delivered to the tumor and then are heated by light at a specific wavelength, which causes heating of the tumor. Work has been done using gold nanoshells [55], fullerenes [66], and carbon nanotubes [67-69].

Carbon nanotubes have several intriguing properties that make them interesting candidates for biological research, including their electrical, optical, and thermal properties. For this work, the property of interest is their strong near-infrared light absorbance from 700 to 1400 nm [70, 71]. Human tissue is known to be relatively transparent in this range of light and will allow the use of carbon nanotubes in combination with NIR to produce thermal cell injury. Additionally, with their extreme length to diameter ratio, carbon nanotubes are able to transverse mammalian cell membranes with little effect on the cell [72]. Because of this, carbon nanotubes have been investigated as delivery vehicles for biological molecules.

Several studies have used carbon nanotubes combined with NIR light as a way to treat cancer (see the review by Harrison et al. [73]). To prepare carbon nanotubes for use as an injectable agent, usually a surfactant must be employed with sonication to mechanically break up aggregates [74]. Being made from all carbon atoms, the surface of nanotubes is extremely hydrophobic which prohibits suspension in aqueous solutions. To circumvent the problem, conjugation of water-soluble polyethylene glycol (PEG) to the nanotube surface [75] or use of heterobifunctional linkers have been used previously [76]. Single-walled and multi-walled carbon nanotubes (SWNTs and MWNTs, respectively) have been employed in several cancer studies. A 2005 study

proved that HeLa cells cultured *in vitro* could be killed using a combination of folate-targeted SWNTs and NIR light while cells receiving no SWNTs were unharmed [71]. Studies targeting different moieties have also been done on neuroblastoma [77], prostate [78], and breast cancer cell lines [79].

F3 Peptide Binds Nucleolin Receptor Expressed on Proliferating Cells

It is known that vascular endothelial cells express specific molecules on their surface depending on where they are located within the body. Extensive work has been done using phage display technology in order to map these vascular addresses and identify targets that are specific to healthy organs or tumor tissues. Phage display techniques employ bacterial viruses, or phage, expressing short amino acid sequences on their surface protein coat [80], and have discovered numerous peptides that home to specific tissues, both healthy and malignant [81, 82]. Some of the peptides also act as cell-penetrating peptides as they become internalized by the cells that express their specific receptor [83]. One such sequence is the F3 peptide.

The F3 peptide is a 31-amino-acid peptide fragment of the high mobility group protein 2 [84]. Upon binding to its cell surface receptor, F3 becomes internalized and homes towards the nucleus. Tumor vascular endothelial cells and tumor cells have been used to demonstrate the F3 shuttling to the nucleus [84, 85]. The cell receptor that binds F3 is called nucleolin and is sequestered in the cytoplasm of healthy cells. Nucleolin is known to have the ability to catalyze its own degradation. However, when a cell receives the signal to begin proliferation, this 105 kDa nucleolar phosphoprotein [86] gets transported to the cell surface of and is exposed to the extracellular environment [87, 88]. While undergoing proliferation, the ability of nucleolin to

degrade itself is thought to be inhibited. A study done in 1991 proved that cells in the process of actively dividing have a majority of intact nucleolin versus stationary phase cells that contain higher amounts of fragmented nucleolin [89]. Additionally, the amount of nucleolin presented by proliferating cells is approximately 10 times that expressed by non-dividing cells [86]. To prove the shuttling of F3 to the nucleus, MDA-MB-435 human breast cancer cells were found to internalize fluorescently-labeled F3 and translocate it to the cell nucleus *in vitro* and in mice [84]. This was confirmed by another group [90]. The expression of nucleolin on the cell surface of tumor vascular endothelial cells and tumor cells provide an excellent target for a new cancer therapy.

Mechanism of Cell Death via Carbon Nanotube Heating

This therapeutic strategy reported here exploits the naturally occurring deficit of NIR-absorbing molecules in most tissue, permitting transmission of NIR light through tissue with little attenuation and minimal heating. Light within this spectral region has been shown to penetrate tissue at depths around 1 cm with no observable damage to the tissue [91]. The combination of SWNTs targeted to the tumor vasculature using the F3 peptide, which binds to nucleolin, and NIR laser light presents a new therapy that allows for a targeted delivery of heat to tumor tissue.

Overall Hypothesis and Experimental Plan

The hypotheses that are tested in this work are: 1) a cytosine deaminase-annexin V fusion protein can be expressed in *E. coli* and then purified, and this fusion protein will have cytosine deaminase enzymatic activity; 2) the L-methioninase-annexin V and cytosine deaminase-annexin V fusion proteins will bind to the surface of endothelial

cells (non-confluent) and breast cancer cells *in vitro* with good binding strength (dissociation constants under 10 nM); 3) L-methioninase-annexin V and cytosine deaminase-annexin V fusion proteins will convert nontoxic prodrugs to active drugs that will kill endothelial and breast cancer cells; 4) the L-methioninase-annexin V/selenomethionine enzyme prodrug system will kill or inhibit the growth of a human breast tumor in mice with the fusion protein and prodrug delivered by i.p. injection; 5) targeting single-walled carbon nanotubes to the surface of endothelial and breast cancer cells via the F3 peptide will cause internalization of the nanotubes; 6) application of a near-infrared laser in the presence of single-walled carbon nanotubes with F3 attached will cause thermal injury and death to cells grown *in vitro*.

The following experimental strategies were used to test the above hypotheses:

1. Creation of a cytosine deaminase-annexin V fusion protein

Nucleotide primers will be designed and manufactured for use in the polymerase chain reaction. A flexible triple repeat glycine-serine linker will be built in to fuse the cytosine deaminase gene (N-terminal) to the annexin V gene (C-terminal). The linker will allow for the enzyme to remain active by preventing interference of the active site and maintain available binding residues of annexin V.

The fused gene will then be cloned into a bacterial expression vector for recombinant expression in *E. coli*. The vector codes for a histidine tag at the N-terminal, and a specific protease site will be added immediately prior to the fusion gene. The fusion protein is expected to be produced as a soluble protein with an active cytosine deaminase enzyme and functional annexin V. The (His)₆ tag will allow for use of a purification column containing nickel for immobilized metal affinity

chromatography, followed by cleavage of the (His)₆ tag using a protease to yield a high purity fusion protein. The Bradford protein assay and an enzymatic assay will be used to track the protein quantity and enzyme activity of the fusion throughout the purification process. Denaturing sodium dodecyl sulfate polyacrylamide gel electrophoresis (SDS-PAGE) will be used to determine for during the various purification steps.

Yeast CD was chosen since previous work has demonstrated a greater ability of yeast CD to convert 5-FC to 5-FU than bacterial CD [92]. Intravenous injection of this fusion protein will allow annexin V to bind rapidly to exposed PS on endothelial cells in the tumor vasculature, and the FP will also be transported from the bloodstream to tumor cells via the well-known enhanced permeability and retention (EPR) effect [10]. Following clearance of unbound FP, 5-FC would be injected and converted to 5-FU within the tumor both at the surface of the tumor vasculature and at the surface of the cancer cells.

2. Fusion proteins bind PS exposed on the surface of endothelial and cancer cells

To prove the methioninase-annexin V and cytosine deaminase-annexin V proteins can be used to effectively target cancer cells and remain bound to convert the prodrug to active drugs, binding tests will be done to determine specific binding dissociation constants for both fusion proteins on endothelial cells and MCF-7 and MDA-MB-231 breast cancer cells using the interaction of biotin and streptavidin tagged with an enzyme to developed a colorimetric substrate for quantification. The duration of binding to these cells is also going to be tested using a modified binding test in

combination with a metabolic assay to produce binding data on a per-cell basis. This will be important to aid in designing subsequent experiments.

3. Fusion proteins convert specific prodrugs into active drugs that kill cancer cells

A metabolic activity assay will be used to determine cytotoxic effects of the fusion proteins, their prodrugs, and the combination of fusion proteins with their prodrugs. Following binding of the fusion proteins to the surface of endothelial and cancer cells, the prodrug will be added and cell viability determined after a given period of time specific for each system. Comparison of treated to untreated cells is expected to result in significant cell death of cells treated with the enzyme prodrug combinations with minimal effect of the prodrug alone.

4. L-methioninase-annexin V with selenomethionine will reduce or inhibit MDA-MB-231 tumor growth in immunodeficient mice

Using a mouse xenograft model, MDA-MB-231 breast cancer cells will be inoculated in the flank region of immunodeficient mice. Once the tumors show signs of growth, three consecutive cycles of treatment with methioninase-annexin V and selenomethionine will begin with each cycle lasting 4 days. The treatment is expected to produce toxic methylselenol that will rupture endothelial cells lining blood vessels within the tumor and cause clotting that will cut off the supply of oxygen and nutrients needed for continued tumor growth. It is anticipated that the tumor will halt or even reduce the size of the tumor.

5. Carbon nanotubes functionalized with the F3 peptide are internalized by endothelial and MCF-7 breast cancer cells

The F3 peptide has been shown to be internalized in previous reports. By attaching the peptide to the surface of single-walled carbon nanotubes, it is expected that the conjugate will be taken up by the cells following incubation with endothelial and cancer cells. Fluorescence and confocal microscopy will be used for that determination.

6. Application of near-infrared light will heat internalized carbon nanotubes to induce death in endothelial cells and 4T1 and MCF-7 breast cancer cells

The use of near-infrared light at specific wavelengths has been shown to produce heat when absorbed by carbon nanotubes. Endothelial and the breast cancer cells will be incubated with the SWNT-F3 conjugate for varying times followed by NIR light to induce heating of the nanotubes. The amount of toxicity will be determined by a metabolic activity assay and is expected to be increased when combining the SWNT-F3 with NIR light.

Note: Some of the information presented in the following sections has previously been published [56, 93, 94].

2. MATERIALS

Bacterial Plasmids, Strains, and Mutagenesis

L-methioninase-annexin V was previously constructed and cloned in this lab (reference Naveen's thesis) using the linear pET-30 Ek/LIC vector from EMD Chemicals (Gibbstown, NJ). Cytosine deaminase-annexin V also was cloned into the linear pET-30 Ek/LIC vector. **Figure 2.1** shows the layout of the vector and some of its general features and ligation independent cloning sequence. NovaBlue Gigasingles were used for the amplification of the pET-30 Ek/LIC plasmid containing the two fusion genes (EMD Chemicals). *E. coli* BL21(DE3) cells were used as the expression host of the fusion genes (EMD Chemicals). Site-directed mutagenesis products used XL10-Gold Ultracompetent cells from Agilent Technologies (Santa Clara, CA).

DNA Manipulation and Protein Purification

Oligonucleotide primers were synthesized by Integrated DNA Technologies (Coralville, IA) with standard desalting. The polymerase chain reaction was done using the Expand High Fidelity PCR system (Boehringer Mannheim, Indianapolis, IN). The DNA sequences encoding for the cytosine deaminase-annexin V gene were amplified from pQE30Xa/CD [95] (obtained from Dr. Maurizio Cianfriglia at the Superior Health Institute, Rome, Italy) and pET-22b(+)/STF-ANX (obtained from Dr. Stuart Lind at the University of Colorado). T4 DNA polymerase and HRV 3C protease were obtained from EMD Chemicals. BamHI restriction enzyme and T4 DNA ligase were purchased from New England Biolabs (Ipswich, MA). The Qiaquick PCR purification kit, Qiaquick agarose gel purification kit, and Qiaquick plasmid purification kit were purchased from Qiagen (Vista, CA). SeaKem® LE agarose was purchased from

Cambrex Bio Science Rockland, Inc. (Rockland, ME). LB medium contained yeast extract Hy-Yest[®] 412 and tryptone from Sigma Aldrich (St. Louis, MO). IPTG, TPCK, PMSF, β -mercaptoethanol, pyridoxal phosphate, MBTH, acrylamide, and Triton X-114 were all from Sigma Aldrich. HisTrap HP columns containing nickel sepharose were purchased from GE Healthcare Biosciences (Piscataway, NJ). Imidazole, BCA protein assay kit, and cellulose acetate filters were from Thermo Fisher Scientific (Waltham, MA). The Bradford protein reagent was from Bio-Rad (Hercules, CA).

Mammalian Cell Lines and Culture Media

HAAE-1 endothelial cells were from Coriell Cell Repositories (Camden, NJ). MCF-7, MDA-MB-231, and 4T1 cells were obtained from the American Type Culture Collection (Manassas, VA). F-12K (Kaighn's modification of Ham's F-12 medium), Eagle's minimum essential medium (EMEM), Leibovitz's L-15 medium, and RPMI-1640 medium were also purchased from American Type Culture Collection. Premium heat inactivated fetal bovine serum and trypsin were from Atlanta Biologicals (Lawrenceville, GA). Heparin sodium salt was from Polysciences.com (Warrington, PA). Endothelial cell growth supplement, bovine insulin, and matrigel were purchased through Fisher Scientific. Penicillin/streptomycin was from Life Technologies (Carlsbad, CA). MDA-MB-231 cells expressing GFP were from Cell Biolabs (San Diego, CA).

In Vitro Binding, Binding Duration, and Cytotoxicity Assays

SureLINK chromophoric biotin and streptavidin-HRP was purchased from KPL (Gaithersburg, MD). Bovine serum albumin, EDTA, O-phenylenediamine, phosphate citrate buffer, fluorescein isothiocyanate (FITC), 5-fluorocytosine, and 5-fluorouracil

were obtained from Sigma Aldrich. Alamar Blue solution was obtained from BioSource (Camarillo, CA). Selenomethionine and Fluoro-gel were from Fisher Scientific. Chambered microscope slides, streptavidin coated 96-well plates, dialysis tubing, and dialysis cassettes were from Thermo Fisher Scientific.

In Vivo Pharmaokinetics, Enzyme Prodrug, Phosphatidylserine Detection, Biodistribution and Tumor Blood Flow Assays in Mice

Inbred NU/J and outbred SCID mice were purchased from Jackson Labs (Bar Harbor, ME), and outbred athymic nu/nu mice were from Charles River (Wilmington, MA). Mice were maintained on a 5053 lab rodent diet 20 from Lab Supply (labsupplytx.com, Fort Worth, TX). Modified L-amino acid defined Lombardi choline and methionine deficient diet with 1.7 g/kg DL-homocysteine added (pelleted #518787GI) was purchased from Dyets, Inc (Bethlehem, PA). Anti-human annexin V antibody produced in rabbit was purchased from Abcam (Cambridge, MA). Tween 20 and anti-rabbit IgG (whole molecule)–horseradish peroxidase secondary antibody produced in goat were from Sigma Aldrich. The DAB reagent kit was bought from KPL and hematoxylin was from Fisher Scientific. DyLight 680 fluorescent dye was from Thermo Fisher Scientific.

In vitro Assays for Single-Walled Carbon Nanotubes with F3 Peptide

CoMoCAT® Single-walled (SG 6,5) carbon nanotubes were provided courtesy of Dr. Daniel Resasco and SouthWest NanoTechnologies (Norman, OK). DSPE-PEG-maleimide (1,2-distearoyl-sn-glycero-3-phosphoethanolamine-polyethylene glycol-maleimide) linker was obtained from Creative PEGworks (Winston Salem, NC). The F3 peptide (KDEPQRRSARLSAKPAPPKPEPKPKKAPAKKC) with FITC added to

the N-terminus was synthesized by Biomatik, Inc (Wilmington, DE). CellMask™ deep red plasma membrane stain was bought from Life Technologies. Fluoro-gel was from Fisher Scientific.

3. METHODS

Primer Design for PCR

Primers for the construction of the cytosine deaminase-annexin V fusion gene were designed to contain the reverse complement of a region of template DNA. In order to insert the fusion gene into the pET-30 Ek/LIC linear vector, ligation independent cloning (LIC) sites needed to be incorporated at the N- and C- terminals of the gene. The cytosine deaminase gene was positioned at the N-terminal, so its forward primer contained the ligation independent cloning sequence and also the HRV 3C protease site sequence to allow for removal of the histidine tag during the purification process. The reverse primer for the cytosine deaminase gene and the forward primer for the annexin V gene contained BamHI restriction enzyme sites to fuse the genes together. The forward primer for annexin V followed the BamHI site with a sequence encoding a 6-amino acid flexible linker before the start of annexin V. Its reverse primer added the C-terminal ligation independent cloning. The following are the complete primer sequences.

Sequence of the primers for amplifying the cytosine deaminase gene:

Forward primer:

5'-gAC/ gAC /gAC/ AAg/ ATg/ CTT/ gAA/ gTC/ CTC/ TTT/ CAg/ ggA/ CCC/
gTg/ ACA/ ggg/ ggA/ ATg/ gCA/ AgC -3'

Reverse primer:

5'- gC/ CgC/ ATT/ ggA/ TCC/ AgA/ ACC/ gTC/ gCC/ CTC/ ACC/ AAT/ ATC/
TTC/ AAA/ CC -3'

Sequence of the primers for amplifying the annexin V gene:

Forward primer:

5'- Cg/ ATT/ CgC/ *ggA*/ TCC/ gCA/ CAg/ gTT/ CTC/ AgA/ ggC -3'

Reverse primer:

5'-gA/ ggA/ gAA/ gCC/ Cgg/ TTA/ gTC/ ATC/ TTC/ TCC/ ACA/ gAg/ C -3'

Notes: Underlined = Ligation independent cloning sites

BOLD = HRV 3C protease site

Italics = BamHI sites

The melting temperature (T_m) of primers and the dimer formation with itself were calculated by using a program provided by the website <http://www.basic.northwestern.edu/biotools/oligocalc.html>. All primers were designed with these criteria: 1) length of primers were ≥ 17 bases, 2) G + C composition was at least 50%, 3) 3' end of primer was G or C, or CG or GC, 4) T_m of primers was between 55-80°C, and 5) ability of primer to form secondary structure was minimized. Integrated DNA Technologies synthesized all the primers with standard desalting in aqueous solution.

Construction of Cytosine Deaminase-Annexin V Fusion Gene

The polymerase chain reaction was used to amplify the cytosine deaminase gene from the pQE30Xa/CD plasmid obtained from the Cianfriglia lab in Italy using the above-mentioned primers. The annexin V gene was amplified from the pET-22b(+)/STF-ANX plasmid previously obtained. The Expand High Fidelity PCR system was used for all reactions. **Table 3.1** contains the composition of the PCR reactions for cytosine deaminase and annexin V. The difference in the size of the specific primers caused the amount of each primer to vary. **Table 3.2** gives the PCR cycling parameters that were used. Following the PCR reactions, the Qiaquick PCR purification kit was used to remove reaction components to retain pure DNA (Appendix B has the complete

PCR Reaction Mixtures for Yeast Cytosine Deaminase (pQE30Xa/CD)			
Mix 1	Volume (μl)	Mix 2	Volume (μl)
PCR nucleotide mix	1	Enzyme mix	0.75
Sense primer	1.1	10X Buffer, w/ MgCl ₂	5
Antisense primer	1.4	ddH ₂ O, Sterile	19.25
Template DNA	1		
PCR grade water	20.5		
TOTAL	25		25

PCR Reaction Mixtures for Annexin V (pET 22b/STF-annexin)			
Mix 1	Volume (μl)	Mix 2	Volume (μl)
PCR nucleotide mix	1	Enzyme mix	0.75
Sense primer	1.2	10X Buffer, w/ MgCl ₂	5
Antisense primer	1.2	ddH ₂ O, Sterile	19.25
Template DNA	2.5		
PCR grade water	19.1		
TOTAL	25		25

Table 3.1. The polymerase chain reaction setup for cytosine deaminase and annexin V construction.

Step	# of Cycles	Temperature	Time
Initial Denaturation	1	94°C	2 min
Amplification	31		
-Denaturation		94°C	15 sec
-Annealing	(CD)	55°C	30 sec
	(annexin V)	55°C	30 sec
-Elongation		72°C	90 sec
Final Elongation	1	72°C	7 min
Cooling	1	4°C	∞

Table 3.2. The polymerase chain reaction setup for cytosine deaminase and annexin V construction.

protocol). [96] To verify the PCR amplification was successful, agarose gel electrophoresis was performed (see Appendix B). Both correctly-sized genes were digested separately with the BamHI restriction enzyme for 1 hr at 37°C to make them compatible. The Qiaquick PCR purification kit was used again to retain only digested genes. T4 DNA ligase was used to fuse the digested cytosine deaminase and annexin V genes together for 10 min at room temperature. Another agarose gel was run to confirm the ligation work. From the gel, the band of the appropriate size was cut out, and the DNA was purified using the Qiaquick gel extraction kit (see Appendix B). Sticky ends were created on the LIC portions of the fusion gene by treatment with T4 DNA polymerase at room temperature for 30 min followed by inactivating the polymerase by incubation at 75°C for 20 min. Table 3.3 gives the reaction composition to create the sticky ends. The sticky ends were used to anneal the fusion gene to the pET-30 Ek/LIC vector. Table 3.4 shows the annealing reaction. An agarose gel was run to confirm the successful annealing to the linear vector, which will close the vector into a circular plasmid. The pET-30 Ek/LIC/CD-Anx plasmid was transformed into NovaBlue GigaSingles for amplification. Following an overnight liquid culture in LB media containing 30 mg/L kanamycin, the cells were harvested by centrifugation, and the plasmid was extracted using the QIAprep spin mini-prep kit (see Appendix B). The plasmid was sent for gene sequencing using the T7 promoter and T7 terminator primers at Oklahoma Medical Research Foundation (Oklahoma City, OK). With confirmation of the correct fusion gene sequence, the plasmid was transformed into *E. coli* BL21(DE3) cells that are used as the expression host.

Component	Volume (μ l)
0.2 pmol purified PCR product	4
10X T4 DNA Polymerase Buffer	2
25 mM dATP	2
100 mM DTT	1
Nuclease-free Water	10.6
2.5 U/ μ l T4 DNA Polymerase	0.4
TOTAL	20

Table 3.3. Composition of the T4 DNA polymerase reaction.

Component	Volume (μ l)
pET-30 Ek/LIC vector	1
Treated Ek/LIC insert (0.02 pmol)	2
Incubate for 5 min at 22°C, then add:	
25 mM EDTA	1
TOTAL	4

Table 3.4. Annealing of cytosine deaminase-annexin V to the pET-30 Ek/LIC vector.

Site-Directed Mutagenesis of L-Methioninase-Annexin V Fusion Gene

It was determined that the methioninase-annexin V fusion gene constructed previously in this laboratory contained two separate point mutations. Methioninase arginine 326 (CGC) needed to be corrected to glycine 326 (GGC), and annexin V phenylalanine 11 (TGC) needed to be corrected to cysteine 11 (TTC). Primers were designed as follows with the correct sequence:

Forward primer for methioninase 326 mutation:

5' - gAg/gCC/ggg/Cgg/ggC/TTC/ATg/AAT/gC -3' T_m = 69.6 °C

Reverse primer for methioninase 326 mutation:

5' - gCA/TTC/ATg/AAg/CCC/CgC/CCg/gCC/TC -3' T_m = 69.6 °C

Forward primer for annexin V 11 mutation:

5' - ggC/ACT/gTg/ACT/gAC/TTC/CTT/ggA/TTT/gAT/gAg -3' T_m = 63.1 °C

Reverse primer for annexin V 11 mutation:

5' - CTC/ATC/AAA/TCC/Agg/gAA/gTC/AgT/CAC/AgT/gCC -3' T_m = 64.3 °C

The Quikchange II XL site-directed mutagenesis kit was used to make the corrections. **Tables 3.5** and **3.6** contain the composition of the mutagenesis PCR reactions and thermocycling conditions, respectively (see Appendix B for complete protocol). Following thermocycling, the *Dpn I* enzyme (10 U) provided was used to digest the parental plasmid for 1 hr at 37°C. *E. coli* XL10-Gold ultracompetent cells were transformed with the mutated plasmid and plated on agar with IPTG and X-gal. The plates were allowed to incubate for at least 16 hr at 37°C. Several colonies that appeared blue in color were selected, and an overnight liquid culture of each was done

Component	Volume (μ l)
10X reaction buffer	5
dsDNA template	4
oligonucleotide primer #1	1.25
oligonucleotide primer #2	1.25
dNTP mix	1
QuikSolution	33.5
ddH ₂ O	3
Then add:	
PfuUltra HF DNA polymerase	1
TOTAL	50

Table 3.5. Site-directed mutagenesis polymerase chain reaction composition.

Segment	Cycles	Temperature	Time
1	1	95°C	1 min
2	18	95°C	50 sec
		60°C	50 sec
		68°C	1 min/kb of plasmid
3	1	68°C	7 min

Table 3.6. PCR thermocycling parameters for site-directed mutagenesis.

to amplify the plasmid for extraction using the mini-prep protocol. The plasmid was sent for sequencing.

The length of the methioninase-annexin V fusion gene (2268 bases) requires an additional set of primers to sequence the middle section of the gene. Primers can identify approximately 600 bases from each end with accuracy. These sequencing primers were used to detect the middle of the gene:

Forward sequencing primer 1:

5' - ggC/TTg/CCg/TCg/TTT/gCC/CAg/TAC/g -3' $T_m = 66.2^\circ\text{C}$

Forward sequencing primer 2:

5' - g/TTT/gAT/ggC/TCT/CAg/TTC/TTC/Agg -3' $T_m = 57.7^\circ\text{C}$

Sequencing of Fusion Proteins

All DNA samples requiring sequencing were sent to Oklahoma Medical Research Foundation (OMRF) DNA sequencing core facility. An ABI 3730 capillary sequencer analyzed all samples. The T7 promoter and T7 terminator primers were provided by OMRF. Primers were made to overlap by 30-60 bases to ensure quality sequencing.

Fusion Protein Expression, Purification, Analysis, and Storage

The *E. coli* BL21(DE3) expression host was transformed with the pET-30 Ek/LIC plasmid containing methioninase-annexin V or cytosine deaminase-annexin V and kanamycin resistance. Luria Bertani (LB) medium containing yeast extract (5 g/L), tryptone (10 g/L), NaCl (10 g/L), and kanamycin (35 mg/L) was used to grow the bacteria. A 10 ml pre-culture was done for ~10 h at 37°C and shaking at 200 rpm

before being added to the remaining 990 ml of LB medium. The 1 L culture was split into four 1-L Erlenmeyer flasks and grown for ~4 h to achieve mid-log phase growth (optical density in the range of 0.6-0.8). Fusion protein production was induced using isopropyl β -D-thiogalactopyranoside (IPTG) at a total concentration of 0.4 mM with the temperature lowered to 30°C and shaking at 180 rpm for 5 h. Cells were harvested by centrifugation at 1,000 x *g* for 10 minutes and resuspended in sonication buffer containing 0.05 mM *N-p*-tosyl-L-phenylalanine chloromethyl ketone (TPCK), 1 mM phenylmethylsulfonyl fluoride (PMSF), 1% HPLC grade ethanol, 0.01% β -mercaptoethanol, and 20 mM sodium phosphate dibasic and adjusted to pH 7.4. The methioninase-annexin V fusion requires 0.02 mM pyridoxal 5'-phosphate as a cofactor throughout to maintain enzymatic activity but is not included for cytosine deaminase-annexin V purification. Sonication of the suspension was done to lyse the cells in an ice bath at 4.5 W for 30 s followed by 30 s of rest and repeated four times. Centrifugation of the entire suspension at 12,000 x *g* for 30 min separated the soluble proteins from the cell debris.

All the following purification steps were performed at 4°C. Samples were taken during each step to track the protein concentration and enzyme activity. An absorbance detector at 280 nm and fraction collector assisted throughout the chromatography. Imidazole (40 mM) and NaCl (500 mM) were used to reduce non-specific binding when the soluble protein lysate was fed into the 5 ml HisTrap HP chromatography column with immobilized Ni²⁺. Wash buffer #1 containing 20 mM sodium phosphate, 40 mM imidazole, 500 mM NaCl, and 0.02 mM pyridoxal phosphate at pH 7.4 was used to equilibrate the column prior to applying the lysate. With the fusion protein secured to

the column by the (His)₆-tag, 70 column volumes of wash buffer #2 (wash buffer #1 plus 0.1% Triton X-114) removed endotoxin bound to the protein. The column was washed with 20 column volumes of wash buffer #1 to remove residual Triton X-114 detergent. By applying elution buffer (20 mM sodium phosphate, 500 mM imidazole, 500 mM NaCl, and 0.02 mM pyridoxal phosphate at pH 7), the fusion protein was removed from the column. Eluted fractions were pooled and dialyzed for 3 h against 20 mM sodium phosphate and 0.02 mM pyridoxal phosphate at pH 7.4 to remove NaCl and ready the protein for cleavage using the HRV 3C protease. The protease was used at 10 U/mg of fusion protein with the addition of 10X cleavage buffer provided with the protease for 16 h at 4°C with gentle agitation. Again, imidazole (40 mM) and NaCl (500 mM) were added to the cleaved protein to reduce non-specific binding and applied to same HisTrap HP column that was regenerated. Lacking the (His)₆-tag, the cleaved fusion protein flows through the column. Any uncleaved fusion protein and the HRV 3C protease remained in the column because both have the (His)₆-tag. The cleaved protein collected from the column was dialyzed against 20 mM sodium phosphate, 100 mM NaCl, and 0.02 mM pyridoxal phosphate at pH 7.4 for 3 hr at 4°C. The protein solution was sterilized by passing the protein solution through a 0.2 µm cellulose acetate filter. The final purified protein was put into 1-ml aliquots in cryovials and flash frozen in liquid nitrogen. The HisTrap HP columns can be used many times if the regeneration is done after each use and then stored in 1 M HPLC grade ethanol to prevent the nickel sepharose resin from drying out. Regeneration of the column is done using 25 ml of 1 M KCl, 1 M NaOH, DI water, and then 1 M HPLC grade ethanol.

Samples were taken at each step to track the purification. The protein

concentration of each sample was determined using either the Bradford protein assay or the BCA protein assay. Bovine serum albumin was used as the standard for both protein assays. Methioninase activity was determined by converting methionine to α -ketobutyrate and developing it with colorimetric substrate 3-methyl-2-benzothiazolinone hydrazone hydrochloride hydrate (MBTH). Cytosine deaminase activity is measured by the change in absorbance as 5-FC is deaminated to 5-FU. Samples were analyzed for size and purity by denaturing gel electrophoresis using the SDS-PAGE method with Coomassie blue staining method [97]. The Limulus Amebocyte Lysate (LAL) QCL-1000 testing kit was used to determine the amount of endotoxin remaining in the fusion protein samples at the conclusion of the purification. Briefly, the endotoxin converts a proenzyme to an enzyme, which then converts a substrate into a peptide and p-nitroaniline that is measured. Appendix B has the complete protocols for methods of analysis.

Flash frozen proteins underwent lyophilization to convert the liquid solution into a dried powder. Holes were punched in caps of cryovials to allow the moisture to be vacuumed out. Protein samples were freeze-dried overnight, recapped to have no holes, and stored at -80°C .

Binding of Fusion Proteins to Exposed Phosphatidylserine on Endothelial and Cancer Cells

Human HAAE-1 aortic endothelial cells were grown in F-12K medium with 2 mM L-glutamine and 1.5 g/L sodium bicarbonate and supplemented with 10% fetal bovine serum (FBS), 0.03 mg/ml endothelial cell growth supplement, and 0.1 mg/ml heparin. MCF-7 human breast cancer cells were maintained as monolayer cultures in

Eagle's minimum essential medium containing Earle's balanced salt solution, non-essential amino acids, 2 mM L-glutamine, 1 mM sodium pyruvate, 1.5 g/L sodium bicarbonate, and supplemented with 10% FBS and 0.01 mg/ml bovine insulin. MDA-MB-231 human breast cancer cells were grown in Leibovitz's L-15 medium supplemented with 10% FBS and 2 mM L-glutamine. Penicillin (100 U/ml) and streptomycin (100 µg/ml) were also added to each medium. HAAE-1 and MCF-7 cells were grown at 37°C in a 5% CO₂ atmosphere, while MDA-MB-231 cells were grown without additional CO₂ at 37°C, as recommended by the American Type Culture Collection. Each cell line was grown to 70–80% confluence in T-75 flasks. Cells were transferred to 24-well culture plates (5x10⁴ cells/well) and grown to 80–85% confluence. Cells were fixed to the plate using 0.25% glutaraldehyde in binding buffer (phosphate buffer saline, or PBS, with 2 mM Ca²⁺). Excess aldehyde groups were quenched using 50 mM NH₄Cl in binding buffer. Varying concentrations of biotinylated fusion proteins, using SureLINK Chromophoric Biotin in a 60 molar excess during biotinylation (see Appendix B), were diluted in binding buffer containing 0.5% BSA and incubated at 37°C for 2 h. After washing with binding buffer with 0.5% BSA, streptavidin-HRP was added at 2 µg/ml and incubated at room temperature for 1 h. Following washing with binding buffer, HRP was measured by adding the chromogenic substrate O-phenylenediamine (0.4 mg/ml) and hydrogen peroxide (0.012 vol.%) in 0.05 mM phosphate-citrate buffer (pH 5.0). After 30 min at room temperature in the dark, the solution was transferred to a transparent 96-well plate, and the absorbance was read at 450 nm on a BioTek Synergy HT microtiter plate reader (Winooski, VT). All experiments had a blank that was subjected to the same procedure but with no fusion

protein added. To determine non-specific binding, the same procedure was performed with no Ca^{2+} and 5 mM EDTA in the binding buffer, with the addition of a 1 h BSA (0.5%) pretreatment for the cancer cells prior to adding the fusion protein. The complete protocol for measuring fusion protein binding is given in Appendix B.

To assess how long the fusion proteins remain bound to the surface of the endothelial and cancer cells, a modified binding assay was used. Cells on 24-well plates were first incubated for 2 hr at 37°C in a saturating concentration of biotinylated fusion protein (100 nM) in complete growth medium with 2 mM Ca^{2+} . The Alamar Blue assay was done on separate sets of cells at days 0–3 to determine viability, followed by fixing with 0.25% glutaraldehyde in binding buffer. Excess aldehyde groups were quenched by incubation in a 50 mM NH_4Cl in binding buffer. The binding of fusion protein was then quantified using streptavidin-HRP and OPD as above. The complete protocol for quantifying the stability of fusion protein binding is given in Appendix B.

To prove the fusion proteins bind to the surface of the cells and not to the 24-well plate surface, a visualization procedure was used. Cells were plated into chambered slides at 80–85% confluence. Fusion proteins tagged with FITC (see Appendix B), were diluted to 100 nM in binding buffer and incubated with the cells for 2 h at 37°C . Cells were washed with binding buffer to remove unbound protein. The chamber was removed from the slide, a drop of fluoro-gel in TES buffer was placed over the cells, and a coverslip was applied. Alternatively, 35 mm petri dishes could be used with 22 mm square coverglasses with the cells seeded on top. The coverglass would be removed from the petri dish after the protein binding, fluoro-gel applied, and

then flipped over onto a microscope slide. A Nikon Eclipse E800 fluorescence microscope with a Nikon DXM1200F digital camera was used to document FITC fluorescence on the cells. The complete protocol for visualizing fusion protein binding is found in Appendix B.

Cytotoxicity of the Enzyme Prodrug Systems to Endothelial and Cancer Cells

The experiment was carried out over 3 days for methioninase-annexin V, using the same cells for each of the days. Cells were grown and plated in 24-well plates with respective growth media using the same procedure as for the binding assay (see above). Each medium was supplemented with 2 mM Ca^{2+} and 0.02 mM pyridoxal phosphate and the level of L-methionine was adjusted to 1000 μM . On day 0, the cells were incubated in medium containing 100 nM methioninase-annexin V for 2 h at 37°C. The plates were washed, and medium containing selenomethionine varying from 0 to 1000 μM was added. The Alamar Blue assay was performed on all wells on day 1. The Alamar Blue assay was performed by adding Alamar Blue solution to each well to give 10% Alamar Blue and then incubated for 4 h at 37 °C. The solution (250 μl) was transferred to an opaque 96-well plate, and the fluorescence was read at 590 nm using excitation at 530 nm. The blank consisted of wells containing only medium and Alamar Blue solution. After the fluorescence reading, the plates were washed, replaced with fresh medium containing appropriate levels of selenomethionine, and placed in the incubator. The readings were taken every 24 h for the duration of the experiment. The complete protocol is given in Appendix B.

The experiment with cytosine deaminase-annexin V was carried out over 9 days using the same set of cells. Cells were grown and plated out in 24-well plates with

respective growth media using the same procedure as for the binding assay above. Each medium was supplemented with 2 mM Ca^{2+} . On day 0, the cells were incubated in medium containing 100 nM cytosine deaminase-annexin V for 2 hr at 37°C. The plates were washed and medium containing 5-FC or 5-FU varying from 0 to 2000 μM was added. Cells receiving 5-FU did not receive cytosine deaminase-annexin V. Each day throughout the experiment, the medium was replaced with fresh medium containing 5-FC or 5-FU. The Alamar Blue assay was performed on all wells on days 3, 6, and 9 (as above). After the fluorescence readings on days 3 and 6, the plates were washed, and the cells were incubated with new cytosine deaminase-annexin V using the same procedures as before. The cells were washed again, and fresh medium containing appropriate levels of 5-FC or 5-FU was added before further incubation.

ELISA for L-Methioninase-Annexin V Detection in Mouse Serum

All work involving the use of mice was done in accordance with the Institutional Animal Care and Use Committee at the University of Oklahoma Health Sciences Center. The complete ELISA protocol is presented in Appendix B. NU/J mice were injected i.p. with 1 and 10 mg/kg of biotinylated methioninase-annexin V. At 1, 4, 8, and 24 h post injection, four mice for each dosage level were sacrificed following a cardiac blood draw. As a blank sample, four mice did not receive any injection. The blood was centrifuged, serum was collected, and flash frozen. Using a streptavidin-coated 96-well plate, serum samples were added and allowed to incubate for 1 h at 37°C to allow the biotinylated methioninase-annexin V to bind to the streptavidin. Wells were washed with wash buffer containing 0.05% Tween 20 in PBS. Polyclonal anti-annexin V antibody was diluted in diluting buffer (0.005% Tween 20 and 0.25% BSA

in PBS) and added to each well. Plates were incubated for 1 h at 37°C and washed as above. Anti-rabbit IgG-HRP conjugate was diluted in diluting buffer and added to the wells and incubated for 1 h at 37°C and washed. O-phenylenediamine was added, incubated for 30 min at room temperature in the dark, and the absorbance was read at 450 nm.

The strain of mice used was changed to SCID mice. To prove that methioninase-annexin V was cleared from the bloodstream in a similar time as in NU/J mice, the above procedure was done using three mice that were sacrificed 14 hr post-injection. Serum samples were compared to mice that did not receive methioninase-annexin V. The complete protocol for the ELISA is given in Appendix B.

Dose Safety Injections of Selenomethionine

Selenomethionine is known to have a toxic limit, so the appropriate level must be determined. Thirty total NU/J mice were injected with selenomethionine at varying dosages to determine the level of prodrug that could be tolerated by the mice. Dosages of 0, 6, 12, 24, and 60 mg/kg were administered via i.p. injection every 24 h for three consecutive days to simulate the anticipated enzyme prodrug treatment schedule. Mice were monitored for three days after the injections to determine an acceptable selenomethionine level.

Development of Tumor Xenografts in Mice

MDA-MB-231 breast cancer cells expressing GFP were grown at 37°C. For each mouse to be injected, two 150-mm petri dishes containing cells were grown to give $\sim 7-8 \times 10^6$ cells. The day prior to the cell injections, the medium was changed to contain no penicillin/streptomycin. Cells were lifted using typical cell culture procedures and

resuspended so each mouse will receive 100 μ l of cell suspension. Matrigel basement membrane matrix was thawed overnight in a water bath at 4°C. Cell suspension was mixed with matrigel at a 1:1 ratio and immediately injected into the flank of mice under anesthesia using a 25G needle. The needle was left in the flank for ~1-2 min to allow for the matrigel to solidify. Tumor volumes, in cubic millimeters using $V = (\text{width})^2 \times \text{length}/2$, were measured every 3-4 days thereafter using digital calipers. The detailed protocol for the injection of cancer cells into mice is given in Appendix B.

Detection of Externally Positioned Phosphatidylserine in MDA-MB-231 Tumor Vasculature

This enzyme prodrug therapy is based on binding of the methioninase-annexin V fusion protein to phosphatidylserine exposed on the surface of endothelial cells that line the blood vessels within a tumor. SCID mice were injected MDA-MB-231/GFP cancer cells as above, and the tumors were allowed to develop. Biotinylated methioninase-annexin V was injected i.p. at 10 mg/kg. One h after injection, the mice placed under anesthesia, and the chest cavity was opened to expose the heart. A 27G butterfly needle was inserted into the left ventricle, and the ascending vena cava was cut. Heparinized saline with 2 mM Ca^{2+} was used to perfuse the circulation, followed by fixation with 0.25% glutaraldehyde in saline with calcium. The tumor was immediately resected and soaked in 20% sucrose and calcium overnight at 4°C. Tumor samples were sent to the imaging core facility at OMRF for cryoembedding and cryosectioning. A slide stained with hematoxylin and eosin (H&E) and slides unstained were obtained. Slides were incubated with streptavidin-HRP to bind biotinylated methioninase-annexin V, washed, and developed with 3,3'-diaminobenzidine (DAB).

Counterstaining was done with hematoxylin to visualize cell nuclei and slides were preserved with ImmuniHistoMount (Santa Cruz Biotechnology, Santa Cruz, CA). The fluorescence microscope above was used for brightfield detection and documentation. Appendix B has the complete protocol.

Biodistribution of Methioninase-Annexin V in SCID Mice

The conversion of selenomethionine prodrug into toxic methylselenol is expected to occur only within the local tumor environment to prevent systemic drug toxicity. To evaluate the location of methioninase-annexin V binding, SCID mice (n = 3) with developed MDA-MB-231/GFP tumors were injected i.p. with methioninase-annexin V tagged with DyLight 680 fluorescent dye. At 1, 12, and 24 h post-injection, whole-body images of the mice were taken with the IVIS Spectrum small animal imaging system located in the Rodent Barrier Facility (OU HSC). After the last images, the tumor, kidneys, lungs, heart, stomach, and spleen were removed and imaged *ex vivo*. The complete protocol is given in Appendix B.

Treatment of MDA-MB-231 Breast Tumors in Mice with Methioninase-Annexin V

Methioninase-annexin V in combination with selenomethionine produced significant endothelial and cancer cell death *in vitro*. To determine the efficacy of this enzyme prodrug system in a living system, mice bearing MDA-MB-231/GFP breast xenografts were treated with three cycles of methioninase-annexin V and selenomethionine. Each cycle consisted of a methioninase-annexin V injection at 10 mg/kg, followed by three consecutive days of selenomethionine (10 mg/kg). The experiment included four groups (n = 7 mice/group): 1) untreated control, 2) methioninase-annexin V only, 3) selenomethionine only, and 4) methioninase-annexin

V with selenomethionine. Mice were maintained on a normal mouse chow diet. Tumor volumes and mouse weight were measured two or three times per week to track the effect of the treatment. Post-treatment observation was done until the tumor volumes required the mice to be sacrificed at which time the lungs, liver, and tumor were removed and soaked in formaldehyde. Samples were delivered to Dr. Stanley Kosanke (OU HSC Pathology) for paraffin embedding. Precision Histology Lab, Inc (Oklahoma City, OK) sectioned and stained the slides with H&E. Dr. Kosanke performed histological analysis for all mice samples.

Knowing methionine is an essential amino acid required for the continued growth of cancer cells and that methioninase enzyme catalyzes the conversion of methionine to byproducts, an experiment was done to see the effect of the methioninase-annexin V with selenomethionine treatment of MDA-MB-231/GFP breast tumors with mice on a methionine-deficient diet. The same treatment schedule of three cycles was used as above, with the selenomethionine dosage lowered to 5 mg/kg. Experiment groups of 1) untreated control, 2) methioninase-annexin V only, and 3) methioninase-annexin V were done with $n = 7$ mice/group. One the day before the treatment began, the mice were changed from the normal diet to the methionine-deficient diet. Histological analysis at the end of the experiment was done as above. The complete protocol for the treatment of tumors in mice is given in Appendix B.

Determination of Blood Flow Through MDA-MB-231/GFP Tumors

The main effect of the methioninase-annexin V with selenomethionine treatment is expected to be the generation of toxic methylselenol at the surface of the endothelial cells lining the tumor vasculature ultimately resulting in clot formation and blood flow

interruption. SCID mice (n = 3 for treated and control groups) bearing MDA-MB-231/GFP tumors were subjected to the above treatment (10 mg/kg of methioninase-annexin V + 10 mg/kg of selenomethionine for three cycles). The day after the conclusion of the treatment, all six mice were injected with DyLight 680 fluorescent dye at 1 mg/kg. The IVIS imaging system was used to document the amount of dye flowing through the control and treated tumors. Then, the circulation of the mice was perfused with heparinized saline with 2 mM Ca²⁺. The same procedure used for detection of PS was used for fixation, resection of the tumor, and preparation for H&E staining was done prior to delivering to Dr. Kosanke. The complete protocol for the experiments to determine blood flow through the tumors is given in Appendix B.

Conjugation of F3 Peptide to Single-Walled Carbon Nanotubes with a Phospholipid Linker

Functionalizing the carbon nanotubes allows them to be targeted to specific cells. To get the single-walled carbon nanotubes (6 mg) into aqueous solution, 1% sodium dodecyl sulfate (SDS, 5 ml) was used with sonication. For producing long nanotubes, samples underwent two rounds of sonication at 7 W for 30 min and a 30 min centrifugation at 15,680 x g in a microcentrifuge. Short and very short nanotubes were produced using two rounds of 3 and 6 hr of sonication, respectively.

The F3 peptide was manufactured by Biomatik, Inc with a lysine residue at the N-terminal for attachment of FITC and an additional cysteine residue at the C-terminal. The initial reaction was a 15 h overnight incubation of 1 mg of F3 (0.33 mg/ml) diluted in phosphate-buffered saline with 2 mg of DSPE-PEG-maleimide linker (2 mg/ml) in deionized water at room temperature with gentle shaking. Unreacted maleimide groups

were blocked with the addition of a 4-molar excess of L-cysteine to linker. The nanotube suspension was combined with the F3-linker and mixed for 30 min at room temperature followed by an 8 h dialysis against deionized water using a 50k MWCO cellulose acetate membrane water to remove SDS. The SWNT-F3 conjugate was centrifuged at 15,680 x g for 1 h to remove any aggregates [98] and stored at 4°C. The complete protocol for the conjugation of F3 to the nanotubes is given in Appendix B.

Analysis of the F3 content in the SWNT-F3 conjugate was done using a Bradford protein microassay (see Appendix B). Nanotube concentration was determined by measuring the absorbance at 800 nm using a BioTek Synergy HT microtiter plate reader and comparing the results to a standard curve developed by sonicating a nanotube suspension for 1 h and making dilutions without centrifuging. It was assumed that 100% of the nanotubes were in suspension.

SWNT-F3 Cell Binding Using Fluorescence and Confocal Microscopy

The SWNT-F3 conjugate is expected to bind to the nucleolin receptor on the surface of dividing endothelial cells and cancer cells and become internalized. Cells were plated into chambered slides at 80–85% confluence. During conjugation procedure, all steps were done wrapped in foil to protect the FITC attached to the F3 peptide from exposure to light. The SWNT-F3 conjugate was diluted to 60 mg/L (nanotube concentration) in cold cell medium and incubated with the cells for varying times at 37°C. Cells were washed, the chamber was removed, a drop of Fluoro-gel was placed on the cells, and a coverslip was applied. Alternatively, 35 mm petri dishes have been used with 22 mm square coverglasses with the cells seeded on top. The coverglass would be removed from the petri dish after the protein binding, Fluoro-gel applied, and

then flipped over onto a microscope slide. A Nikon Eclipse E800 fluorescence microscope with a Nikon DXM1200F digital camera was used to document FITC fluorescence on the cells. To prove the SWNT-F3 conjugate was internalized, cells were stained with 7.5 $\mu\text{g/ml}$ CellMask deep red plasma membrane stain for 30 min at 37°C, washed, and fixed with formalin. Fluoro-gel was used to preserve the fluorescence signal for viewing under an Olympus Fluoview laser scanning microscope.

Cytotoxicity of Varying Length SWNT-F3 Conjugates with NIR Laser

Endothelial and MCF-7 cells were grown and plated at ~80% confluence in 24-well plates (see Appendix B for the layout of plates) in a manner that prevents the use of adjacent wells. Cells were incubated for 24 h at 37°C to allow firm attachment to the plates. The varying length SWNT-F3 conjugates was diluted to 60 mg/L in cold cell medium, added to the wells, and incubated for 2, 8, 16, and 24 h at 37°C. Cells were washed with medium and irradiated with a Diodevet-50 Laser (B&W TEK, Inc., Newark, DE). Previous work in the lab determined that MCF-7 cells can be irradiated at 350 J/cm². All cell plates were incubated at 37°C for 1 h following the laser before measurement of cell viability using the Alamar Blue assay (as above). Fresh medium was replaced in the wells and the cells were incubated for another 13 h, at which time another Alamar blue assay was done. The complete protocol for the treatment with the laser is given in Appendix B.

Data Analysis

Dissociation constant determination was done using GraphPad software (GraphPad, La Jolla, CA). *In vitro* cytotoxicity and *in vivo* tumor volumes were

compared using a one-way ANOVA employing a Tukey-Kramer multiple comparisons test was performed using GraphPad InStat software.

4. RESULTS AND DISCUSSION

Construction of Cytosine Deaminase-Annexin V Fusion Gene

The cytosine deaminase-annexin V fusion gene was successfully produced using PCR. The template pQE30Xa/CD was used to clone the cytosine deaminase gene, while annexin V was from pET-22b(+)/STF-ANX. Primers were synthesized to add useful features to assist in the cloning, ligation, and annealing process. The amplification of cytosine deaminase added an N-terminal ligation independent cloning site (LIC) and an engineered protease site, while a BamHI restriction enzyme site was added to the C-terminal. Annexin V had a BamHI site added to its N-terminal and a LIC site to the C-terminal. **Figure 4.1A** shows an agarose gel following the PCR amplification of cytosine deaminase and annexin V genes with the additions mentioned above. The sizes of the annexin V and cytosine deaminase genes (988 and 524 base pairs, respectively) are consistent with the sizes of the PCR fragments shown in **Figure 4.1A**. Both genes were digested with the BamHI restriction enzyme for 1 h at 37°C to create compatible ends, which were fused together for 10 min at room temperature using T4 DNA ligase. **Figure 4.1B** presents the results of the ligation reaction. The genes for cytosine deaminase-annexin V (1449 base pairs), cytosine deaminase-cytosine deaminase (~1040 base pairs), and annexin V-annexin V (~1980 base pairs) were observed following the ligation. The cytosine deaminase-annexin V gene was extracted from the gel and purified using the Qiaquick agarose gel purification kit (see Appendix B). Purified product was treated with T4 DNA polymerase to create sticky ends and annealed to the linear pET-30 Ek/LIC vector. *E. coli* NovaBlue GigaSingles were transformed with the plasmid for amplification. An overnight culture was done, and the plasmid was extracted using the QIAprep spin mini-prep protocol (see Appendix B).

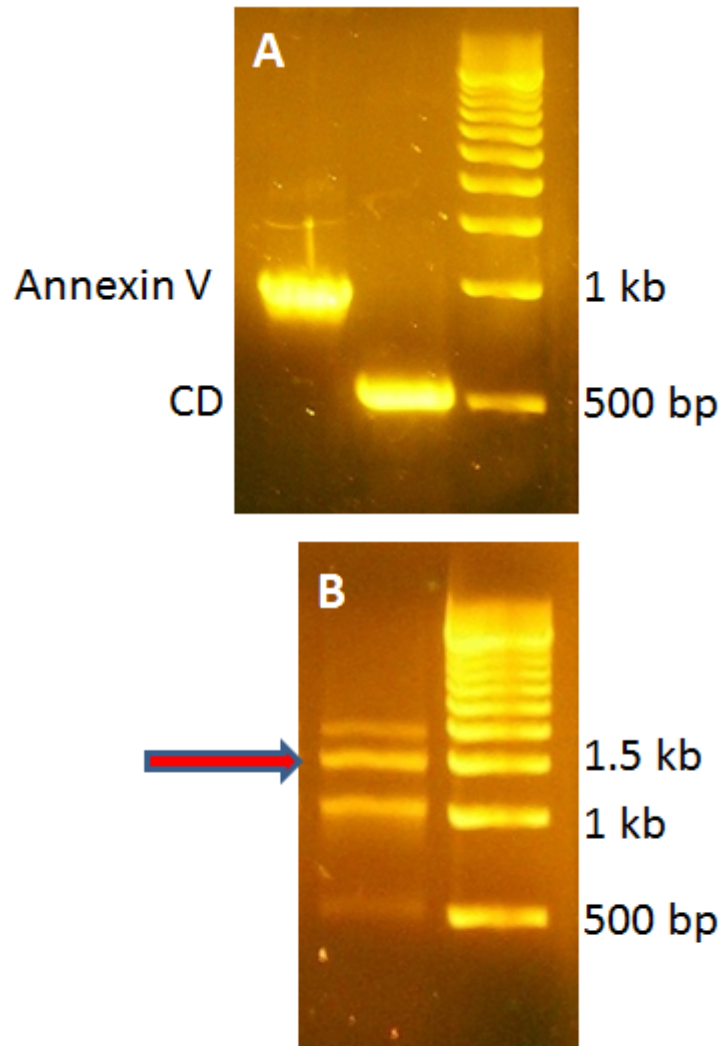


Figure 4.1. Agarose gels of cytosine deaminase-annexin V fusion gene construction. A) Annexin V and cytosine deaminase amplification. B) Ligation of cytosine deaminase to annexin V (indicated by the arrow).

Plasmid samples were sent for sequencing, and results for the cytosine deaminase-annexin V sequence are presented in Appendix A. No mutations were found in the sequence.

For the correct protein to be produced by the plasmid, the proper DNA reading frame must be maintained following the insertion of the fusion gene into the vector. The pET cloning system makes this easy since both LIC sites have distinctive complementary overhangs following treatment with the T4 DNA polymerase, which results in only one direction of gene insertion. The polymerase uses its 3' → 5' endonuclease activity to remove bases on each side of double-stranded DNA until it reaches a dATP base (the kit provided contains dATP bases for use in creating sticky ends). The polymerase activity then adds the dATP base to leave an overhang of single-stranded DNA. Insertion of the cytosine deaminase-annexin V fusion gene into the vector was efficient and required only one attempt.

Site-Directed Mutagenesis of L-Methioninase-Annexin V

It was determined that the methioninase-annexin V gene that was constructed previously in the lab [99] contained point mutations within the sequence, with one mutation in methioninase (arginine 326) and the other in annexin V (phenylalanine 11). Before continuing *in vitro* experimentation, site-directed mutagenesis was performed using the Quikchange II XL site-directed mutagenesis kit, which employs PCR with new primers designed to incorporate the correct base. Parental pET-30 Ek/LIC/METHANX was digested using 10 U of *Dpn I* enzyme for 1 h. The remaining plasmid in solution was used to transform *E. coli* XL10-Gold ultracompetent cells. Blue colonies were observed on the agar plates containing IPTG and X-gal after at least

16 h at 37°C. Several colonies were chosen for sequence analysis following a mini-prep plasmid preparation. The sequence was found to be correct after the site-directed mutagenesis (see Appendix A).

The *Dpn I* enzyme is able to recognize the parental plasmid in the PCR mutagenesis reaction because the plasmid has been methylated during replication in *E. coli* [100]. PCR does not have the ability to methylate plasmids, so the *Dpn I* will leave the mutated plasmid unharmed. Methylation of *E. coli* has been discussed previously [101].

Fusion Protein Expression, Purification, Analysis, and Storage

E. coli BL21(DE3) cells were transformed with the pET-30 Ek/LIC/CD-Anx or pET-30 Ek/LIC/METHANX plasmids to serve as the bacterial host for fusion protein expression. Cells were grown at 37°C in either 250 ml or 4 L flasks using 1 L of LB culture medium containing yeast extract, salt, and tryptone. The temperature was lowered to 30°C and IPTG (0.4 mM final concentration) was added to induce the expression of cytosine deaminase-annexin V or methioninase-annexin V for 5 h. Cells were harvested, lysed by sonication, and the soluble proteins were collected in the supernatant after centrifugation.

IPTG binds to the repressor in the *lac* operon, which inactivates it and allows gene expression to proceed. Induction at 37°C resulted in the majority of fusion protein expression to be contained in inclusion bodies. However, when the temperature was lowered to 30°C, both cytosine deaminase-annexin V and methioninase-annexin V were expressed in soluble form.

The (His)₆ tag added to the N-terminal of both fusion proteins enabled immobilized metal affinity chromatography (IMAC) to be used to purify the fusion proteins with a nickel HisTrap HP column. Applying the soluble protein fraction to the column allowed the fusion protein to bind to the column and unwanted proteins were washed out. A wash of the column with a buffer containing Triton X-114 was performed to remove endotoxin associated with the fusion protein. The application of a high concentration of imidazole eluted the fusion proteins by displacing the (His)₆ tag bound to the nickel column. Following dialysis to remove NaCl and imidazole, the (His)₆ tag was cleaved off using 10 U/mg of HRV 3C protease for 16 h at 4°C. The cleaved protein solution was applied to the regenerated column where only uncleaved protein and protease bound. The flow-through was collected, dialyzed, and sterile-filtered. Aliquots were flash frozen in liquid nitrogen in preparation for freeze-drying.

Table 4.1 shows a summary of a typical purification from a 1 L culture. Each peak was pooled together, and samples were taken after each step throughout the purification process for analysis of protein and enzymatic activity. A typical chromatograph of the chromatography portion of the purification is given in Appendix A is given in Appendix A. **Figure 4.2** is an SDS-PAGE gel image with Coomassie blue staining showing the purification of the methioninase-annexin V fusion protein at different stages. Lane 1 represents the total soluble protein lysate. Lanes 2 and 3 are the unwanted protein flow-through and the eluted methioninase-annexin V, respectively. Lane 4 corresponds to methioninase-annexin V that has been cleaved with the HRV 3C protease. **Figure 4.3** is an SDS-PAGE gel for cytosine deaminase-annexin V purification with the same samples as methioninase-annexin V.

Step	Volume (mL)	Protein concentration (mg/mL)	Total amount of protein (mg)	Activity in sample (U/mL)	TOTAL UNITS	Specific activity (U/mg protein)	Recovery Yield (%)
Before Centrifugation	40	7.16	286.40	1.31	52.4	0.18	
Supernatant after sonication	38	7.10	269.80	1.15	43.70	0.16	100%
Chromatography 1 - flow-thru (feed)	31	2.74	84.94	0.03	0.93	0.01	2%
Chromatography 1 - flow-thru (wash buffer #2)	340	0.31	105.40	0.00	0.00	0.00	0%
Chromatography 1 - flow-thru (wash buffer #1)	94	0.00	0.00	0.00	0.00	0.00	0%
Chromatography 1 - elution	33	1.88	62.04	1.61	53.13	0.86	122%
After 1st dialysis	35	1.30	45.50	1.13	39.55	0.87	91%
After cleavage	38	1.17	44.46	1.18	44.84	1.01	103%
Chromatography 2 - flow-thru	45	0.92	41.40	1.16	52.20	1.26	119%
Chromatography 2 - elution	3	0.26	0.78	0.04	0.12	0.15	0%
After 2nd dialysis	47	0.95	44.65	0.86	40.42	0.91	92%
Sterile filtration	45	0.94	42.30	0.95	42.75	1.01	98%
Biotinylated samples	5.32	0.87	4.63	0	0	0.00	0.00
Lyophilized samples (1 ml)	40	0.94	37.60	0.95	38.00	1.01	87%

Table 4.1. Summary of methioninase-annexin V purification.

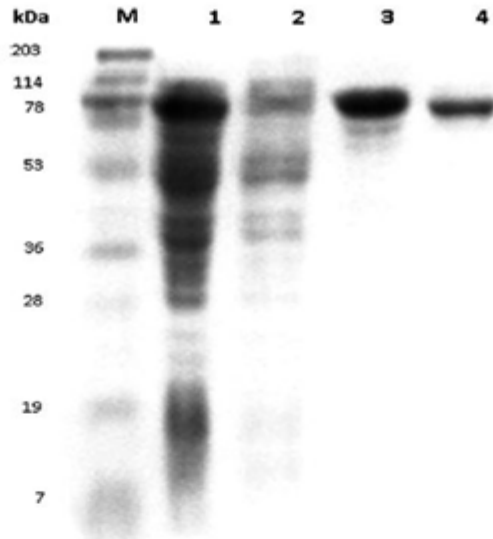


Figure 4.2. SDS-PAGE of methioninase-annexin V. Coomassie blue was used to stain the gel. Lane 1, total soluble cell lysate; lane 2, unwanted flow-through; lane 3, eluted methioninase-annexin V; lane 4, methioninase-annexin V with the (His)₆ tag removed.

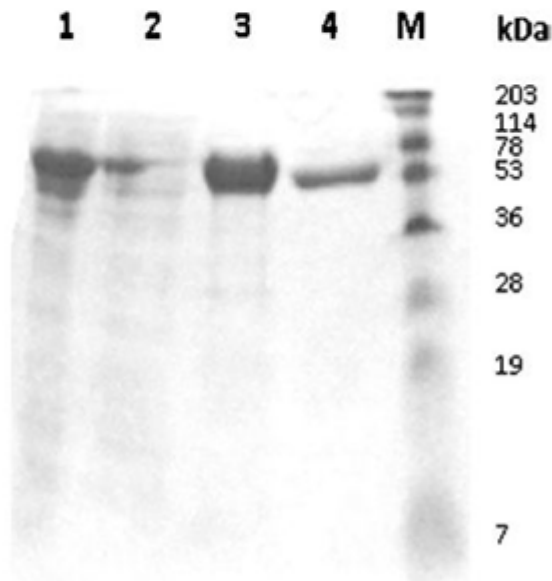


Figure 4.3. SDS-PAGE of cytosine deaminase-annexin V. Coomassie blue was used to stain the gel. Lane 1, total soluble cell lysate; lane 2, unwanted flow-through; lane 3, eluted cytosine deaminase-annexin V; lane 4, cytosine deaminase-annexin V with the (His)₆ tag removed.

Previous work regarding freezing and storing of proteins was done by Naveen Palwai [99] in the laboratory. The buffer used most often throughout the purification is 20 mM sodium phosphate, and a different fusion protein containing methioninase, ATF-methioninase, was shown to retain 69% of its activity following flash freezing in that buffer. It was hypothesized that small ice crystals were formed during flash freezing, which came into contact with the protein to cause denaturation. The addition of 100 mM NaCl resulted in a loss of only 6% when flash frozen and an additional 7% after freeze-drying. This is believed to be caused by a reduction of ice crystal interaction with the protein [102]. Because of this, both methioninase-annexin V and cytosine deaminase-annexin V proteins were stored in 20 mM sodium phosphate and 100 mM NaCl. Both enzymes retained nearly all activity for at least 3 months when stored in a freezer at -80°C as lyophilized powder.

Specific Fusion Protein Binding to Endothelial and Cancer Cells *In Vitro*

The ability of the fusion proteins to bind to endothelial cells and breast cancer cells with PS exposed on the cell surface was evaluated by equilibrium binding experiments in which increasing concentrations of biotinylated fusion protein were used. In initial experiments with endothelial cells, hydrogen peroxide was used at a low concentration (1 mM) to induce exposure of PS. In later experiments, the H_2O_2 was omitted with little change in the results; therefore, the data reported here is with no H_2O_2 added. No H_2O_2 was added in the experiments with the breast cancer lines, since it has been reported that cancer cells express PS *in vitro* [103, 104]. A typical equilibrium binding result is shown in **Figure 4.4** for the binding of methioninase-annexin V to endothelial cells. The non-specific binding, obtained in the absence of

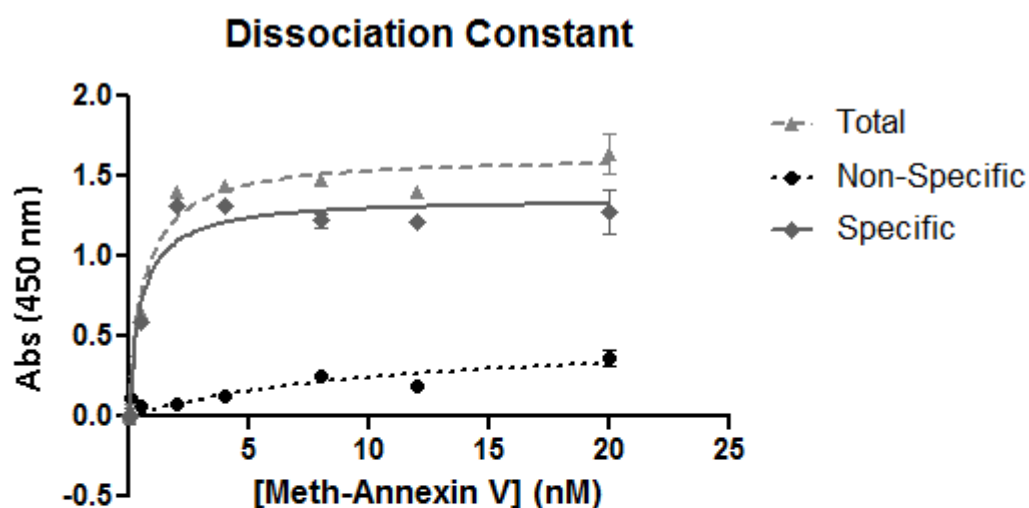


Figure 4.4. Determination of dissociation constant for methioninase-annexin V binding to human endothelial cells. Methioninase-annexin V was biotinylated and streptavidin-HRP was used to quantify the binding. Total binding was obtained using 2 mM Ca^{2+} in the binding buffer. Non-specific binding was obtained by removing the Ca^{2+} from the binding buffer and replacing it with 5 mM of EDTA to chelate Ca^{2+} . Specific binding was obtained by subtracting the non-specific binding from the total binding. GraphPad Prism 5 software determined the specific binding to have a $K_d = 0.5 \pm 0.2$ nM. Data are presented as mean \pm SE ($n = 3$).

Ca^{2+} , was subtracted from the total binding to obtain the specific binding. The dissociation constant (K_d) for each cell line tested was obtained from the specific binding data using GraphPad Prism 5 software to give the following results for methioninase-annexin V: 0.5 ± 0.2 nM for endothelial cells (with saturation $A_{450 \text{ nm}} = 1.3$), 6.2 ± 1.6 nM for MCF-7 breast cancer cells (with saturation $A_{450 \text{ nm}} = 0.9$), and 4.9 ± 0.9 nM (with saturation $A_{450 \text{ nm}} = 1.8$) for MDA-MB-231 breast cancer cells. Similarly, cytosine deaminase-annexin V binding results were the following: 1.5 ± 0.2 nM for the endothelial cells (with saturation $A_{450 \text{ nm}} = 0.6$), 0.6 ± 0.4 nM for MCF-7 cells (with saturation $A_{450 \text{ nm}} = 0.5$), and 4.2 ± 1.8 nM (with saturation $A_{450 \text{ nm}} = 1.2$) for MDA-MB-231 cells. An equilibrium binding result for the binding of cytosine deaminase-annexin V to endothelial cells is shown in Appendix A. These results indicate that the binding of the fusion proteins to these cells is relatively strong. In a control test, the specific binding assay was performed on endothelial cells that were 100% confluent. The result was that the total and non-specific data were essentially identical, indicating no specific binding. The binding of annexin V to endothelial cells was determined using the same procedures. The K_d for the specific binding data was found using GraphPad Prism 5 software to be 0.9 ± 0.2 nM (with saturation $A_{450 \text{ nm}} = 1.2$), which is similar to the K_d determined for the binding of the fusion proteins to endothelial cells. Literature values of annexin V binding alone to endothelial cells have been reported from 2.7–15.5 nM [105, 106].

The low K_d values for the endothelial cells is favorable for these enzyme prodrug systems because they are primarily directed to the tumor vasculature. The fact that the fusion proteins exhibit the same degree of binding to endothelial cells with or

without hydrogen peroxide leads us to believe that endothelial cells grown *in vitro* by our techniques expose PS on their surface. It has been shown previously in tumor-bearing mice that PS is exposed on the external surface of vascular endothelial cells in tumor blood vessels but not on endothelial cells outside of the tumor; this was demonstrated using biotinylated annexin V [25, 26]. When endothelial cells were grown to confluence, no specific binding was observed, meaning there was a lack of PS expression on the cell surface. Normal vasculature does not express PS, as proven by the lack of biotinylated annexin V binding to endothelial cells in healthy tissue [25, 26]. The strength and specificity of binding of annexin V not part of a fusion protein to endothelial cells is very similar to that of the fusion proteins using the same procedures; therefore, there is no reason to believe that the fusion proteins will bind with any different strength or specificity *in vivo* compared to annexin V.

As further evidence of the fusion proteins binding to exposed PS on the surface of cells, MDA-MB-231 cells were incubated with FITC-labeled methioninase-annexin V or cytosine deaminase-annexin V. **Figure 4.5** shows a light microscopy image (left) of MDA-MB-231 cells and a fluorescence microscopy image (right) of cytosine deaminase-annexin V bound to the cell surface. As hypothesized, the fusion protein remains on the cell surface after binding to exposed PS on the surface. Similar experiments with endothelial cells showed fluorescence only at the cell surface when they were 70-80% confluent, but no fluorescence was observed when endothelial cells were 100% confluent. This indicates binding of the fusion proteins and thus no expression of PS on the surface of the cells.

The stability of both fusion proteins binding to the cell surface was determined

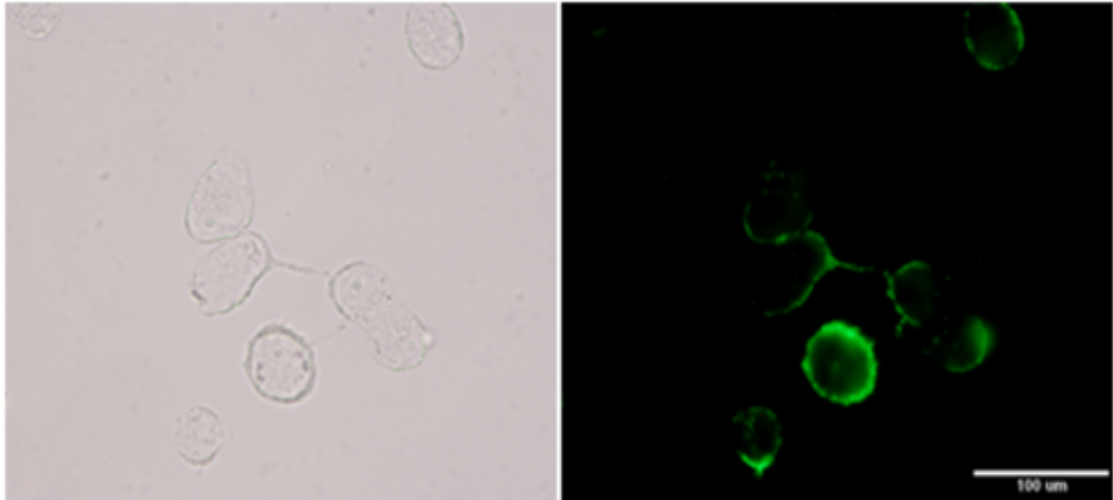


Figure 4.5. Visualization of fluorescent cytosine deaminase-annexin V binding to MDA-MB-231 breast cancer cells. Cells were seeded onto a cover glass and allowed to adhere. Cytosine deaminase-annexin V labeled with FITC was added, allowed to bind for 2 h, and washed to remove unbound fusion protein. Corresponding light (left) and fluorescence (right) images were acquired with a 40X objective to verify binding to the cell surface. The bar represents 100 μm .

and used to design cytotoxicity experiments. Fusion protein bound per cell was studied over 3 days for the three cell lines by measuring the absorbance at 450 nm, determined by the binding assay, and dividing by the fluorescence at 590 nm, determined by the Alamar Blue assay. **Figure 4.6** indicates that binding methioninase-annexin V declined over 3 days for all three cell lines, with the MDA-MB-231 cancer cells showing the most rapid decline; however, the fusion protein was still present at day 3 for all three cell lines. Similar results were obtained for the cytosine deaminase-annexin V fusion protein (see Appendix A). Cell viability, as measured by the Alamar Blue assay, was found to be linearly proportional to the number of cells.

Cytotoxicity of Methioninase-Annexin V + Selenomethionine *In Vitro*

The ability of the enzyme prodrug system to eliminate human endothelial cells and breast cancer cells was evaluated using a saturating concentration (100 nM) of methioninase-annexin V, followed by concentrations of selenomethionine ranging from 0 to 1000 μ M (**Figures 4.7, 4.8, 4.9**). The methionine concentration in the medium was set at a level (1000 μ M) that would not lead to a significant decrease in cell viability because of methionine depletion with methioninase-annexin V present. Each of the cell lines metabolized the Alamar Blue reagent to produce a fluorescence that was measured to quantify total cell viability. The fluorescence data from the Alamar Blue assay was expressed as a percentage of the fluorescence for the cells with no methioninase-annexin V and 0 μ M selenomethionine (control). Cells that were treated with different selenomethionine concentrations but no methioninase-annexin V were compared to the control on the same day, whereas cells that had methioninase-annexin V were compared to cells with the same selenomethionine concentration but no methioninase-annexin V

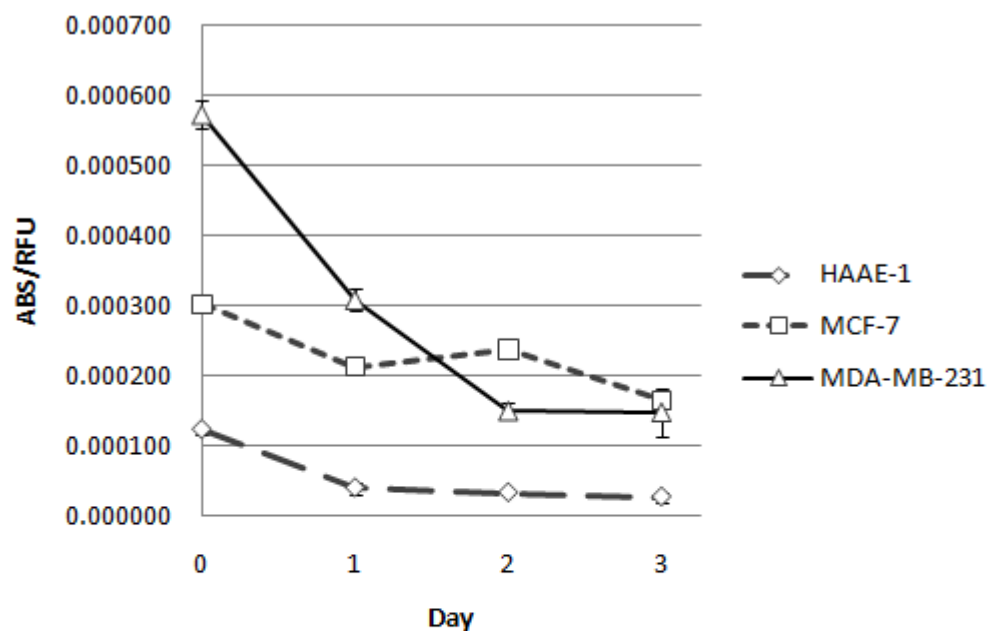


Figure 4.6. Methioninase-annexin V fusion protein binding stability. The Alamar Blue assay for cell viability was performed each day, followed by the binding assay to determine the duration of binding of the fusion protein to exposed PS on the surface of each cell line. ABS/RFU is the absorbance at 450 nm, determined by the binding assay, divided by the relative fluorescence units at 590 nm, determined by the Alamar Blue assay. Data are presented as mean \pm SE (n = 3).

on the same day.

The cytotoxicity results for the endothelial cells are shown in **Figure 4.7**. Treatment with methioninase-annexin V gave significant cell killing for 500 and 1000 μM selenomethionine on days 1–3 ($p < 0.001$). With no methioninase-annexin V present, significant cell cytotoxicity was not observed at the levels of selenomethionine tested.

Cytotoxicity results for the two breast cancer cell lines are shown in **Figure 4.8 and 4.9**. For MCF-7 cells with FP present, there was significant killing at days 2 and 3 with 50–1000 μM SeMet (**Figure 4.8**, $p < 0.001$). Cell killing without FP present was not significant on day 3 until the SeMet concentration reached 1000 μM . MDA-MB-231 cells showed a greater sensitivity to the SeMet than MCF-7 and endothelial cells (**Figure 4.9**); significant cell cytotoxicity was observed with the FP present on days 1–3 with 10–1000 μM SeMet ($p < 0.001$). Even without the addition of the SeMet, binding of the FP alone produced significant cell killing. With no FP present, cell killing did not occur until the SeMet level was 1000 μM and was relatively small and not statistically significant ($p < 0.001$).

In an attempt to remove what was thought to be methionine depletion-related cell death with methioninase-annexin V and 0 μM selenomethionine, an experiment was done adding up to 20,000 μM methionine for MDA-MB-231 cells. A steady decline in cell viability was observed as the level of methionine increased for the 2 days of the experiment after the addition of the extra methionine (**Figure 4.10**). Methionine toxicity is believed to be contributing to the cell death, but has not been confirmed.

The effectiveness of the enzyme in the methioninase-annexin V during the test

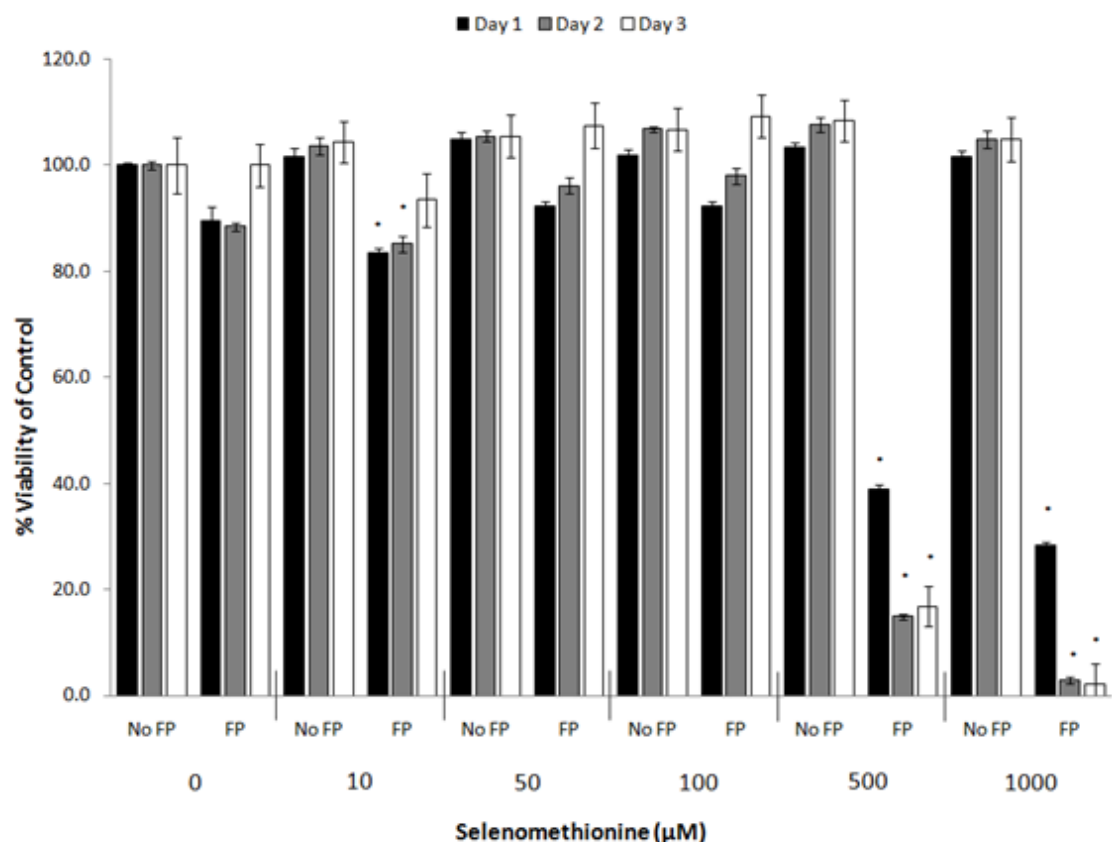


Figure 4.7. Effect of selenomethionine conversion to methylselenol on HAAE-1 endothelial cells. Cells were grown in medium adjusted to 1000 μM of L-methionine. Cell viability was assessed using the Alamar Blue assay for cell viability and normalized to the control (i.e. no methioninase-annexin V and no selenomethionine). A one-way ANOVA was performed for statistical analysis. Cells treated with different selenomethionine concentrations but with no methioninase-annexin V were compared to the control on the same day, and statistical significance was denoted by # ($p < 0.001$). Cells treated with methioninase-annexin V were compared to cells with no methioninase-annexin V on the same day at the same selenomethionine concentration, and statistical significance was denoted by * ($p < 0.001$). Data are presented as mean \pm SE ($n = 3$).

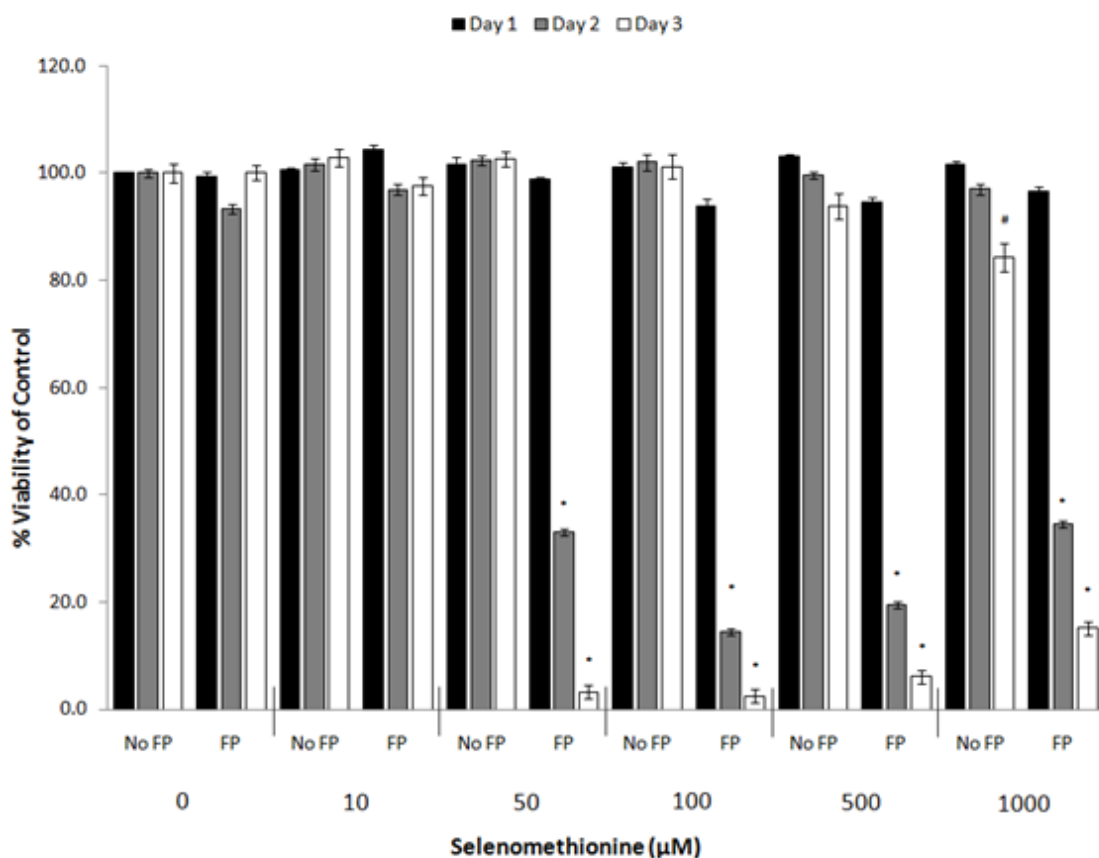


Figure 4.8. Effect of selenomethionine conversion to methylselenol on MCF-7 breast cancer cells. Cells were grown in medium adjusted to 1000 μM of L-methionine. Cell viability was assessed using the Alamar Blue assay for cell viability and normalized to the control (i.e. no methioninase-annexin V and no selenomethionine). A one-way ANOVA was performed for statistical analysis. Cells treated with different selenomethionine concentrations but with no methioninase-annexin V were compared to the control on the same day, and statistical significance was denoted by # ($p < 0.001$). Cells treated with methioninase-annexin V were compared to cells with no methioninase-annexin V on the same day at the same selenomethionine concentration, and statistical significance was denoted by * ($p < 0.001$). Data are presented as mean \pm SE ($n = 3$).

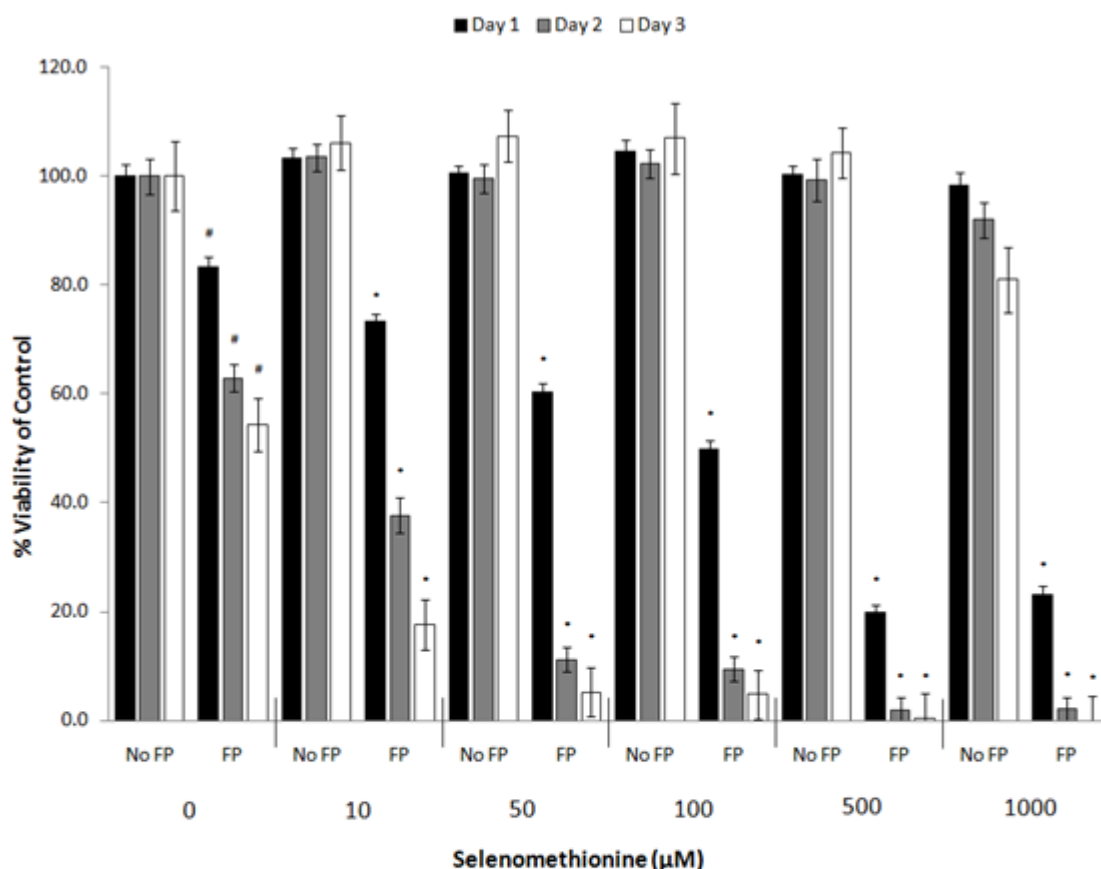


Figure 4.9. Effect of selenomethionine conversion to methylselenol on MDA-MB-231 breast cancer cells. Cells were grown in medium adjusted to 1000 µM of L-methionine. Cell viability was assessed using the Alamar Blue assay for cell viability and normalized to the control (i.e. no methioninase-annexin V and no selenomethionine). A one-way ANOVA was performed for statistical analysis. Cells treated with different selenomethionine concentrations but with no methioninase-annexin V were compared to the control on the same day, and statistical significance was denoted by # ($p < 0.001$). Cells treated with methioninase-annexin V were compared to cells with no methioninase-annexin V on the same day at the same selenomethionine concentration, and statistical significance was denoted by * ($p < 0.001$). Data are presented as mean \pm SE ($n = 3$).

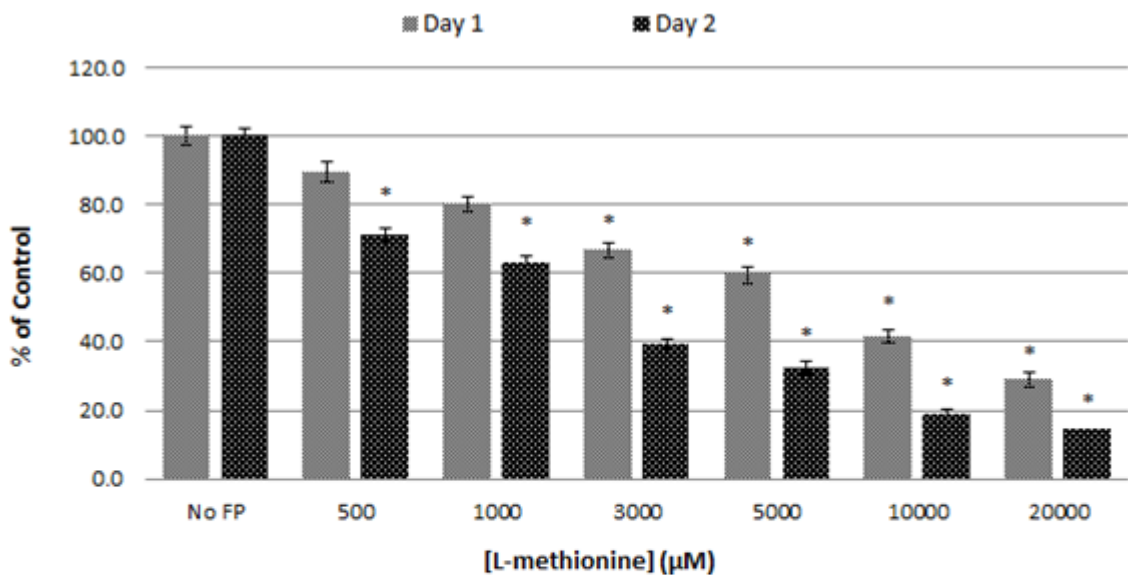


Figure 4.10. Addition of methionine to eliminate MDA-MB-231 breast cancer cell death from methionine-depletion effects. Cells were grown in medium increasing amounts of L-methionine. Cell viability was assessed using the Alamar Blue assay for cell viability and normalized to the control (i.e. no methioninase-annexin V and no selenomethionine). A one-way ANOVA was performed for statistical analysis. Cells treated with extra methionine were compared to cells grown in Lebovitz's L-15 medium that received no fusion protein, and statistical significance was denoted by * ($p < 0.001$). Data are presented as mean \pm SE ($n = 3$).

period is reinforced by the cytotoxicity data for the endothelial cells and breast cancer cell lines (**Figures 4.7, 4.8, and 4.9**) for the selenomethionine concentrations at which there was a statistically significant decline in cell viability compared to the same selenomethionine concentrations with no methioninase-annexin V present on the same day (indicated by a *); for this data there was in almost every case a decline in cell viability from days 1 to 2 and from days 2 to 3. The medium for the cells was changed at days 1 and 2, meaning the enzyme would have to produce additional methylselenol for more cells to be killed; if additional methylselenol were not produced, then no methylselenol would be present (since the medium was changed), and additional cell killing would likely not occur.

In the enzyme prodrug test of cytotoxicity for the endothelial cells, which are the primary target in the tumor for this enzyme prodrug therapy, the cytotoxic effect was evident after only one day of treatment at 500 μM selenomethionine. At either 500 μM or 1000 μM selenomethionine, there was no effect on endothelial cell viability with no methioninase-annexin V present; this indicates that endothelial cells in the normal vasculature, which will not bind to the methioninase-annexin V (since PS is not externalized), will not be affected by these concentrations of selenomethionine. At selenomethionine concentrations well below 500 μM , however, the cancer cells will be killed by toxic methylselenol being carried across the artery wall by fluid permeation; the effect of methylselenol on normal cells outside of the tumor is expected to be minimal or none because it will be greatly diluted by the bloodstream before it reaches the normal cells. MDA-MB-231 breast cancer cells were found to be the more sensitive to the enzyme prodrug treatment than MCF-7 breast cancer cells, even producing killing

when the methioninase-annexin V was bound but no selenomethionine prodrug was added.

We have not found evidence that the sensitivity of the three cell lines to the enzyme prodrug treatment is dependent on the degree of exposure of PS on the cell surface. The saturation A_{450} values measured in the methioninase-annexin V binding assay, which are a measure of the amount of methioninase-annexin V bound to PS, do not correlate with the sensitivity to the enzyme prodrug treatment indicated. Therefore, other cell properties besides the degree of PS exposure are contributing to the sensitivity to the effect of methylselenol.

Cytotoxicity of Cytosine Deaminase-Annexin V + 5-Fluorocytosine *In Vitro*

Cell viability was determined on days 3, 6, and 9 to demonstrate the cytotoxic effects of 5-FC, with or without cytosine deaminase, against human endothelial cells and breast cancer cells (**Figures 4.11, 4.12, and 4.13**). In addition, treatment with commercially available 5-fluorouracil was performed. The viability data is presented as the percentage of fluorescence produced relative to control samples (no cytosine deaminase-annexin V and 0 μ M 5-fluorocytosine). All of the experimental groups were compared to the control for that day (no cytosine deaminase-annexin V and the same 5-fluorocytosine or 5-fluorouracil concentration). For all three cell lines, no significant cell death was found with 5-fluorocytosine present and cytosine deaminase-annexin V absent, or with 5-fluorocytosine absent but cytosine deaminase-annexin V present.

For the endothelial cells (**Figure 4.11**), there was negligible cell killing in the first 3 days of the experiments; however, significant killing ($p < 0.001$) was observed on

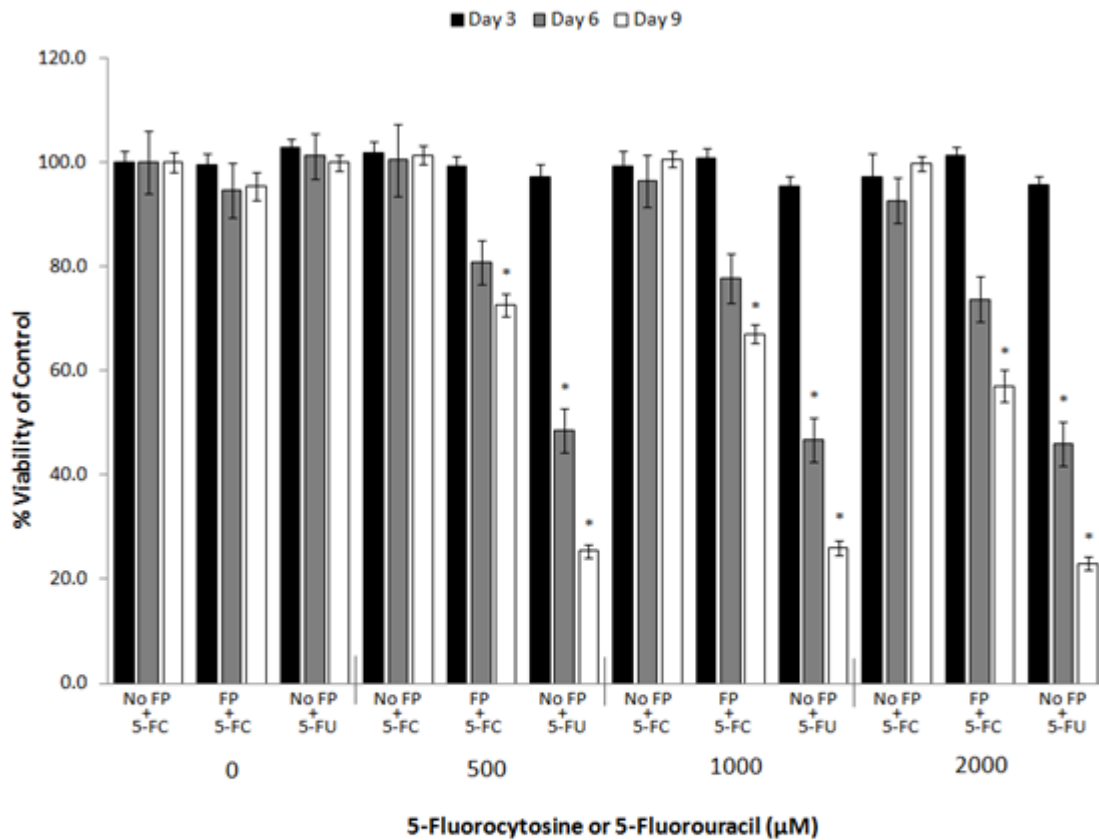


Figure 4.11. Effect of 5-fluorocytosine conversion to 5-fluorouracil on HAAE-1 endothelial cells. Cell viability was assessed using the Alamar Blue assay and normalized to the control (i.e. no cytosine deaminase-annexin V and no 5-fluorocytosine). A one-way ANOVA was performed for statistical analysis. Cells treated with cytosine deaminase-annexin V or cells treated with only 5-fluorouracil were compared to cells with no cytosine deaminase-annexin V on the same day at the same 5-fluorocytosine concentration, and statistical significance was denoted by * ($p < 0.001$). Data are presented as mean \pm SE ($n = 3$).

day 9 for cells with cytosine deaminase-annexin V plus 5-fluorocytosine and on days 6 and 9 for cells with 5-fluorouracil. Killing was observed to be dose-dependent.

The breast cancer cell lines exhibited similar patterns of cell death. Both MCF-7 (**Figure 4.12**) and MDA-MB-231 (**Figure 4.13**) cells receiving the cytosine deaminase-annexin V plus 5-fluorocytosine showed significant cell killing that was dose-dependent, compared to the control group, on days 3, 6, and 9 ($p < 0.001$). By day 9, treatment with the cytosine deaminase-annexin V plus 5-fluorocytosine resulted in less than 10% viability at 500 μM 5-fluorocytosine for MCF-7 cells and at 1000 μM 5-fluorocytosine for MDA-MB-231 cells. As for the endothelial cells, the combination of 5-fluorocytosine and the cytosine deaminase-annexin V gave less cytotoxicity than with 5-fluorouracil directly at the same 5-fluorocytosine concentration and incubation time.

Comparison between the efficacy of the enzyme prodrug treatment and 5-fluorouracil at the same concentration as 5-fluorocytosine resulted in higher toxicity with 5-fluorouracil alone (**Figures 4.11, 4.12, 4.13**). This finding is consistent with other reports comparing drug and prodrug toxicity [92, 107].

Pharmacokinetics of Methioninase-Annexin V in Mice

The relatively small size of the methioninase-annexin V fusion protein (~316 kDa) allows for rapid diffusion into the bloodstream following i.p. injection. A pharmacokinetics test was done by injecting NU/J mice ($n = 4/\text{dosage}/\text{time point}$) with 1 and 10 mg/kg of biotinylated methioninase-annexin V. After 1, 4, 8, and 24 h post-injection, a blood sample was extracted from each mouse by cardiac draw. Mice that did not receive methioninase-annexin V were used as the control. The serum was collected and flash frozen for analysis after all samples were taken.

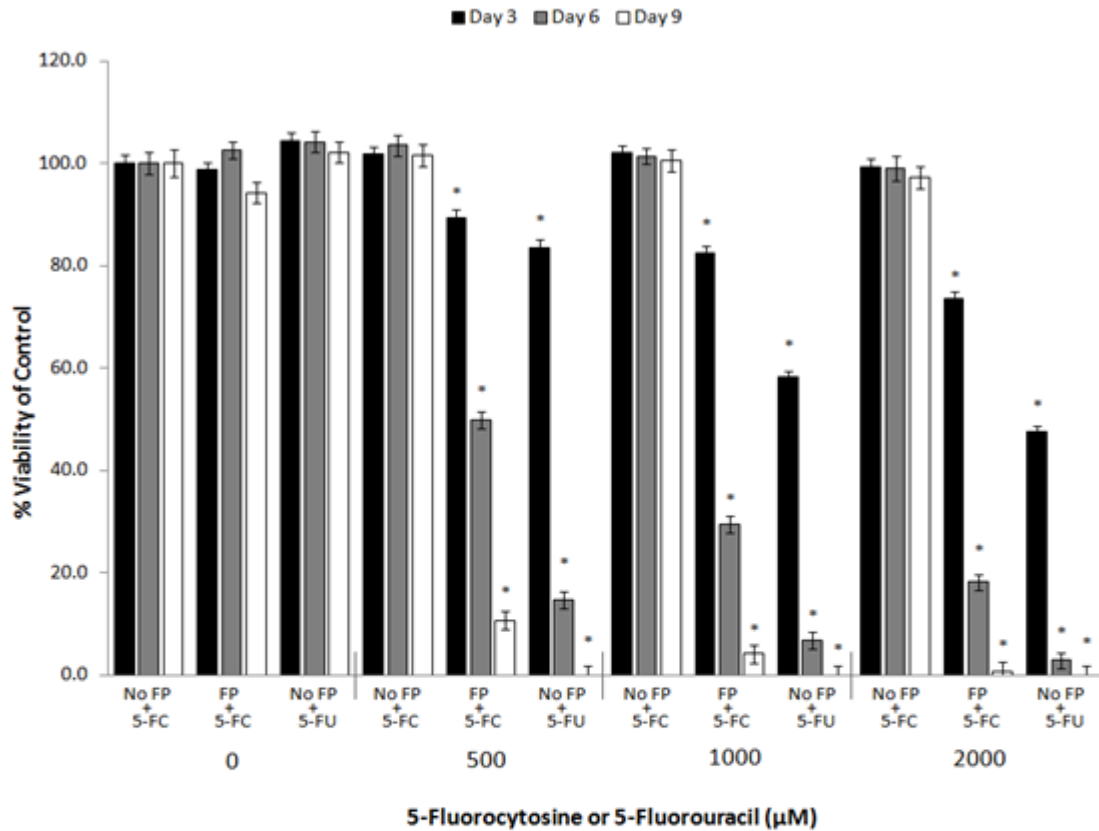


Figure 4.12. Effect of 5-fluorocytosine conversion to 5-fluorouracil on MCF-7 breast cancer cells. Cell viability was assessed using the Alamar Blue assay and normalized to the control (i.e. no cytosine deaminase-annexin V and no 5-fluorocytosine). A one-way ANOVA was performed for statistical analysis. Cells treated with cytosine deaminase-annexin V or cells treated with only 5-fluorouracil were compared to cells with no cytosine deaminase-annexin V on the same day at the same 5-fluorocytosine concentration, and statistical significance was denoted by * ($p < 0.001$). Data are presented as mean \pm SE ($n = 3$).

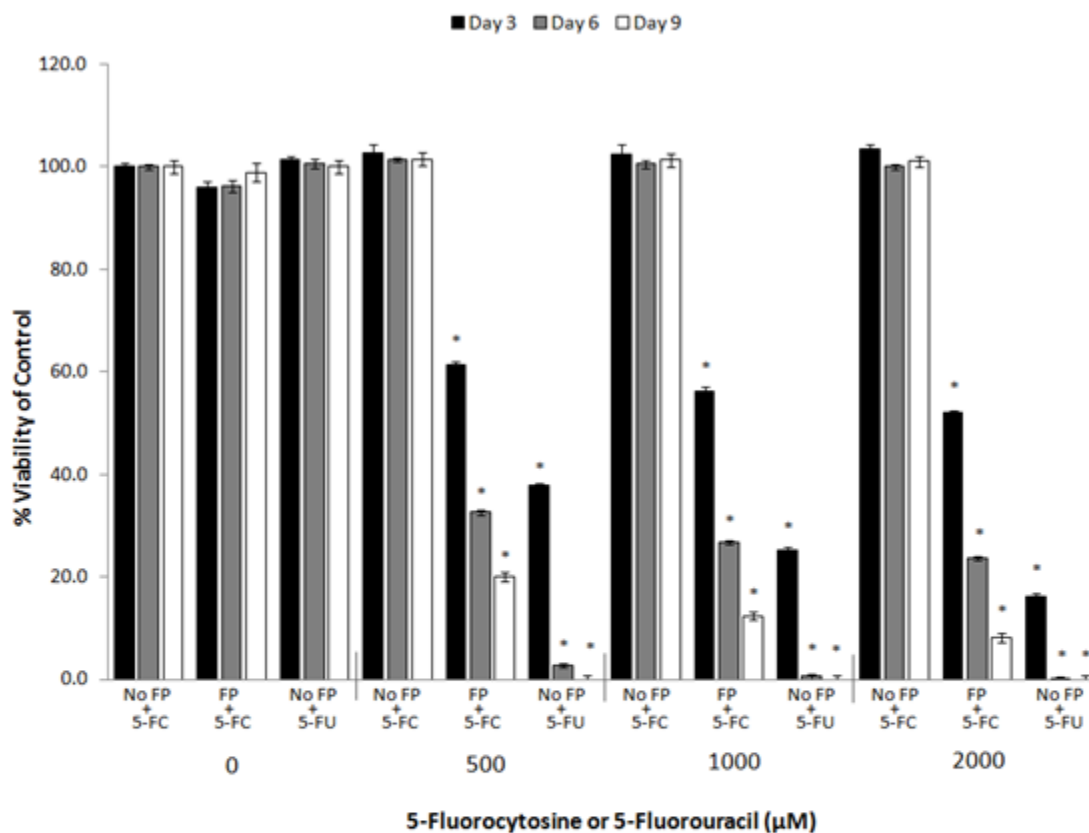


Figure 4.13. Effect of 5-fluorocytosine conversion to 5-fluorouracil on MDA-MB-231 breast cancer cells. Cell viability was assessed using the Alamar Blue assay and normalized to the control (i.e. no cytosine deaminase-annexin V and no 5-fluorocytosine). A one-way ANOVA was performed for statistical analysis. Cells treated with cytosine deaminase-annexin V or cells treated with only 5-fluorouracil were compared to cells with no cytosine deaminase-annexin V on the same day at the same 5-fluorocytosine concentration, and statistical significance was denoted by * ($p < 0.001$). Data are presented as mean \pm SE ($n = 3$).

An ELISA was used to determine the time required for clearance from the bloodstream. Serum samples were incubated for 1 h at 37°C in streptavidin-coated plates. A rabbit polyclonal antibody against annexin V was added to bind methioninase-annexin V and incubated for 1 h at 37°C. The amount of fusion protein binding was then determined by adding an anti-rabbit IgG secondary antibody conjugated to horseradish peroxidase (1 h at 37°C) and developing with the chromogenic substrate OPD (**Figure 4.14**). Both 1 and 10 mg/kg doses were detected in the bloodstream after 1 h of circulation, with the concentrations falling to near undetectable levels at 4 h and complete clearance by 8 h. The results of this experiment were used to design the experimental design of treating mice with MDA-MB-231 breast tumors using methioninase-annexin V and selenomethionine.

Selenomethionine Toxicity in Mice

Methylselenol is known to be 200 times more toxic to various cancer cells than selenomethionine [36]. To determine a selenomethionine dosage level that can be used for the treatment of MDA-MB-231 breast tumors, NU/J mice (n = 6/dosage level) were injected i.p. with selenomethionine ranging up to 60 mg/kg every 24 h for three consecutive days. After only one dose, all mice receiving 60 mg/kg were found dead, indicating severe toxicity. At 24 mg/kg, only one mouse survived the injections but appeared sick, had noticeable behavioral changes, and lost significant weight. However, all mice receiving either 6 or 12 mg/kg selenomethionine survived a week of post-injection observation and did not show any signs of changed behavior or movement, with only minimal weight-loss that was recovered after the injections ended.

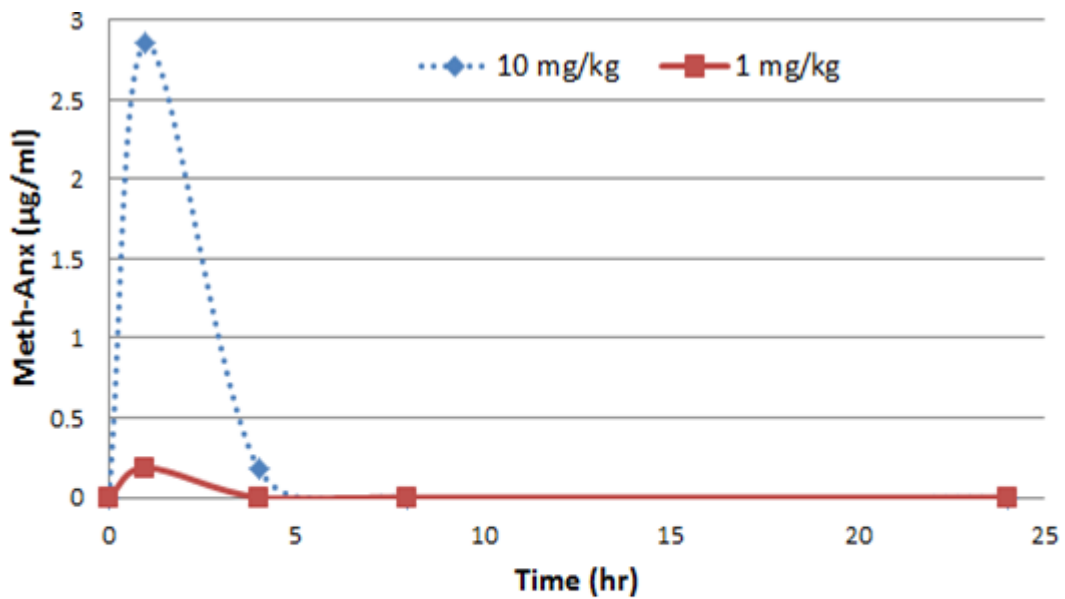


Figure 4.14. Clearance time of methioninase-annexin V in the bloodstream of nude mice. Methioninase-annexin V was injected i.p. at 1 and 10 mg/kg. An ELISA was used to detect biotinylated methioninase-annexin V in mouse serum, followed by an antibody against annexin V. A secondary antibody IgG conjugated to peroxidase was with chromogenic substrate to develop the results. Data are presented as mean \pm SE (n = 4).

Detection of Exposed Phosphatidylserine in Tumor Vasculature in Mice

Annexin V is known to bind to exposed PS on the surface of endothelial cells and cancer cells. This was demonstrated by Ran et al. [25] in mice bearing MDA-MB-231 xenografts using biotinylated annexin V. Similarly, SCID mice bearing MDA-MB-231 tumors were injected i.p. with 10 mg/kg of biotinylated methioninase-annexin V. At 1 h post-injection, their circulation was perfused with heparinized saline with calcium and by glutaraldehyde. Tumors were removed and stored in sucrose in preparation for cryosectioning at OMRF. Streptavidin-HRP was used to bind to any biotinylated methioninase-annexin V, and bound streptavidin-HRP was developed with DAB substrate to produce a dark brown image. **Figure 4.15** shows a stained section of the MDA-MB-231 tumor. The presence of activated DAB is shown on the perimeter of a blood vessel within the tumor tissue. This experiment was done to demonstrate annexin V has retained its ability to bind to PS *in vivo* as part of a fusion protein and allows the presentation of methioninase at the blood vessel surface. This allows for the rapid conversion of selenomethionine upon intravenous administration into toxic methylselenol. The methylselenol will act on the endothelial cells and also penetrate into the tumor parenchyma via permeation and diffusion.

Biodistribution of Methioninase-Annexin V in Mice

Methioninase-annexin V is expected to bind to PS that is exposed by tumor vascular endothelial cells and tumor cells. To detect the location of methioninase-annexin V after i.p. injection, three mice with MDA-MB-231 tumors were injected with the fusion protein labeled with DyLight 680 red fluorescent dye. After 1, 12, and 24 h post-injection, the mice were imaged using the IVIS Spectrum small animal imaging



Figure 4.15. Detection of methioninase-annexin V bound to exposed PS on the surface of a blood vessel in an MDA-MB-231 tumor grown in SCID mice. Biotinylated fusion protein was injection i.p.. Cryosections were stained using streptavidin-HRP and developed with DAB to prove methioninase-annexin V binding. Counterstaining was done with hematoxylin.

system looking for the GFP signal from the tumor cells and the red signal from methioninase-annexin V. After the final images were acquired, the tumor, heart, lungs, liver, kidneys, and spleen were removed and imaged *ex vivo* to detect the DyLight 680 signal.

Figure 4.16 shows the three mice at 1 h (A), 12 h (B), and 24 h (C) post-injection. In **Figure 4.16A**, it appears that the fusion protein has not diffused away from the site of injection in one mouse, but the other mice show a systemic signal indicating the methioninase-annexin V made it into the bloodstream. **Figure 4.16B** shows one mouse has a very weak signal signifying near complete clearance of the fusion protein, while the others show a vibrant red signal near the tumor region, near the bladder, and in the tail. At 24 h, all mice once again have a bright signal near the tumor region and a signal near the bladder (**Figure 4.16C**). The red signal coming from above the tumor appeared to represent the spleen, however, after resection of the organs, no DyLight 680 signal was observed from any of the tissues collected. It is possible that the injected protein contained free DyLight 680 even though an extensive dialysis was done with two buffer changes following protein labeling. The GFP signal was easily detectable *ex vivo* and only coming from the tumor sample.

MDA-MB-231 Breast Tumor Treatment with Methioninase-Annexin V Plus Selenomethionine in Mice

NU/J mice were initially used to test the efficacy of the methioninase-annexin V enzyme prodrug system. Tumor formation of MDA-MB-231 cells expressing GFP appeared to be normal, indicating treatment needed to begin. The experimental treatment design consisted of three cycles, with each cycle beginning with an injection

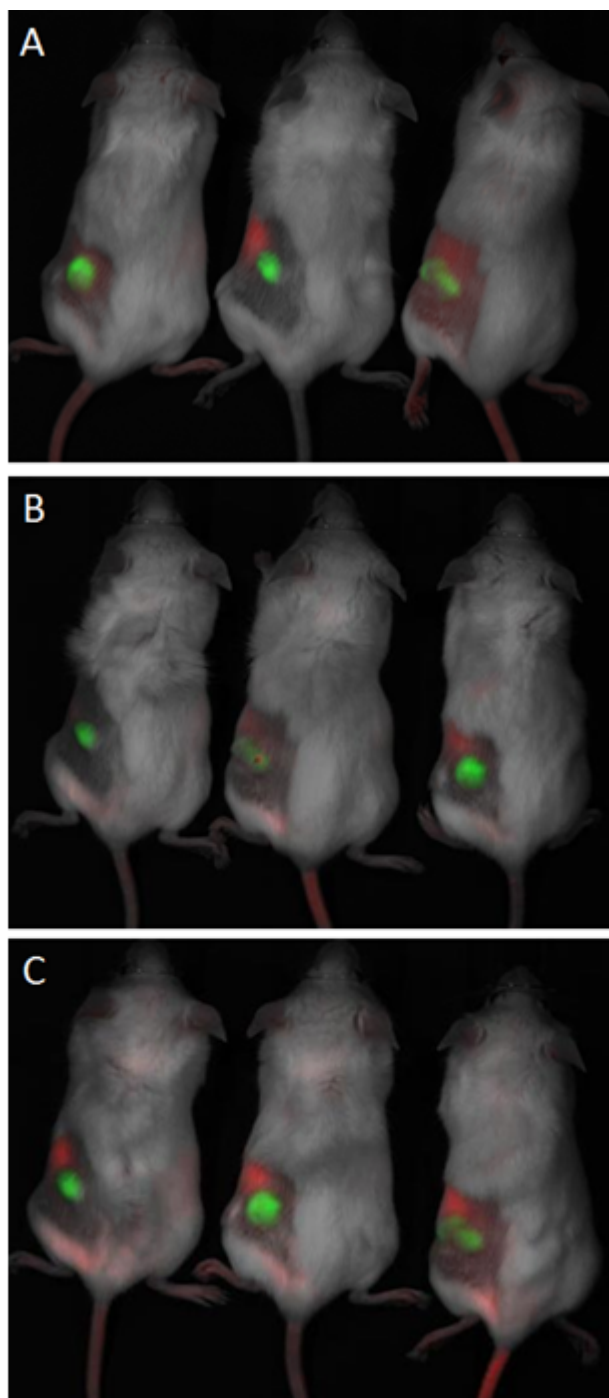


Figure 4.16. Biodistribution of methioninase-annexin V. Mice were injected with methioninase-annexin V labeled with DyLight 680 fluorescent dye. At 1 h (A), 12 h (B), and 24 h (C) post-injection, images were taken to detect the fusion protein. Red signal is DyLight 680 and green signal is GFP from the MDA-MB-231 cancer cells.

of methioninase-annexin V (10 mg/kg), followed by a 2-week observation period. Based on the pharmacokinetics data, a minimum of 8 h was allowed for unbound methioninase-annexin V clearance, followed by three consecutive injections of selenomethionine (10 mg/kg) every 24 h. **Figure 4.17** shows the results of the treatment and observation of period of the NU/J mice. Noticeably, the tumors in the treatment group steadily declined in volume; however, the tumors in the control groups only maintained similar sizes but did not grow, except for tumors in the selenomethionine group that grew after 67 days post-inoculation. Two mice in the selenomethionine group and one in the treatment group died during the treatment period. For each methioninase-annexin V and selenomethionine injection, each group was weighed. The average group weight was used to determine the injection dose for those mice, presumably the reason for the dead mice, since some of the mice actually received more than 10 mg/kg selenomethionine. The stagnant growth of the tumors was hypothesized to be because the cells inoculated had been passaged too long and had lost their tumorigenicity. New MDA- MB-231 cells expressing GFP were purchased to repeat the study. The new cells produced inconsistent formation in the NU/J mice as only 4 of 26 mice developed stable tumors. It is unclear why the tumors were not forming as expected.

Before more treatment experiments were done, it was necessary to find a mouse model that would allow for consistent, repeatable MDA-MB-231 tumor development. In addition to NU/J, SCID and athymic nude (NU/NU) mice were tested (n = 3). As shown in **Figure 4.18A**, NU/J and athymic nude mice did not form stable tumors; however, all three SCID mice developed large tumors in 25 days. IVIS Spectrum

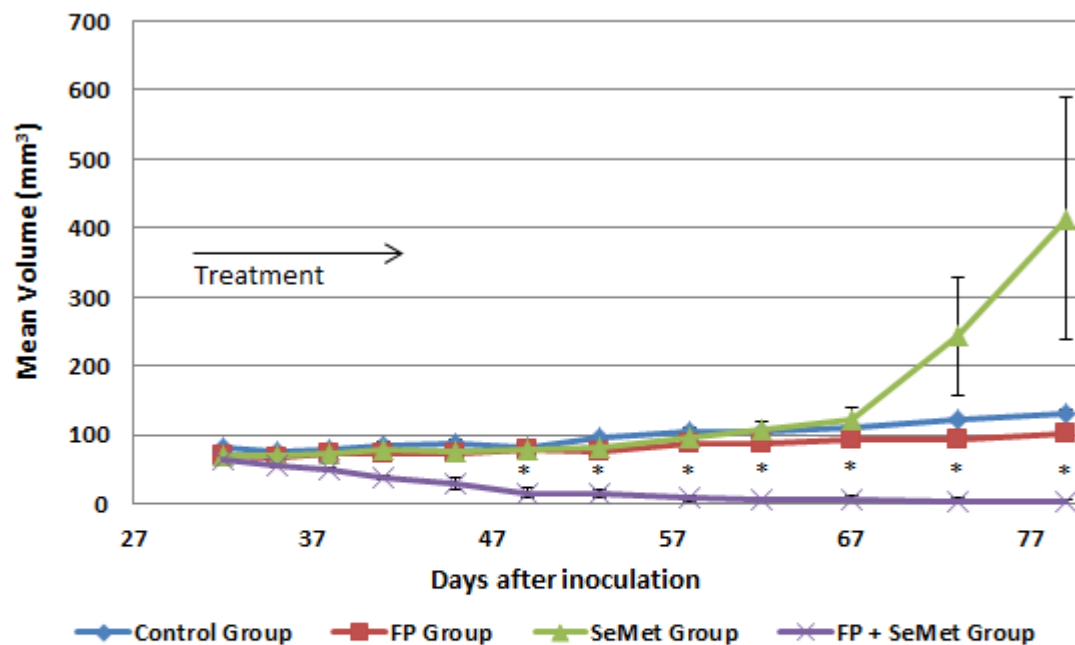


Figure 4.17. Treatment of MDA-MB-231 breast tumors in NU/J mice. Treatment consisted of three consecutive cycles, where each cycle was as follows: 10 mg/kg methioninase-annexin V injected on day 0 and 10 mg/kg selenomethionine injected on days 1, 2, and 3. Tumor volume data are presented as mean \pm SE (n = 3-5) with statistical significance denoted by * ($p < 0.001$)

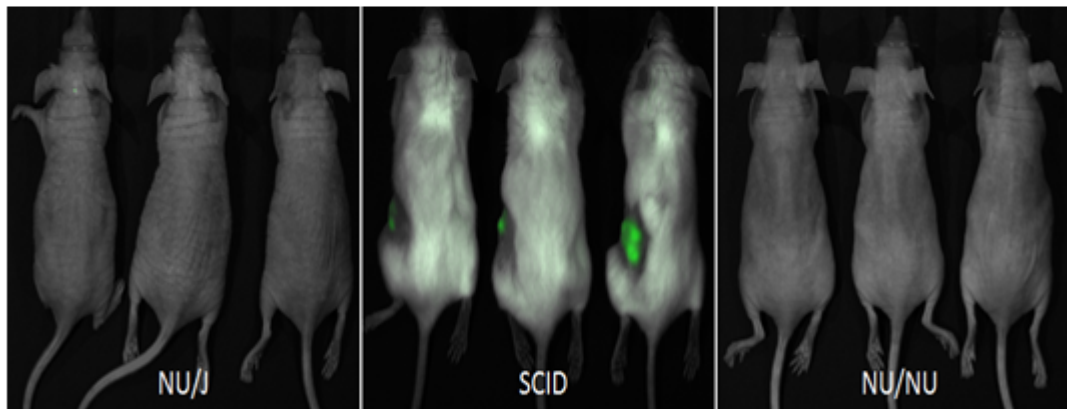
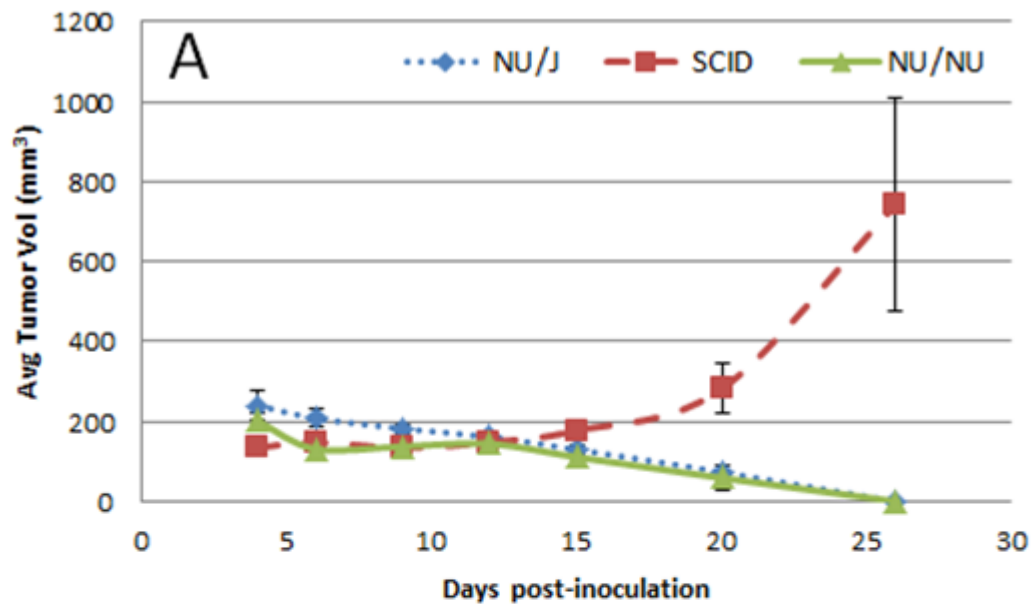


Figure 4.18. MDA-MB-231 tumor growth in various immunodeficient mouse models. A. Tumor volume data for NU/J, SCID, and NU/NU mice bearing MDA-MB-231 breast tumor xenografts. Data are presented as mean \pm SE ($n = 3$) with statistical significance denoted by * ($p < 0.001$). B. Fluorescence images of NU/J, SCID, and NU/NU mice taken with the IVIS Spectrum small imaging system showing GFP signal from MDA-MB-231 cells.

images taken of the SCID mice showed the presence of GFP signal, confirming the MDA-MB-231 cells were alive and growing at day 25 (**Figure 4.18B**), while NU/J and NU/NU mice showed no GFP. Based on this result, SCID mice were used for the remaining tests *in vivo*.

Pharmacokinetics and selenomethionine dosage experiments were initially done using NU/J mice and needed to be confirmed in SCID mice. The experimental design calls for the injection of methioninase-annexin V in the afternoon and selenomethionine the following mornings, an average of 14 h later. The ELISA assay was repeated using SCID mouse blood samples (n = 3) taken 14 h after the injection of biotinylated methioninase-annexin V. No difference in signal was observed for the 14 h sample compared to a blank sample. The prodrug toxicity study was done with three SCID receiving 10 mg/kg of selenomethionine for three consecutive days, 24 h apart. The mice tolerated the selenomethionine with no behavioral changes.

For the enzyme prodrug study using SCID mice (n = 7 per group), the MDA-MB-231 cells were injected, and all tumors developed as expected. When the tumors began to increase in size, the IVIS imaging system was used, and the GFP signal was documented for all mice, indicating living MDA-MB-231 cells. The treatment was done as described above with mice on a normal chow diet, and the results are presented in **Figure 4.19**. The tumors in mice receiving methioninase-annexin V and selenomethionine reduced in size throughout the treatment period, while mice receiving no treatment, methioninase-annexin V, or selenomethionine only steadily increased. One mouse in the selenomethionine group died during the treatment period. All mice in the treatment group tolerated the selenomethionine, presumably because the

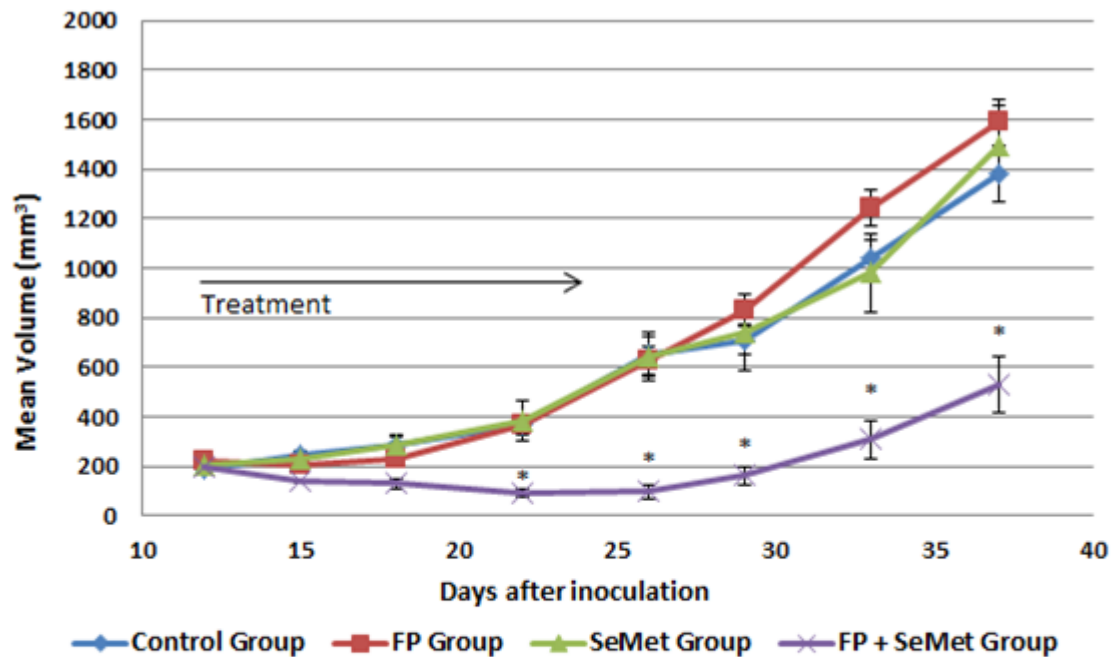


Figure 4.19. Enzyme prodrug treatment of MDA-MB-231 breast tumors in SCID mice. Treatment consisted of three consecutive cycles, where each cycle was as follows: 10 mg/kg methioninase-annexin V injected on day 0 and 10 mg/kg selenomethionine injected on days 1, 2, and 3. Tumor volume data are presented as mean \pm SE (n = 7) with statistical significance compared to the control group denoted by * (p < 0.001).

selenomethionine was converted to methylselenol and did not build up in tissue. During the 2-week observation period, mice in the treatment group showed tumor regrowth, indicating that all the cancer cells were not killed. Still, tumors in the treated group were only a third of the size of the control groups. Histological analysis of three mice per control group and all seven treated mice revealed there were no metastatic lesions found in lungs or liver of any of the mice (see Appendix A for the complete pathology report).

From the data in **Figure 4.19**, it is apparent that the enzyme prodrug treatment did not kill all of the tumor cells. This could have occurred because the period of hypoxia was not long enough or because the duration of exposure to the methylselenol generated was not long enough. Also, some tumor cells still alive at the end of the 3-day selenomethionine treatment could have regrown during the day of treatment with the fusion protein, when no methylselenol is being produced.

Methionine dependence in cancer cells has been well-documented [32, 108]. The methioninase enzyme has the ability to convert selenomethionine; additionally, methionine required for protein production and sustained cancer cell proliferation is cleaved. While healthy cells are able to produce methionine for protein synthesis from its precursor homocysteine, cancer cells typically express below normal levels of the enzyme methionine synthase that is responsible for making methionine from homocysteine [33, 34]. To determine the therapeutic potential of the enzyme prodrug therapy with reduced methionine available, a diet containing no methionine replaced the normal mouse chow was used. The experimental design was similar to that above, with methioninase-annexin V fusion protein administered at 10 mg/kg, but the

selenomethionine dosage was cut in half (5 mg/kg). The mice were placed on a methionine-deficient diet supplemented with D,L-homocysteine 24 h prior to the start of treatment. The selenomethionine dosage was reduced for two reasons: 1) to prevent unwanted selenomethionine-related toxicity, and 2) the methionine-deficient diet had previously been shown to cause reversible weight loss in mice [109], as has the selenomethionine in control mice (data not shown).

Figure 4.20 shows the tumor volume curves obtained throughout the treatment and observation period. As expected, the methioninase-annexin V plus selenomethionine treatment resulted in a significant reduction in tumor growth compared to the untreated control. During the treatment period, the size of the tumors in the group of mice receiving the enzyme prodrug treatment increased slightly, and there was regrowth of the tumors after the end of the treatment. When the tumor volumes of the control group required the mice to be sacrificed (tumor weight was ~10% of body weight), the average size of the tumors in the group treated with methioninase-annexin V and selenomethionine was 42% of that in the control group, which is similar to what was found in the study with mice on a normal diet. In addition, although not significant, methioninase-annexin V only showed an effect during the treatment period, but its efficacy did not last after the conclusion of the therapy.

Significant attention has been given to enzyme prodrug systems as potential therapeutic strategies for cancer. As shown in **Figures 4.19 and 4.20**, the combination of methioninase-annexin V and selenomethionine leads to a significant inhibition of tumor growth compared to those untreated. These findings are consistent with other enzyme prodrug systems, which inhibit tumor growth during treatment, but fail to kill

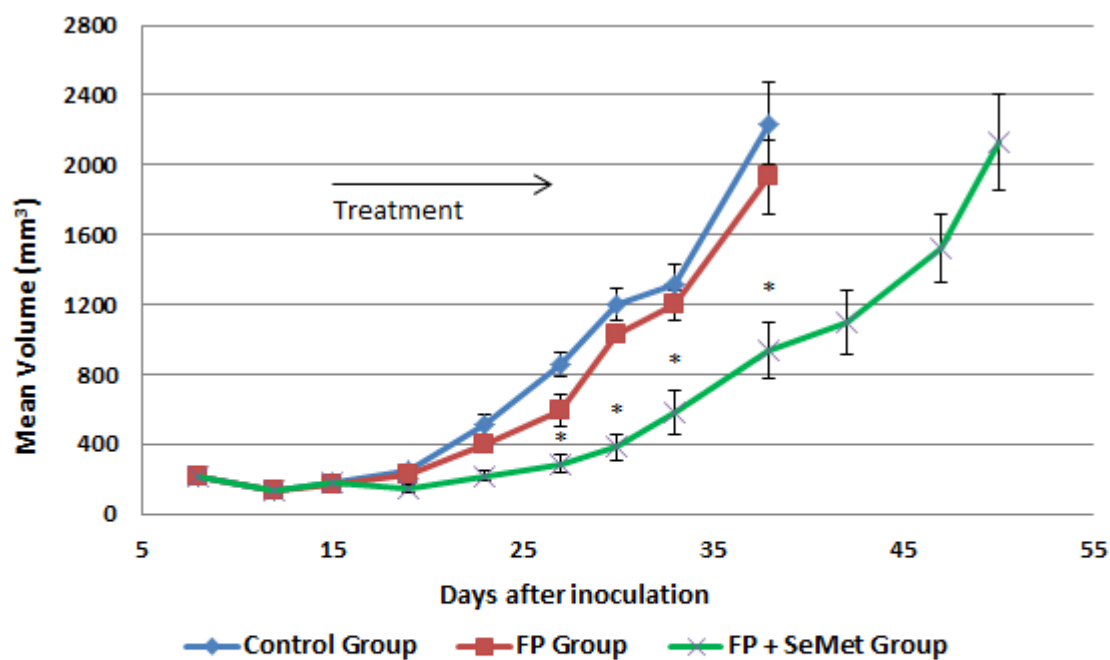


Figure 4.20. Enzyme prodrug treatment of MDA-MB-231 breast tumors in SCID mice on a methionine-deficient diet. Treatment consisted of three consecutive cycles, where each cycle was as follows: 10 mg/kg methioninase-annexin V injected on day 0 and 5 mg/kg selenomethionine injected on days 1, 2, and 3. Tumor volume data are presented as mean \pm SE (n = 7) with statistical significance compared to the control group denoted by * (p < 0.001).

all malignant cells, which results in tumor regrowth. Vrudhula et al. [110] used a monoclonal antibody to target β -lactamase in a lung adenocarcinoma model. A cephalosporin prodrug was used to generate toxic cephalosporin mustard, which was shown to inhibit lung tumor growth by roughly 60%. A different type of mustard drug developed by carboxypeptidase G2 was compared to treatment with 5-fluorouracil and showed complete tumor regression in a colorectal model, but tumor regrowth was eventually observed [111]. Other groups have shown different enzyme prodrug combinations can cause prolonged tumor growth inhibition [112, 113], including a therapy targeting cytosine deaminase to colon cancer with 5-fluorocytosine prodrug [114].

Tumor Blood Flow Interrupted After Methioninase-Annexin V + Selenomethionine Treatment

The methylselenol generated by the conversion of selenomethionine by L-methioninase at the surface of the endothelial cells in the tumor vasculature will cause destruction of these cells, which leads to clotting in the tumor vasculature and a cutoff of the supply of oxygen to the tumor. To test this hypothesis, SCID mice with MDA-MB-231 tumor xenografts underwent the standard three-cycle treatment of methioninase-annexin V (10 mg/kg) and selenomethionine (10 mg/kg). The day after treatment concluded, untreated and treated mice (n = 3) were injected i.p. with DyLight 680 fluorescent dye at 1 mg/kg. The dye was allowed to circulate for 1 h followed by imaging with the IVIS Spectrum system. **Figure 4.21** contains images from untreated (**4.21A**) and treated (**4.21B**) mice, in which the DyLight 680 signal was spectrally unmixed using the IVIS Spectrum's Living Image software. The outline of the GFP

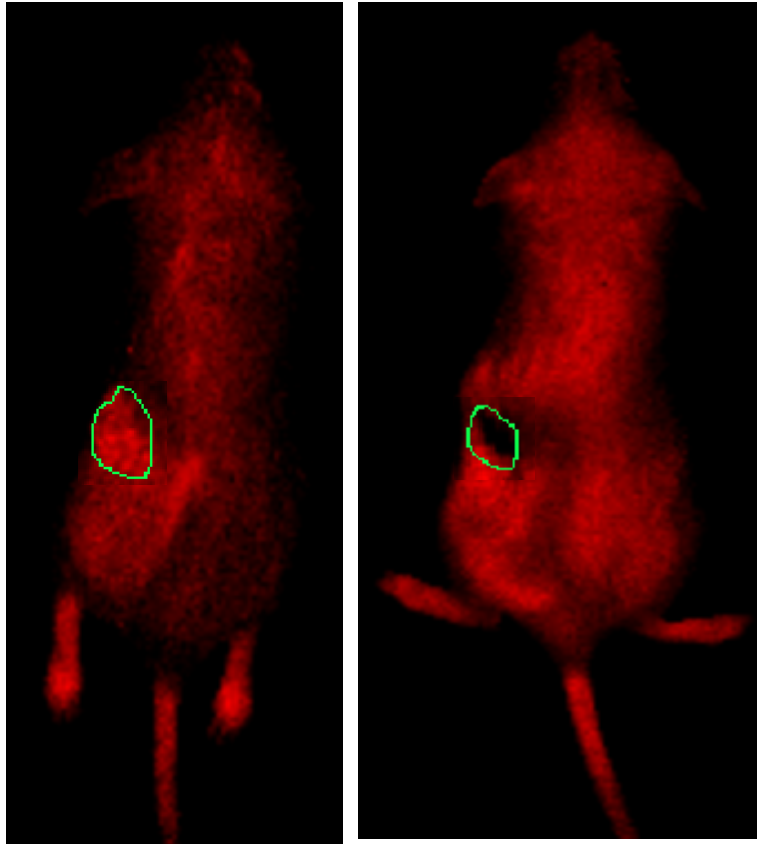


Figure 4.21. Interruption of blood flow through tumor vasculature. Female SCID mice were injected with DyLight 680 red fluorescent dye the day after the completion of the three-cycle enzyme prodrug treatment with methioninase-annexin V and selenomethionine. The outline of the GFP signal showing the living tumor cell perimeter is in green. Mice were either untreated (A) or treated with methioninase-annexin V (B) to compromise tumor vasculature.

signal showing the living tumor cell perimeter is in green on both figures. Untreated mice showed significant red fluorescence in the tumor area, indicating blood flow through the tumor vasculature, while treated mice showed much less red fluorescence, indicating a lack of blood in the tumor region. This suggests that treated mice had compromised tumor vasculature resulting from the production of methylselenol from selenomethionine. The black hole on the left side of the mice in **Figure 4.21B** is the tumor void of blood flow. The area of the untreated tumor was 100% red fluorescence, while that in the treated tumor was 66% fluorescent. Thus, the percentage of the treated tumor tissue receiving blood flow was approximately 66% based on the pictures showing red fluorescence. This result provides significant support of the hypothesis that methioninase-annexin V and selenomethionine are able to selectively destroy tumor vasculature.

SWNT-F3 Internalization Confirmed by Fluorescence and Confocal Microscopy

F3 peptide was commercially synthesized to contain an N-terminal FITC attached to a lysine residue and an extra cysteine residue at the C-terminus. The cysteine was used to react with a maleimide group of a heterobifunctional polyethylene glycol linker to create a stable disulfide bond. The other end of the linker contained a DSPE phospholipid that is used to for attachment to SWNTs suspended in 1% sodium dodecyl sulfate through hydrophobic interaction. Appendix A contains a table with results of numerous SWNT-F3 conjugate preparations. SWNT concentrations approaching 300 mg/L were observed after the conjugation to F3, giving a final yield of nearly 25% of the SWNTs put into the initial suspension. The absorbance spectra of

stable SWNT-F3 conjugate has been described previously in the laboratory [56, 115]. Optimizing the conjugation parameters still needs to be done.

The F3 peptide is known to be a cell-penetrating peptide that binds to surface nucleolin, becomes internalized, and homes to the nuclei of tumor endothelial cells and tumor cells. Following the attachment of F3 to SWNTs, it is believed that the F3 homing activity will be retained. Human endothelial cells, used to confirm the internalization ability, were seed onto chambered microscope slides, allowed to adhere for 24 h, and incubated with SWNT-F3 conjugate for 12 h at 37°C. The cells were washed, stained with CellMask deep red plasma membrane stain, and fixed to the slides with formalin. Fluorescence from FITC and CellMask were verified to be present using a Nikon Eclipse E800 fluorescence microscope. To prove the SWNT-F3 conjugate was internalized, the same slides were visualized using an Olympus Fluoview laser scanning microscope. **Figure 4.22** shows the fluorescent signals obtained from a scan at the center of the cell layer. Each cell in the image emitted a green signal indicating presence of the F3 peptide. Previous work in the laboratory proved that SWNTs were also present inside the cells with a Raman spectra [56, 115].

Cell Death Induced by SWNT-F3 Incubation and Near-Infrared Light

Dividing MCF-7 and 4T1 cancer cells were grown in 24-well plates and incubated with 60 mg/L of SWNT-F3 conjugate containing different length nanotubes for varying time up to 24 h. The cells were washed and subjected to photothermal treatment using a Diodevet-50 980 nm laser. Previously, MCF-7 cells were shown to handle an energy density of 350 J/cm² [56, 115], so that energy density was used for the tests. Cell viability results for the test with MCF-7 cells were determined using the

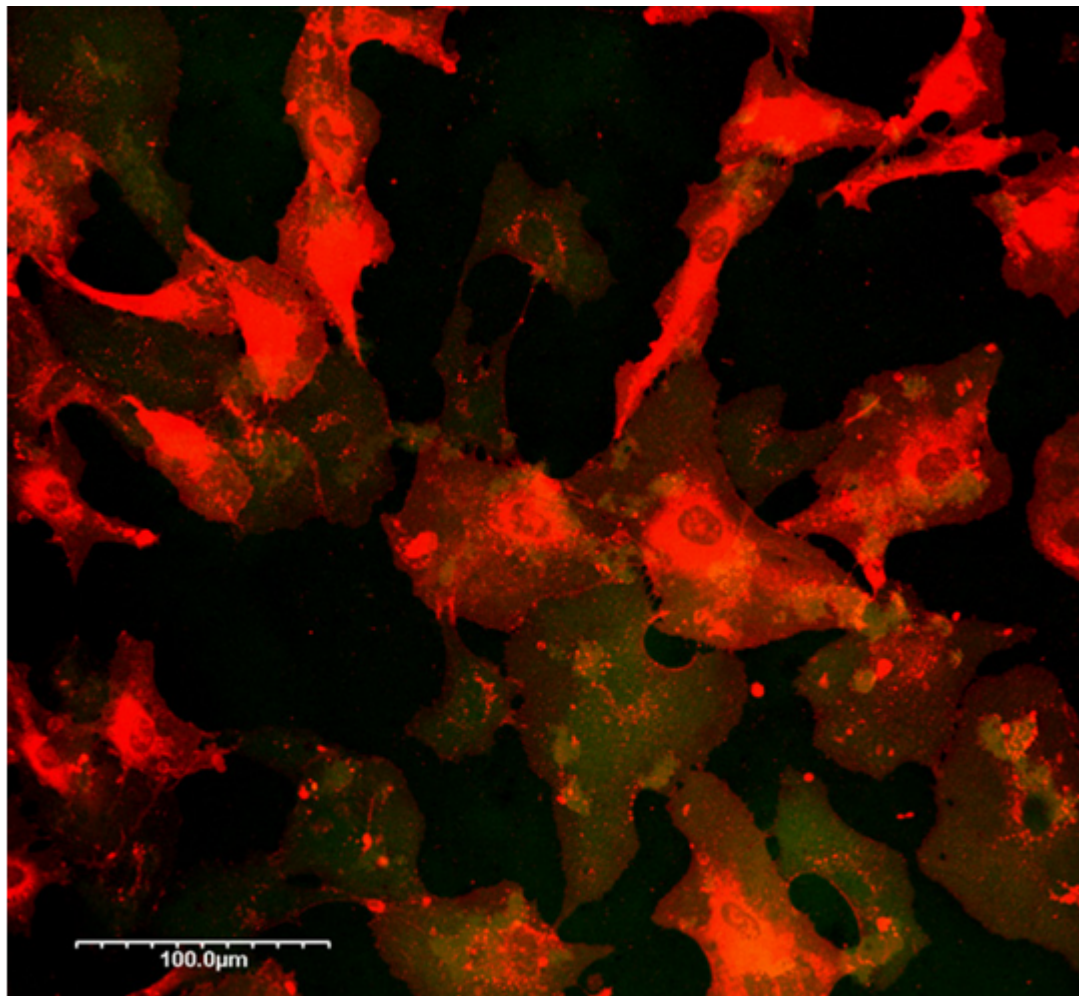


Figure 4.22. Internalization of SWNT-F3 by endothelial cells. Confocal image of dividing endothelial cells following 12 h of incubation with the SWNT-F3 conjugate. Cellular membranes are stained in red with CellMask Deep Red. The green fluorescence is from the SWNT-F3 conjugate (F3 tagged at the N-terminus with FITC).

Alamar Blue assay on the same cells at 1 h (**Figure 4.23**) and 18 h (**Figure 4.24**) after the laser irradiation. **Figure 4.23** shows SWNT-F3 conjugates with long nanotubes (graph A) showed significant killing with and without the laser at 16 and 24 h of incubation, while experiments with short (graph B) and very short (graph C) nanotubes showed minimal cell death. **Figure 4.24** shows reduced viability for cells receiving the SWNT-F3 conjugate at all nanotube lengths with laser irradiation. Long nanotubes with the laser completely killed the cells, while short and very short nanotubes produced ~80% cell death. Mouse mammary tumor cells were found to be much more sensitive to the laser irradiation only, significantly reducing the cell viability of cells not treated with SWNT-F3. The data are shown in Appendix A, with short and very short nanotubes represented as graphs A and B, respectively. The uptake of SWNTs by the cells is thought to cause cell lysis and could explain the reason for death of cells that receive only the SWNT-F3 conjugate.

The actual lengths of the long, short, and very short nanotubes have yet to be determined, but it was the difficulty of injecting a single-walled carbon nanotube-annexin V conjugate into the tail vein of mice for a different project that led to experimenting with shorter nanotubes. As can be seen from data obtained by colleague Luis Neves (see Appendix A), the absorption peak steadily declines the longer the carbon nanotubes are sonicated during preparation of the suspension for the conjugation. The decline in the absorption peak as sonication time increases is likely due to the walls of the nanotubes being damaged as a result of collisions.

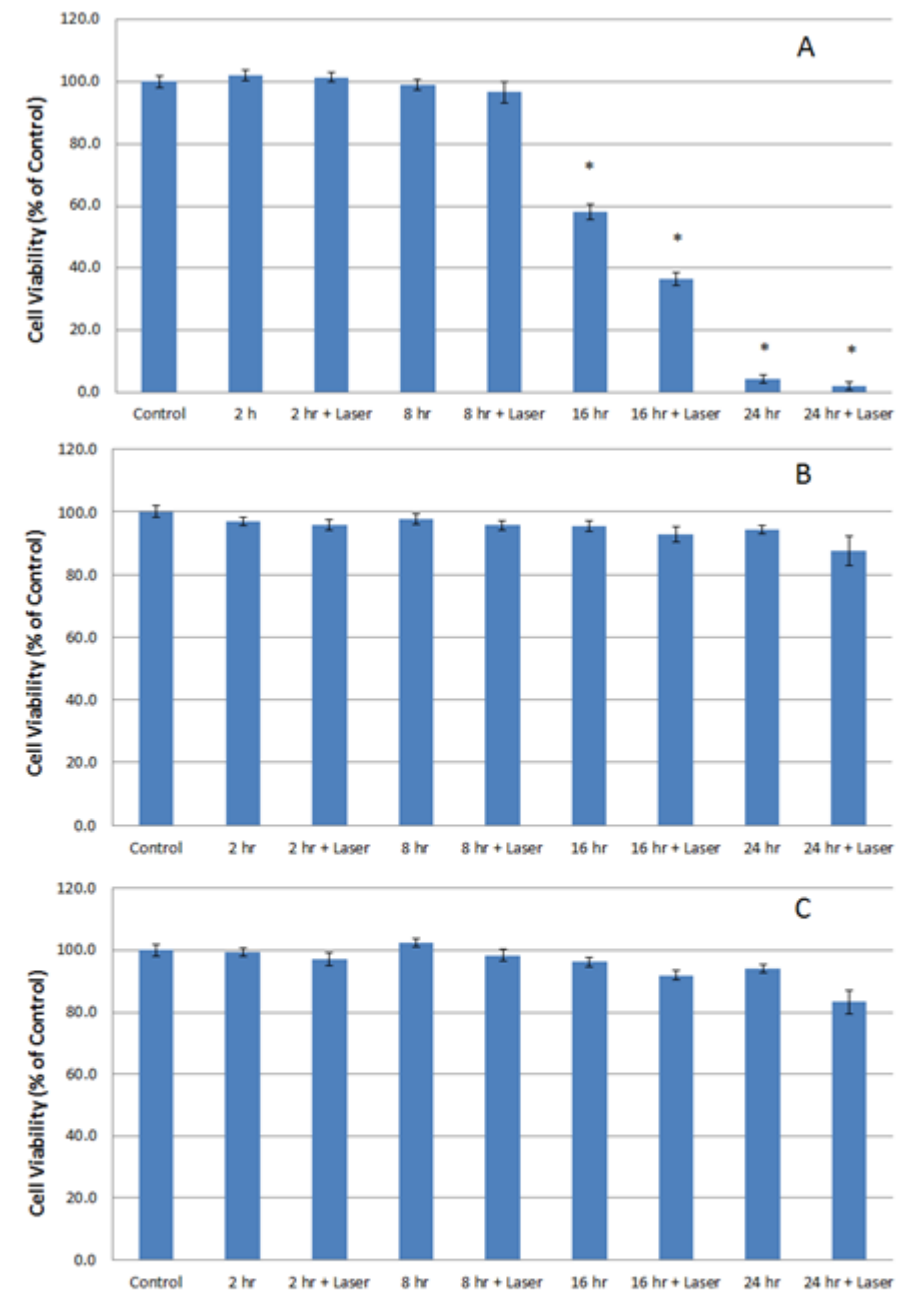


Figure 4.23. Effect of SWNT-F3 with NIR laser 1 h post-irradiation. MCF-7 cells incubated for varying times with SWNT-F3 containing long (A), short (B), and very short (C) SWNTs were irradiated with NIR light at 980 nm. Cell viability was measured by the Alamar Blue assay with statistical significance was denoted by * ($p < 0.01$). Data are presented as mean \pm SE ($n = 3$).

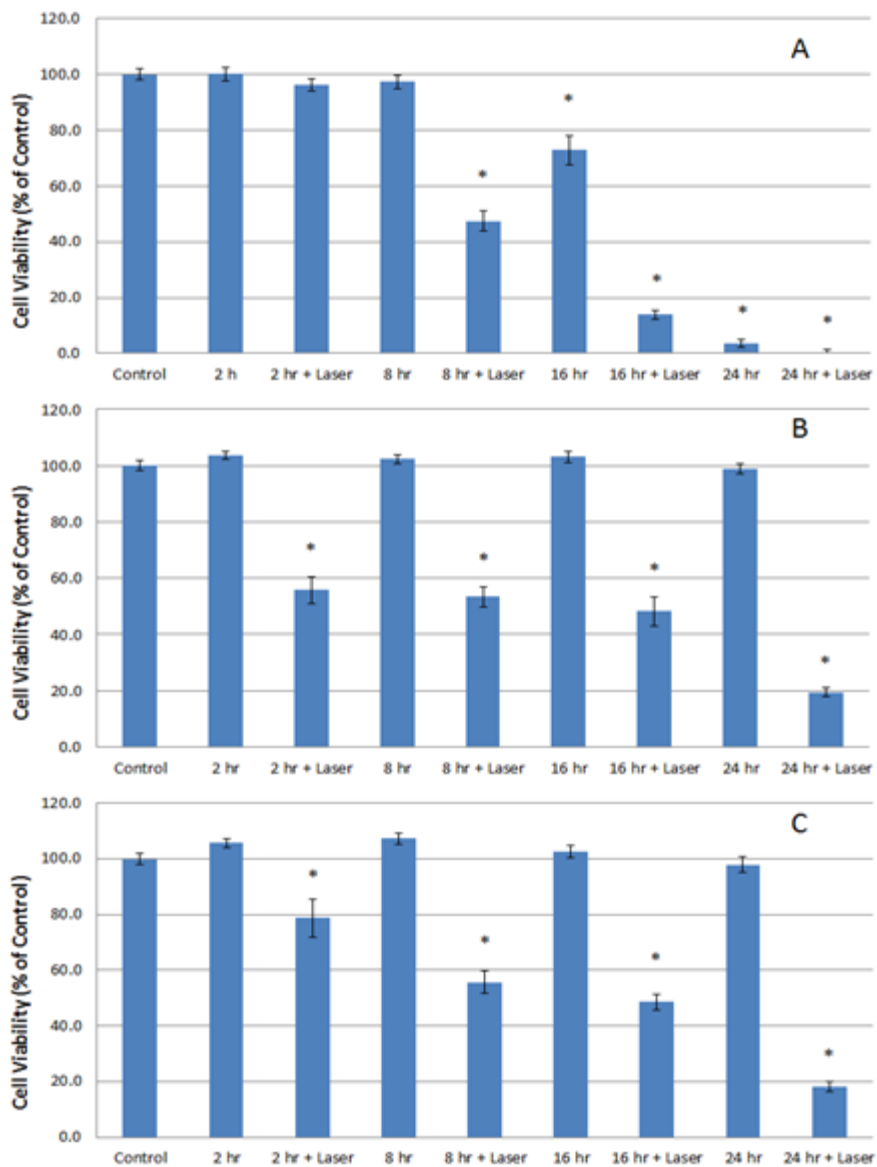


Figure 4.24. Effect of SWNT-F3 with NIR laser 18 h post-irradiation. MCF-7 cells incubated for varying times with SWNT-F3 containing long (A), short (B), and very short (C) SWNTs were irradiated with NIR light at 980 nm. Cell viability was measured by the Alamar Blue assay with statistical significance was denoted by * ($p < 0.01$). Data are presented as mean \pm SE ($n = 3$)

5. CONCLUSIONS AND FUTURE DIRECTIONS

The main objective of this work was to investigate the effectiveness of novel cancer therapeutics on two different classes. First, two enzyme prodrug systems (methioninase-annexin V with selenomethionine and cytosine deaminase-annexin V with 5-fluorocytosine) were examined for their ability to selectively target phosphatidylserine exposed on the surface of endothelial cells and two breast cancer cell lines and then induce cell death by the conversion of a specific nontoxic prodrug to an active anti-cancer metabolite. Both systems were tested *in vitro* followed by *in vivo* testing of methioninase-annexin V with selenomethionine in immunodeficient mice. Second, a project using single-walled carbon nanotubes targeted to tumor endothelial cells and tumor cells in combination with near-infrared light as a photothermal therapy was continued with the ultimate goal of performing *in vivo* testing.

The main conclusions of this research are the following:

1. Both the methioninase-annexin V and cytosine deaminase-annexin V fusion proteins could be produced with a high yield in *E. coli* and purified to greater than 96% purity.
2. Binding of both fusion proteins to exposed PS on cells was relatively strong, giving dissociation constant values in the low nanomolar range.
3. A high degree of killing of human endothelial and breast cancer cells was achieved by both enzyme prodrug systems *in vitro*. Cell killing in the methioninase-annexin V/selenomethionine system was much faster (by about three times) than in the cytosine deaminase/5-fluorocytosine system. This is probably because the methylselenol produced from selenomethionine acts directly to kill cells, while the 5-

fluorouracil produced from 5-fluorocytosine kills cells by incorporation into DNA and RNA and by inhibition of thymidylate synthetase and therefore requires more time.

4. Tests of the methioninase-annexin V/selenomethionine system in SCID mice showed that MDA-MB-231 breast tumor growth could be arrested or greatly slowed but tumor growth resumed after the end of the 11 day treatment period.

5. The two novel fusion proteins were designed to bind to the tumor vasculature, where a prodrug could be converted to a drug to attack the tumor vasculature and the tumor. Two experiments validated this hypothesis. When biotin-labeled methioninase-annexin V was injected into mice, binding in the tumor was observed on stained tissue slides only at the blood vessel surface. In another experiment in mice with MDA-MB-231 tumors that had been subjected to treatment with methioninase-annexin V/selenomethionine, a red fluorescent dye was injected. Using an animal imaging system, dye was seen throughout the untreated tumor, but substantially less dye was observed in the treated tumor. This confirms a substantial cutoff of blood flowing through the treated tumor and means that a substantial degree of hypoxia has been created in the treated tumor.

6. The SWNT-F3 conjugate was shown to be internalized in endothelial cells by confocal laser scanning microscopy. Laser treatment at 980 nm was shown to be significantly more effective in killing cells *in vitro* that previously been incubated with the conjugate, compared to cells that had only been incubated with the conjugate. An important finding in these tests is that more than 1 h is needed for the cell killing process to take place after the laser treatment.

Future experiments that could be done to increase the efficacy of this enzyme prodrug therapy system include:

1. Increasing the methioninase-annexin V dose beyond 10 mg/kg. It is unknown if the 10 mg/kg dose of methioninase-annexin V saturates all the PS molecules exposed by tumor endothelial cells, so increasing the concentration could provide extra methioninase enzyme to convert more selenomethionine into toxic methylselenol.

2. Extending the number of treatment cycles. Because the enzyme prodrug system has been well tolerated, adding more treatment cycles could provide more killing and the potential for eradicating the tumor with minimal side effects. More than an 11-day period of hypoxia may be required to completely kill the tumor.

3. Modifying the dosing schedule. Because the fusion protein completely clears bloodstream in 8 h (see **Figure 4.14**), the dosing schedule could be modified to inject the fusion protein and the prodrug on the same day, 8 h apart. This would increase the amounts of both the fusion protein and the prodrug compared to the treatment schedule that was used in this study.

4. PEGylating the fusion protein so experiments could be performed in immune competent mice. Testing of this enzyme prodrug system in immune competent mice would determine if tumor antigen release directly into the bloodstream would create an immune response that would increase the efficacy of the system in eradicating the primary tumor and distant metastases. An immunostimulant could also be administered simultaneously to boost the immune response. One possible immunostimulant is cyclophosphamide, which has been shown using low doses in combination with

photothermal therapy to greatly increase the cure rate in mice with implanted tumors [116].

5. Combining this enzyme prodrug therapy with treatment with docetaxel to increase the exposure of PS in the tumor vasculature and thus increase the effectiveness of the treatment. Docetaxel has been found to about double the percentage of tumor vessels in mice that expose anionic phospholipids, while not leading to any exposure of these phospholipids in the vasculature of any of the normal organs [117].

BIBLIOGRAPHY

1. Centers for Disease Control and Prevention. <http://www.cdc.gov/cancer/breast/> 2012.
2. American Cancer Society. <http://www.cancer.org/Cancer/BreastCancer/> 2012.
3. Dotan E, Cohen SJ, Alpaugh KR, Meropol NJ, *Circulating tumor cells: evolving evidence and future challenges*. *Oncologist*, 2009. **14**(11): p. 1070-82.
4. Carmeliet P, Jain RK, *Angiogenesis in cancer and other diseases*. *Nature*, 2000. **407**(6801): p. 249-57.
5. National Institute of Health. www.nih.gov, 2012.
6. Hashizume H, Baluk P, Morikawa S, McLean JW, Thurston G, Roberge S, Jain RK, McDonald DM, *Openings between defective endothelial cells explain tumor vessel leakiness*. *Am J Pathol*, 2000. **156**(4): p. 1363-80.
7. Vaupel P, Harrison L, *Tumor hypoxia: Causative factors, compensatory mechanisms, and cellular response*. *The Oncologist*, 2004. **9**(suppl 5): p. 4-9.
8. Thomlinson RF, Gray LH, *The histological structure of some human lung cancers and the possible implications for radiotherapy*. *British Journal of Cancer*, 1955. **9**: p. 539-549.
9. Karmali PP, Kotamraju VR, Kastantin M, Black M, Missirlis D, Tirrell M, Ruoslahti E, *Targeting of albumin-embedded paclitaxel nanoparticles to tumors*. *Nanomedicine*, 2009. **5**(1): p. 73-82.
10. Maeda H, Bharate GY, Daruwalla J, *Polymeric drugs for efficient tumor-targeted drug delivery based on EPR-effect*. *Eur J Pharm Biopharm*, 2009. **71**(3): p. 409-19.
11. Gottesman MM, *Mechanisms of Cancer Drug Resistance*. *Annual Review of Medicine*, 2002. **53**: p. 615-627.
12. Persidis A, *Cancer multidrug resistance*. *Nature Biotechnology*, 1999. **17**: p. 94-95.
13. Bagshawe KD, *Antibody-directed enzyme prodrug therapy (ADEPT) for cancer*. *Expert Rev Anticancer Ther*, 2006. **6**(10): p. 1421-31.
14. Tietze LF, Krewer B, *Antibody-directed enzyme prodrug therapy: a promising approach for a selective treatment of cancer based on prodrugs and monoclonal antibodies*. *Chem Biol Drug Des*, 2009. **74**(3): p. 205-11.
15. Cheng TL, Wei SL, Chen BM, Chern JW, Wu MF, Liu PW, Roffler SR, *Bystander killing of tumour cells by antibody-targeted enzymatic activation of a glucuronide prodrug*. *Br J Cancer*, 1999. **79**(9-10): p. 1378-85.
16. Burnham NL, *Polymers for delivering peptides and proteins*. *Am J Hosp Pharm*, 1994. **51**(2): p. 210-8; quiz 228-9.
17. Williamson P, Schlegel RA, *Back and forth: the regulation and function of transbilayer phospholipid movement in eukaryotic cells*. *Mol Membr Biol*, 1994. **11**(4): p. 199-216.
18. Zwaal RF, Schroit AJ, *Pathophysiologic implications of membrane phospholipid asymmetry in blood cells*. *Blood*, 1997. **89**(4): p. 1121-32.
19. Rao LV, *Mechanisms of activity of lupus anticoagulants*. *Curr Opin Hematol*, 1997. **4**(5): p. 344-50.

20. Utsugi T, Schroit AJ, Connor J, Bucana CD, Fidler IJ, *Elevated expression of phosphatidylserine in the outer membrane leaflet of human tumor cells and recognition by activated human blood monocytes*. *Cancer Res*, 1991. **51**(11): p. 3062-6.
21. Rote NS, Ng AK, Dostal-Johnson DA, Nicholson SL, Siekman R, *Immunologic detection of phosphatidylserine externalization during thrombin-induced platelet activation*. *Clin Immunol Immunopathol*, 1993. **66**(3): p. 193-200.
22. Herrmann A, Devaux PF, *Alteration of the aminophospholipid translocase activity during in vivo and artificial aging of human erythrocytes*. *Biochim Biophys Acta*, 1990. **1027**(1): p. 41-6.
23. Demo SD, Masuda E, Rossi AB, Thronset BT, Gerard AL, Chan EH, Armstrong RJ, Fox BP, Lorens JB, Payan DG, Scheller RH, Fisher JM, *Quantitative measurement of mast cell degranulation using a novel flow cytometric annexin-V binding assay*. *Cytometry*, 1999. **36**(4): p. 340-8.
24. Blankenberg FG, Katsikis PD, Tait JF, Davis RE, Naumovski L, Ohtsuki K, Kapiwoda S, Abrams MJ, Darkes M, Robbins RC, Maecker HT, Strauss HW, *In vivo detection and imaging of phosphatidylserine expression during programmed cell death*. *Proc Natl Acad Sci U S A*, 1998. **95**(11): p. 6349-54.
25. Ran S, Downes A, Thorpe PE, *Increased exposure of anionic phospholipids on the surface of tumor blood vessels*. *Cancer Res*, 2002. **62**(21): p. 6132-40.
26. Ran S, Thorpe PE, *Phosphatidylserine is a marker of tumor vasculature and a potential target for cancer imaging and therapy*. *Int J Radiat Oncol Biol Phys*, 2002. **54**(5): p. 1479-84.
27. Esaki N, Soda K, *L-methionine gamma-lyase from Pseudomonas putida and Aeromonas*. *Methods Enzymol*, 1987. **143**: p. 459-65.
28. Hoffman RM, *Altered methionine metabolism and transmethylation in cancer*. *Anticancer Res*, 1985. **5**(1): p. 1-30.
29. Kokkinakis DM, Hoffman RM, Frenkel EP, Wick JB, Han Q, Xu M, Tan Y, Schold SC, *Synergy between methionine stress and chemotherapy in the treatment of brain tumor xenografts in athymic mice*. *Cancer Res*, 2001. **61**(10): p. 4017-23.
30. Kokkinakis DM, *Methionine-stress: a pleiotropic approach in enhancing the efficacy of chemotherapy*. *Cancer Lett*, 2006. **233**(2): p. 195-207.
31. Halpern BC, Clark BR, Hardy DN, Halpern RM, Smith RA, *The effect of replacement of methionine by homocystine on survival of malignant and normal adult mammalian cells in culture*. *Proc Natl Acad Sci U S A*, 1974. **71**(4): p. 1133-6.
32. Hoffman RM, *Methioninase: a therapeutic for diseases related to altered methionine metabolism and transmethylation: cancer, heart disease, obesity, aging, and Parkinson's disease*. *Hum Cell*, 1997. **10**(1): p. 69-80.
33. Kenyon SH, Ast T, Nicolaou A, Gibbons WA, *Polyamines can regulate vitamin B12 dependent methionine synthase activity*. *Biochem Soc Trans*, 1995. **23**(3): p. 444S.
34. Kenyon SH, Waterfield CJ, Timbrell JA, Nicolaou A, *Methionine synthase activity and sulphur amino acid levels in the rat liver tumour cells HTC and Phi-1*. *Biochem Pharmacol*, 2002. **63**(3): p. 381-91.

35. Esaki N, Tanaka H, Uemura S, Suzuki T, Soda K, *Catalytic action of L-methionine gamma-lyase on selenomethionine and selenols*. *Biochemistry*, 1979. **18**(3): p. 407-10.
36. Miki K, Xu M, Gupta A, Ba Y, Tan Y, Al-Refaie W, Bouvet M, Makuuchi M, Moossa AR, Hoffman RM, *Methioninase cancer gene therapy with selenomethionine as suicide prodrug substrate*. *Cancer Res*, 2001. **61**(18): p. 6805-10.
37. Yamamoto N, Gupta A, Xu M, Miki K, Tsujimoto Y, Tsuchiya H, Tomita K, Moossa AR, Hoffman RM, *Methioninase gene therapy with selenomethionine induces apoptosis in bcl-2-overproducing lung cancer cells*. *Cancer Gene Ther*, 2003. **10**(6): p. 445-50.
38. Kim A, Oh JH, Park JM, Chung AS, *Methylselenol generated from selenomethionine by methioninase downregulates integrin expression and induces caspase-mediated apoptosis of B16F10 melanoma cells*. *J Cell Physiol*, 2007. **212**(2): p. 386-400.
39. Zeng H, Wu M, Botnen JH, *Methylselenol, a selenium metabolite, induces cell cycle arrest in G1 phase and apoptosis via the extracellular-regulated kinase 1/2 pathway and other cancer signaling genes*. *J Nutr*, 2009. **139**(9): p. 1613-8.
40. Rayman MP, *Selenium in cancer prevention: a review of the evidence and mechanism of action*. *Proc Nutr Soc*, 2005. **64**(4): p. 527-42.
41. Zeng H, *Selenium as an essential micronutrient: roles in cell cycle and apoptosis*. *Molecules*, 2009. **14**(3): p. 1263-78.
42. Chen WR, Adams RL, Carubelli R, Nordquist RE, *Laser-photosensitizer assisted immunotherapy: a novel modality for cancer treatment*. *Cancer Lett*, 1997. **115**(1): p. 25-30.
43. Wyatt MD, Wilson III DM, *Participation of DNA repair in the response to 5-fluorouracil*. *Cell Mol Life Sci*, 2009. **66**(5): p. 788-99.
44. Longley DB, Harkin BP, Johnston PG *5-Fluorouracil: mechanisms of action and clinical strategies*. *Nat Rev Cancer*, 2003. **3**: p. 330-338.
45. Cheung WY, Fralick RA, Cheng S, *The confused cancer patient: a case of 5-fluorouracil-induced encephalopathy*. *Curr Oncol*, 2008. **15**(5): p. 234-6.
46. Cutler RE, Blair AD, Kelly MR, *Flucytosine kinetics in subjects with normal and impaired renal function*. *Clinical Pharmacology and Therapeutics*, 1978. **24**: p. 333-342.
47. Coelho V, Dervede J, Petrusch U, Panjideh H, Fuchs H, Menzel C, Dubel S, Keilholz U, Thiel E, Deckert PM, *Design, construction, and in vitro analysis of A33scFv::CDy, a recombinant fusion protein for antibody-directed enzyme prodrug therapy in colon cancer*. *Int J Oncol*, 2007. **31**(4): p. 951-7.
48. Zamboni S, Mallano A, Flego M, Ascione A, Dupuis ML, Gellini M, Barca S, Cianfriglia M, *Genetic construction, expression, and characterization of a single chain anti-CEA antibody fused to cytosine deaminase from yeast*. *International Journal of Oncology*, 2008. **32**: p. 1245-1251.
49. Del Vecchio S, Reynolds JC, Carrasquillo JA, Blasberg RG, Neumann RD, Lotze MT, Bryant GJ, Farkas RJ, Larson SM, *Local distribution and concentration of intravenously injected 131I-9.2.27 monoclonal antibody in human malignant melanoma*. *Cancer Res*, 1989. **49**(10): p. 2783-9.

50. Zeng H, Wei Q, Huang R, Chen N, Dong Q, Yang Y, Zhou Q, *Recombinant adenovirus mediated prostate-specific enzyme pro-drug gene therapy regulated by prostate-specific membrane antigen (PSMA) enhancer/promoter*. J Androl, 2007. **28**(6): p. 827-35.
51. Chaszczewska-Markowska M, Stebelska K, Sikorski A, Madej J, Opolski A, Ugorski M *Liposomal formulation of 5-fluorocytosine in suicide gene therapy with cytosine deaminase--for colorectal cancer*. . Cancer Letters, 2008. **262**(2): p. 164-172.
52. Huber BE, Richards CA, Austin EA, *Virus-directed enzyme/prodrug therapy (VDEPT). Selectively engineering drug sensitivity into tumors*. Ann N Y Acad Sci, 1994. **716**: p. 104-14; discussion 140-3.
53. Harris JD, Gutierrez AA, Hurst HC, Sikora K, Lemoine NR, *Gene therapy for cancer using tumour-specific prodrug activation*. Gene Ther, 1994. **1**(3): p. 170-5.
54. Singh Y, Palombo M, Sinko PJ, *Recent trends in targeted anticancer prodrug and conjugate design*. Curr Med Chem, 2008. **15**(18): p. 1802-26.
55. Hirsch LR, Stafford RJ, J. Bankson, and e. al., *Nanoshell-mediated near-infrared thermal therapy of tumors under magnetic resonance guidance*. Proceedings of the National Academy of Sciences, 2003. **100**(23): p. 13549–13554.
56. Prickett WM, Van Rite BD, Resasco DE, Harrison RG, *Vascular targeted single-walled carbon nanotubes for near-infrared light therapy of cancer*. Nanotechnology, 2011: p. 455101-455108.
57. Hilger I, Hiergeist R, Hergt R, Winnefeld K, Schubert H, Kaiser WA, *Thermal ablation of tumors using magnetic nanoparticles: An in vivo feasibility study*. Investigative Radiology, 2002. **37**: p. 580-586.
58. Gannon CJ, Cherukuri P, Yakobson BI, Cognet L, Kanzius JS, Kittrell C, Weisman RB, Pasquali M, Schmidt HK, Smalley RE, Curley SA, *Carbon Nanotube-enhanced Thermal Destruction of Cancer Cells in a Noninvasive Radiofrequency Field*. Cancer, 2007. **110**(12): p. 2654-2665.
59. Gannon CJ, Patra CR, Bhattacharya R, Mukherjee P, Curley SA, *Intracellular gold nanoparticles enhance non-invasive radiofrequency thermal destruction of human gastrointestinal cancer cells*. Journal of Nanobiotechnology, 2008. **6**(2): p. doi:10.1186/1477-3155-6-2.
60. Glazer ES, Zhu C, Massey KL, Thompson CS, Kaluarachchi WD, Hamir AN, Curley SA, *Noninvasive Radiofrequency Field Destruction of Pancreatic Adenocarcinoma Xenografts Treated with Targeted Gold Nanoparticles*. Clinical Cancer Research, 2010. **16**: p. 5712-5721.
61. Glazer ES, Curley SA, *Radiofrequency Field-Induced Thermal Cytotoxicity in Cancer Cells Treated With Fluorescent Nanoparticles*. Cancer, 2010: p. 3285-3293.
62. Storm FK, Harrison WH, Elliott RS, *Normal Tissue and Solid Tumor Effects of Hyperthermia in Animal Models and Clinical Trials*. Cancer Research, 1979. **39**: p. 2245-2251.

63. Kampinga HH, *Cell biological effects of hyperthermia alone or combined with radiation or drugs: a short introduction to newcomers in the field*. International Journal of Hyperthermia, 2006. **22**: p. 191-196.
64. Tell RA, Harlen F, *A review of selected biological effects and dosimetric data useful for development of radiofrequency safety standards for human exposure*. Journal of Microwave Power, 1979. **14**: p. 405-424.
65. Feng Y, Oden JT, Rylander MN, *A two-state cell damage model under hyperthermic conditions: theory and in vitro experiments*. Journal of Biomechanical Engineering, 2008. **130**: p. 041016.
66. Sharma SK, Chiang LY, Hamblin MR, *Photodynamic therapy with fullerenes in vivo: reality or a dream?* Nanomedicine (Lond), 2011. **6**(10): p. 1813-25.
67. Zhou F, Xing D, Ou Z, Wu B, Resasco DE, Chen WR, *Cancer photothermal therapy in the near-infrared region by using single-walled carbon nanotubes*. J Biomed Opt, 2009. **14**(2): p. 021009.
68. Chakravarty P, Marches R, Zimmerman NS, Swafford AD, Bajaj P, Musselman IH, Pantano P, Draper RK, Vitetta ES, *Thermal ablation of tumor cells with antibody-functionalized single-walled carbon nanotubes*. Proc Natl Acad Sci U S A, 2008. **105**(25): p. 8697-702.
69. Zhou F, Wu S, Wu B, Chen WR, Xing D, *Antitumor immunologically modified carbon nanotubes for photothermal therapy*. Biomaterials, 2012. **33**(11): p. 3235-42.
70. O'Connell MJ, Bachilo SM, Huffman CB, Moore VC, Strano MS, Haroz EH, Rialon KL, Boul PJ, Noon WH, Kittrell C, Ma J, Hauge RH, Weisman RB, Smalley RE, *Band gap fluorescence from individual single-walled carbon nanotubes*. Science, 2002. **297**(5581): p. 593-6.
71. Kam NW, O'Connell M, Wisdom JA, Dai H, *Carbon nanotubes as multifunctional biological transporters and near-infrared agents for selective cancer cell destruction*. Proc Natl Acad Sci U S A, 2005. **102**(33): p. 11600-5.
72. Porter AE, Gass M, Muller K, Skepper JN, Midgley PA, Welland M, *Direct imaging of single-walled carbon nanotubes in cells*. Nat Nanotechnol, 2007. **2**(11): p. 713-7.
73. Harrison RG, Neves LFF, Prickett WM, Luu D, *Cancer Treatment with Carbon Nanotubes, Using Thermal Ablation or Association with Anticancer Agents*. Nanomaterials for the Life Sciences, ed. C.S.S.R. Kumar. Vol. 9: Nanomaterials. 2011, WILEY-VCH Verlag GmbH & Co. KGaA, Weinheim.
74. Strano MS, Moore VC, Miller MK, Allen MJ, Haroz EH, Kittrell C, Hauge RH, Smalley RE, *The role of surfactant adsorption during ultrasonication in the dispersion of single-walled carbon nanotubes*. J Nanosci Nanotechnol, 2003. **3**(1-2): p. 81-6.
75. Bhirde AA, Patel S, Sousa AA, Patel V, Molinolo AA, Ji Y, Leapman RD, Gutkind JS, Rusling JF, *Distribution and clearance of PEG-single-walled carbon nanotube cancer drug delivery vehicles in mice*. Nanomedicine (Lond), 2010. **5**(10): p. 1535-46.
76. Chen H, Ma X, Li Z, Shi Q, Zheng W, Liu Y, Wang P, *Functionalization of single-walled carbon nanotubes enables efficient intracellular delivery of siRNA*

- targeting MDM2 to inhibit breast cancer cells growth*. Biomed Pharmacother, 2012.
77. Wang CH, Huang YJ, Chang CW, Hsu WM, Peng CA, *In vitro photothermal destruction of neuroblastoma cells using carbon nanotubes conjugated with GD2 monoclonal antibody*. Nanotechnology, 2009. **20**(31): p. 315101.
 78. Fisher JW, Sarkar S, Buchanan CF, Szot CS, Whitney J, Hatcher HC, Torti SV, Rylander CG, Rylander MN, *Photothermal response of human and murine cancer cells to multiwalled carbon nanotubes after laser irradiation*. Cancer Res, 2010. **70**(23): p. 9855-64.
 79. Zhou F, Wu S, Wu B, Chen WR, Xing D, *Mitochondria-targeting single-walled carbon nanotubes for cancer photothermal therapy*. Small, 2011. **7**(19): p. 2727-35.
 80. Smith GP, *Filamentous fusion phage: novel expression vectors that display cloned antigens on the virion surface*. Science, 1985. **228**(4705): p. 1315-7.
 81. Arap W, Kolonin MG, Trepel M, Lahdenranta J, Cardo-Vila M, Giordano RJ, Mintz PJ, Ardeli PU, Yao VJ, Vidal CI, Chen L, Flamm A, Valtanen H, Weavind LM, Hicks ME, Pollock RE, Botz GH, Bucana CD, Koivunen E, Cahill D, Troncoso P, Baggerly KA, Pentz RD, Do KA, Logothetis CJ, Pasqualini R, *Steps toward mapping the human vasculature by phage display*. Nature Medicine, 2002. **8**(2): p. 121-127.
 82. Ruoslahti E, *Targeting tumor vasculature with homing peptides from phage display*. Seminars in Cancer Biology, 2000. **10**: p. 435-442.
 83. Ruoslahti E, Duza T, Zhang L, *Vascular homing peptides with cell-penetrating properties*. Curr Pharm Des, 2005. **11**(28): p. 3655-60.
 84. Porkka K, Laakkonen P, Hoffman JA, Bernasconi M, Ruoslahti E, *A fragment of the HMGN2 protein homes to the nuclei of tumor cells and tumor endothelial cells in vivo*. Proc Natl Acad Sci U S A, 2002. **99**(11): p. 7444-9.
 85. Zhang Y, Yang M, Park JH, Singelyn J, Ma H, Sailor MJ, Ruoslahti E, Ozkan M, Ozkan C, *A surface-charge study on cellular-uptake behavior of F3-peptide-conjugated iron oxide nanoparticles*. Small, 2009. **5**(17): p. 1990-6.
 86. Pfeifle J, Anderer FA, *Isolation and characterization of phosphoprotein pp 105 from simian virus 40-transformed mouse fibroblasts*. Biochim Biophys Acta, 1983. **762**(1): p. 86-93.
 87. Derenzini M, Sirri V, Trere D, Ochs RL, *The quantity of nucleolar proteins nucleolin and protein B23 is related to cell doubling time in human cancer cells*. Lab Invest, 1995. **73**(4): p. 497-502.
 88. Christian S, Pilch J, Akerman ME, Porkka K, Laakkonen P, Ruoslahti E, *Nucleolin expressed at the cell surface is a marker of endothelial cells in angiogenic blood vessels*. J Cell Biol, 2003. **163**(4): p. 871-8.
 89. Chen CM, Chiang SY, Yeh NH, *Increased stability of nucleolin in proliferating cells by inhibition of its self-cleaving activity*. J Biol Chem, 1991. **266**(12): p. 7754-8.
 90. Drecoll E, Gaertner FC, Miederer M, Blechert B, Vallon M, Fuller JM, Alke A, Seidl C, Bruchertseifer F, Morgenstern A, Senekowitsch-Schmidtke R, Essler M, *Treatment of peritoneal carcinomatosis by targeted delivery of the radio-*

- labeled tumor homing peptide bi-DTPA-[F3]2 into the nucleus of tumor cells.* PLoS ONE, 2009. **4**(5): p. e5715.
91. Shah N, Cerussi A, Eker C, Espinoza J, Butler J, Fishkin J, Hornung R, Tromberg B, *Noninvasive functional optical spectroscopy of human breast tissue.* Proc Natl Acad Sci U S A, 2001. **98**(8): p. 4420-5.
 92. Kievit E, Bershad E, Ng E, Sethna P, Dev I, Lawrence TS, Rehemtulla A., *Superiority of yeast over bacterial cytosine deaminase for enzyme/prodrug gene therapy in colon cancer xenografts.* Cancer Res, 1999. **59**(7): p. 1417-21.
 93. Van Rite BD, Lazrak Y, Pagnon ML, Palwai NR, Neves LFF, McFetridge PS, Harrison RG, *Enzyme prodrug therapy designed to target L-methioninase to the tumor vasculature.* Cancer Letters, 2011. **301**: p. 177-184.
 94. Van Rite BD, Harrison RG, *Annexin V-targeted enzyme prodrug therapy using cytosine deaminase in combination with 5-fluorocytosine.* Cancer Lett, 2011. **307**(1): p. 53-61.
 95. Mallano A, Zamboni S, Carpinelli G, Santoro F, Flego M, Ascione A, Gellini M, Tombesi M, Podo F, Cianfriglia M, *Generation and characterization of a human single-chain fragment variable (scFv) antibody against cytosine deaminase from Yeast.* BMC Biotechnol, 2008. **8**: p. 68.
 96. *National Cancer Institute.* www.cancer.gov, 2012.
 97. Laemmli UK, *Cleavage of structural proteins during the assembly of the head of bacteriophage T4.* Nature, 1970. **227**(5259): p. 680-5.
 98. Moon HK, Lee SH, Choi HC, *In vivo near-infrared mediated tumor destruction by photothermal effect of carbon nanotubes.* ACS Nano, 2009. **3**(11): p. 3707-13.
 99. Palwai NR, *Targeting Fusion Proteins Containing L-Methioninase to Cancer Cells,* in *School of Chemical, Biological and Materials Engineering2007,* University of Oklahoma: Norman.
 100. Lacks S, Greenberg B, *A deoxyribonuclease of Diplococcus pneumoniae specific for methylated DNA.* J Biol Chem, 1975. **250**(11): p. 4060-66.
 101. Marinus MG, *DNA methylation in Escherichia coli.* Annu Rev Genet, 1987. **21**: p. 113-31.
 102. Van Den Berg L, Rose D, *Effect of freezing on the pH and composition of sodium and potassium phosphate solutions; the reciprocal system KH₂PO₄-Na₂-HPO₄-H₂O.* Archives of Biochemistry and Biophysics, 1959. **84**: p. 305-315.
 103. Utsugi T, Schroit AJ, Connor J, Bucana CD, Fidler IJ, *Elevated expression of phosphatidylserine in the outer membrane leaflet of human tumor cells and recognition by activated human blood monocytes.* Cancer Res, 1991. **51**(11): p. 3062-6.
 104. Sugimura M, Donato R, Kakkar VV, Scully MF, *Annexin V as a probe of the contribution of anionic phospholipids to the procoagulant activity of tumour cell surfaces.* Blood Coagul Fibrinolysis, 1994. **5**(3): p. 365-73.
 105. van Heerde WL, Sakariassen KS, Hemker HC, Sixma JJ, Reutelingsperger CP, de Groot PG, *Annexin V inhibits the procoagulant activity of matrices of TNF-stimulated endothelium under blood flow conditions.* Arterioscler Thromb, 1994. **14**(5): p. 824-30.

106. van Heerde WL, Poort S, van 't Veer C, Reutelingsperger CP, de Groot PG, *Binding of recombinant annexin V to endothelial cells: effect of annexin V binding on endothelial-cell-mediated thrombin formation*. *Biochem J*, 1994. **302** (Pt 1): p. 305-12.
107. Erbs P, Regulier E, Kintz J, Leroy P, Poitevin Y, Exinger F, Jund R, Mehtali M, *In vivo cancer gene therapy by adenovirus-mediated transfer of a bifunctional yeast cytosine deaminase/uracil phosphoribosyltransferase fusion gene*. *Cancer Res*, 2000. **60**(14): p. 3813-22.
108. Mecham JO, Rowitch D, Wallace CD, Stern PH, Hoffman RM, *The metabolic defect of methionine dependence occurs frequently in human tumor cell lines*. *Biochem Biophys Res Commun*, 1983. **117**(2): p. 429-34.
109. Hu J, Cheung NK, *Methionine depletion with recombinant methioninase: in vitro and in vivo efficacy against neuroblastoma and its synergism with chemotherapeutic drugs*. *Int J Cancer*, 2009. **124**(7): p. 1700-6.
110. Vrudhula VM, Svensson HP, Kennedy KA, Senter PD, Wallace PM, *Antitumor activities of a cephalosporin prodrug in combination with monoclonal antibody-beta-lactamase conjugates*. *Bioconjug Chem*, 1993. **4**(5): p. 334-40.
111. Blakey DC, Burke PJ, Davies DH, Dowell RI, East SJ, Eckersley KP, Fitton JE, McDaid J, Melton RG, Niculescu-Duvazm IA, Pinder PE, Sharma SK, Wright AF, Springer CJ, *ZD2767, an improved system for antibody-directed enzyme prodrug therapy that results in tumor regressions in colorectal tumor xenografts*. *Cancer Res*, 1996. **56**: p. 3287-3292.
112. Senter PD, Saulnier MG, Schreiber GJ, Hirschberg DL, Brown JP, Hellstrom I, Hellstrom KE, *Anti-tumor effects of antibody-alkaline phosphatase conjugates in combination with etoposide phosphate*. *Proc Natl Acad Sci U S A*, 1988. **85**(13): p. 4842-6.
113. Senter PD, Schreiber GJ, Hirschberg DL, Ashe SA, Hellstrom KE, Hellstrom I, *Enhancement of the in vitro and in vivo antitumor activities of phosphorylated mitomycin C and etoposide derivatives by monoclonal antibody-alkaline phosphatase conjugates*. *Cancer Res*, 1989. **49**(21): p. 5789-92.
114. Park JI, Cao L, Platt VM, Huang Z, Stull RA, Dy EE, Sperinde JJ, Yokoyama JS, Szoka FC, *Antitumor therapy mediated by 5-fluorocytosine and a recombinant fusion protein containing TSG-6 hyaluronan binding domain and yeast cytosine deaminase*. *Mol Pharm*, 2009. **6**(3): p. 801-12.
115. Prickett WM, *Vascular Targeted Single-Walled Carbon Nanotubes for Cancer Therapy*, in *Bioengineering2011*, University of Oklahoma: Norman.
116. Castano AP, Mroz P, Wu MX, Hamblin MR, *Photodynamic therapy plus low-dose cyclophosphamide generates antitumor immunity in a mouse model*. *Proc Natl Acad Sci U S A*, 2008. **105**(14): p. 5495-500.
117. Huang X, Bennett M, Thorpe PE, *A monoclonal antibody that binds anionic phospholipids on tumor blood vessels enhances the antitumor effect of docetaxel on human breast tumors in mice*. *Cancer Res*, 2005. **65**(10): p. 4408-16.

APPENDIX A

Cytosine Deaminase–Annexin V Fusion Gene Sequence

Note: The flexible (Gly-Ser)₃ linker attaching cytosine deaminase to annexin V is underlined.

gtgacagggggaatggcaagcaagtgggatcagaaaggcatggacattgcctatgaagag
V T G G M A S K W D Q K G M D I A Y E E
gccgactgggctacaagaaggcgggtgtgccgattggcggttgtctgatcaataacaaa
A A L G Y K E G G V P I G G C L I N N K
gacggctccgtgctgggcccgtgggcacaacatgcgcttcagaaaggcagcgcaccctg
D G S V L G R G H N M R F Q K G S A T L
cacggcgaaatctccaccctggaaaactgcgggcgtctcgagggcaaagtgtacaaagat
H G E I S T L E N C G R L E G K V Y K D
accaccctgtatacgaccctgagcccgtgcgacatgtgtacgggcgccatcatcatgtac
T T L Y T T L S P C D M C T G A I I M Y
ggcattccacgctgctggtcggcgaaaacgtgaatttcaaatccaagggcgagaaatac
G I P R C V V G E N V N F K S K G E K Y
ctgcagaccgcgcccacgaagtggctcgtgggtggacgatgaacgctgcaaaaagatcatg
L Q T R G H E V V V V D D E R C K K I M
aacagttcatcgatgagcgtccacaggattggtttgaagatattgggtgagggctccggt
K Q F I D E R P Q D W F E D I G E G S G
tctggatccgcacaggttctcagaggcactgtgactgacttcctggatttgatgagcgg
S G S A Q V L R G T V T D F P G F D E R
gctgatgcagaaactcttcggaaggctatgaaaggcttggggcacagatgaggagagcatc
A D A E T L R K A M K G L G T D E E S I
ctgactctgttgacatcccgaagtaatgctcagcgcaggaaatctctgcagcttttaag
L T L L T S R S N A Q R Q E I S A A F K
actctgtttggcagggatcttctggatgacctgaaatcagaactaactggaaaatttgaa
T L F G R D L L D D L K S E L T G K F E
aaattaattgtggctctgatgaaaccctctcggctttatgatgcttatgaaactgaaacat
K L I V A L M K P S R L Y D A Y E L K H
gccttgaagggagctggaacaaatgaaaaagtactgacagaaattattgcttcaaggaca
A L K G A G T N E K V L T E I I A S R T
cctgaagaactgagagccatcaaacaagtttatgaagaagaatatggctcaagcctggaa
P E E L R A I K Q V Y E E E Y G S S L E
gatgacgtgggtgggggacacttcagggtactaccagcggatgttgggtggttctccttcag
D D V V G D T S G Y Y Q R M L V V L L Q
gctaacagagaccctgatgctggaatcgatgaagctcaagttgaacaagatgctcaggct
A N R D P D A G I D E A Q V E Q D A Q A
ttatttcaggctggagaacttaaatgggggacagatgaagaaaagtttatcaccatcttt
L F Q A G E L K W G T D E E K F I T I F
ggaacacgaagtgtgtctcatttgagaaaggtgtttgacaagtacatgactatatacagga
G T R S V S H L R K V F D K Y M T I S G
tttcaaattgaggaaccattgaccgcgagacttctggcaatttagagcaactactcctt
F Q I E E T I D R E T S G N L E Q L L L
gctggtgtgaaatctattcgaagtatacctgcctaccttgacagagaccctctattatgct
A V V K S I R S I P A Y L A E T L Y Y A

atgaagggagctgggacagatgatcataccctcatcagagtcatggtttccaggagtgag
M K G A G T D D H T L I R V M V S R S E
attgatctgtttaacatcaggaaggagtttaggaagaatgttccacctctctttattcc
I D L F N I R K E F R K N F A T S L Y S
atgattaagggagatacatctggggactataaгааagctcttctgctgctctgtggagaa
M I K G D T S G D Y K K A L L L L C G E
gatgactaa
D D -

DNA Sequence:

gtgacagggggaatggcaagcaagtgggatcagaaaggcatggacattgcctatgaagag
gccgactgggctacaagaaggcggtgtgccgattggcggttgtctgatcaataacaaa
gacggctccgtgctgggccgtgggcacaacatgctctccagaaaggcagcgccaccctg
cacggcgaaatctccaccctggaaaactgcgggcgtctcgagggcaaagtgtacaaagat
accaccctgtatacgaccctgagcccgtgogacatgtgtacgggcccacatcatcatgtac
ggcattccacgctgctgggtcggcgaaaacgtgaatttcaaatccaagggcgagaaatac
ctgcagacccgcggccacgaagtggctcgtgggtggacgatgaacgctgcaaaaagatcatg
aaacagttcatcgatgagcgtccacaggattggtttgaagatatgggtgagggctccgggt
tctggatccgcacaggttctcagaggcactgtgactgacttccttgatttgatgagcgg
gctgatgcagaaactcttcggaaggctatgaaaggcttgggcacagatgaggagagcatc
ctgactctgttgacatcccgaagtaatgctcagcgccaggaaatctctgcagcttttaag
actctgtttggcagggatcttctggatgacctgaaatcagaactaactggaaaatttgaa
aaattaattgtggctctgatgaaaccctctcggctttatgatgcttatgaaactgaaacat
gccttgaagggagctggaacaaatgaaaaagtactgacagaaattattgcttcaaggaca
cctgaagaactgagagccatcaacaagtttatgaagaagaatatggctcaagcctggaa
gatgacgtgggtgggggacacttcagggtactaccagcggatgttggtgggttctccttcag
gctaacagagaccctgatgctggaatcgatgaagctcaagttgaacaagatgctcaggct
ttatttcaggctggagaacttaaatgggggacagatgaagaaaagtttatcaccatcttt
ggaacacgaagtgtgtctcatttgagaaagggtgtttgacaagtacatgactatatcagga

tttcaaattgaggaaaccattgaccgagacttctggcaatttagagcaactactcctt
gctgttgtgaaatctattcgaagtatacctgcctaccttgcagagaccctctattatgct
atgaagggagctgggacagatgatcataccctcatcagagtcatggtttccaggagtgag
attgatctgtttaacatcaggaaggagtttaggaagaattttgccacctctctttattcc
atgattaagggagatacatctggggactataagaaagctcttctgctgctctgtggagaa
gatgactaa

Amino Acid Sequence:

V T G G M A S K W D Q K G M D I A Y E E A A L G Y K E G G V
P I G G C L I N N K D G S V L G R G H N M R F Q K G S A T L
H G E I S T L E N C G R L E G K V Y K D T T L Y T T L S P C
D M C T G A I I M Y G I P R C V V G E N V N F K S K G E K Y
L Q T R G H E V V V V D D E R C K K I M K Q F I D E R P Q D
W F E D I G E G S G S G S A Q V L R G T V T D F P G F D E R
A D A E T L R K A M K G L G T D E E S I L T L L T S R S N A
Q R Q E I S A A F K T L F G R D L L D D L K S E L T G K F E
K L I V A L M K P S R L Y D A Y E L K H A L K G A G T N E K
V L T E I I A S R T P E E L R A I K Q V Y E E E Y G S S L E
D D V V G D T S G Y Y Q R M L V V L L Q A N R D P D A G I D
E A Q V E Q D A Q A L F Q A G E L K W G T D E E K F I T I F
G T R S V S H L R K V F D K Y M T I S G F Q I E E T I D R E
T S G N L E Q L L L A V V K S I R S I P A Y L A E T L Y Y
A M K G A G T D D H T L I R V M V S R S E I D L F N I R K E
F R K N F A T S L Y S M I K G D T S G D Y K K A L L L L C G
E D D **Stop**

Methioninase-Annexin V Sequence Following Site-Directed Mutagenesis

ggaccccgcgactcccataacaacaccgggtttttccacacggggcattcaccacgggtacgacccg
G P R D S H N N T G F S T R A I H H G Y D P
ctttccacgggtggtgccttggtgccaccgggtgtaccagaccgcgacctatgccttcccg
L S H G G A L V P P V Y Q T A T Y A F P
actgtcgaatacggcgctgcgtgcttcgccggggaggaggcggggcacttctacagccgc
T V E Y G A A C F A G E E A G H F Y S R
atctccaacccaccctggccttgctcgagcaacgcatggcctcgttggagggtggtgag
I S N P T L A L L E Q R M A S L E G G E
gcgggattggcgctggcgctcggggatgggagccattacttcgaccctctggaccctgctg
A G L A L A S G M G A I T S T L W T L L
cggcctgggtgatgagctgatcgtggggcgcaccttgtatggctgcacctttgcgttctg
R P G D E L I V G R T L Y G C T F A F L
caccatggcattggcgagttcgggggtcaagatccaccatgtcgcaccttaacgatgccaa
H H G I G E F G V K I H H V D L N D A K
gccctgaaagcggcgatcaacagcaaacgcggatgatctacttcgaaacaccggccaac
A L K A A I N S K T R M I Y F E T P A N
cccaacatgcaactggtggatatagcggcggtcgtcgaggcagtgcgggggagtgatgag
P N M Q L V D I A A V V E A V R G S D V
cttgtgggtggtcgacaacacactactgcacgccctacctgcagcggccactggaactgggg
L V V V D N T Y C T P Y L Q R P L E L G
gcagacctggtggtgcattcggcgaccaagtacctcagtgggccatggcgacatcactgag
A D L V V H S A T K Y L S G H G D I T A
ggcctggtggtggggcgcaaggccttgggtcgaccgcattcggctggaagggtgaaagac
G L V V G R K A L V D R I R L E G L K D
atgaccggggcagccttgtcaccgcatgacgctgcgttgttgatgcgcggcatcaagacc
M T G A A L S P H D A A L L M R G I K T
ctggcgctgcgcatggaccggcattgcgccaacgcctggaggctcgcgcagttcctggcc
L A L R M D R H C A N A L E V A Q F L A
gggcagccccaggtggagctgatccactaccgggcttgccgctcgtttgcccagtagcga
G Q P Q V E L I H Y P G L P S F A Q Y E
ctggcacagcggcagatgcgtttgccggggcgggatgattgcctttgagctcaagggcgg
L A Q R Q M R L P G G M I A F E L K G G
atcgaggccggggcgggcttcatgaatgccctgcagctttttgcccgtgcgggtgagcctg
I E A G R G F M N A L Q L F A R A V S L
ggggatgccgagtcgctggcacagcaccggcgagcatgacgcactccagttacacgccca
G D A E S L A Q H P A S M T H S S Y T P
caagagcggggcgcacacgggatatcagaggggctggtgaggttgcagtggggctggag
Q E R A H H G I S E G L V R L S V G L E
gatgtggaggacctgctggcagatatcgagttggcattggaggcgtgtgcagggcagcgg
D V E D L L A D I E L A L E A C A G S G
tctggatccgcacaggttctcagaggcactgtgactgacttccctggatttgatgagcgg
S G S A Q V L R G T V T D C P G F D E R
gctgatgcagaaactcttcggaaggctatgaaaggcttggggcacagatgaggagagcatc
A D A E T L R K A M K G L G T D E E S I
ctgactctgttgacatcccgaagtaatgctcagcgcaggaaatctctgcagcttttaag
L T L L T S R S N A Q R Q E I S A A F K
actctgtttggcagggatcttctggatgacctgaaatcagaactaactggaaaatttga
T L F G R D L L D D L K S E L T G K F E

aaattaattgtggctctgatgaaaccctctcggtttatgatgcttatgaaactgaaacat
K L I V A L M K P S R L Y D A Y E L K H
gccttgaagggagctggaacaaatgaaaaagtactgacagaaattattgcttcaaggaca
A L K G A G T N E K V L T E I I A S R T
*cctgaagaactgagagccatcaaac***caag**tttatgaagaagaatatggctcaagcctggaa
P E E L R A I K Q V Y E E E Y G S S L E
gatgacgtgggtgggggacacttcagggtactaccagcggatggtgggttctccttcag
D D V V G D T S G Y Y Q R M L V V L L Q
gctaacagagaccctgatgctggaatcgatgaagctcaagttgaacaagatgctcaggct
A N R D P D A G I D E A Q V E Q D A Q A
ttatttcaggctggagaacttaaagggggacagatgaagaaaagtttatcaccatcttt
L F Q A G E L K W G T D E E K F I T I F
ggaacacgaagtgtgtctcatttgagaaaggtgtttgacaagtacatgactatatcagga
G T R S V S H L R K V F D K Y M T I S G
tttcaaattgaggaaaccattgaccgagacttctggcaatttagagcaactactcctt
F Q I E E T I D R E T S G N L E Q L L L
gctgttgtaaacttattcgaagtatacctgcctaccttgacagagaccctctattatgct
A V V K S I R S I P A Y L A E T L Y Y A
atgaagggagctgggacagatgatcataccctcatcagagtcatggtttccaggagtgag
M K G A G T D D H T L I R V M V S R S E
attgatctgtttaacatcaggaaggagtttaggaagaattttgccacctctctttattcc
I D L F N I R K E F R K N F A T S L Y S
atgattaagggagatacatctggggactataagaaagctcttctgctgctctgtggagaa
M I K G D T S G D Y K K A L L L L C G E
gatgactaa

DD -

The regions underlined are the corrected mutations (methioninase 326 and annexin V 11), the sequences in italics are where the forward and reverse mutation sequencing primers aligned, and the bold region is the flexible linker.

BCA Protein Assay Standard Curve

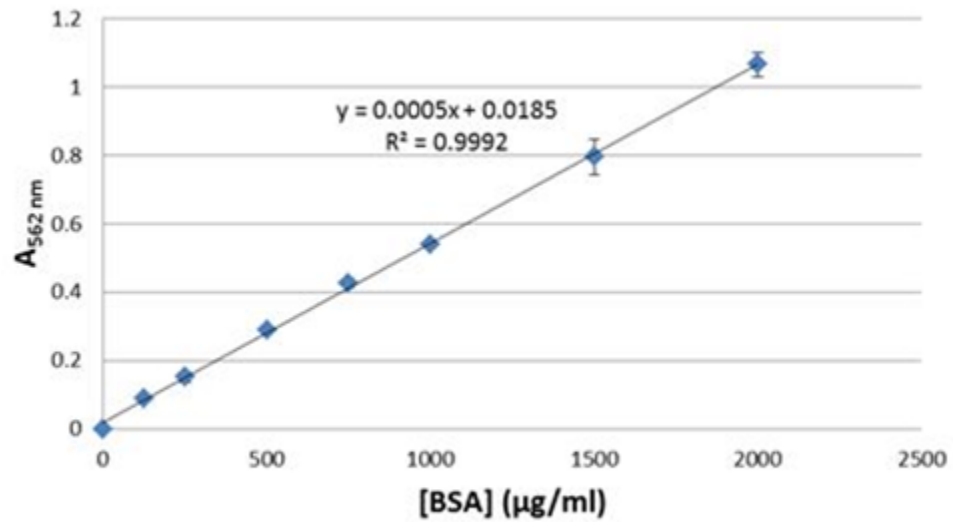


Figure A.1. BCA protein assay standard curve with BSA standard

Bradford Protein Assay Standard Curve

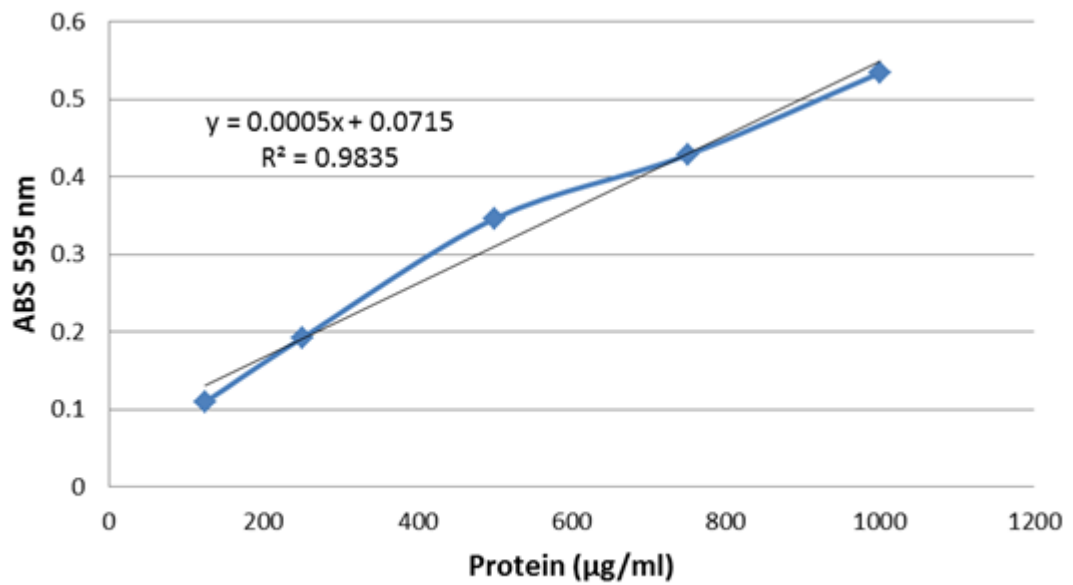


Figure A.2. Bradford protein assay standard curve with BSA standard

Bradford Protein Microassay Standard Curve

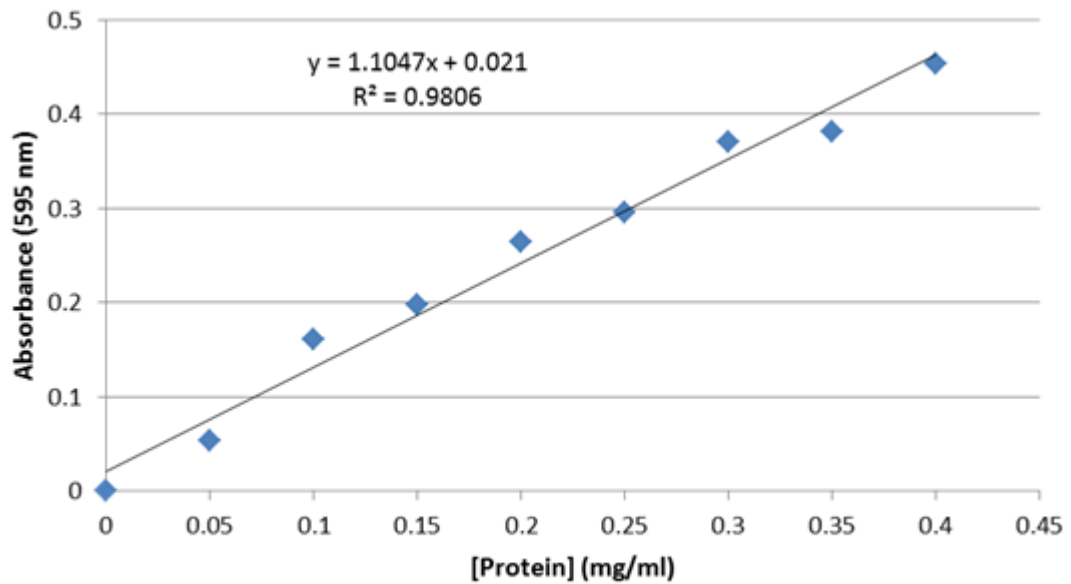


Figure A.3. Bradford protein assay microassay standard curve with BSA standard

L-Methioninase Enzymatic Activity Assay Standard Curve

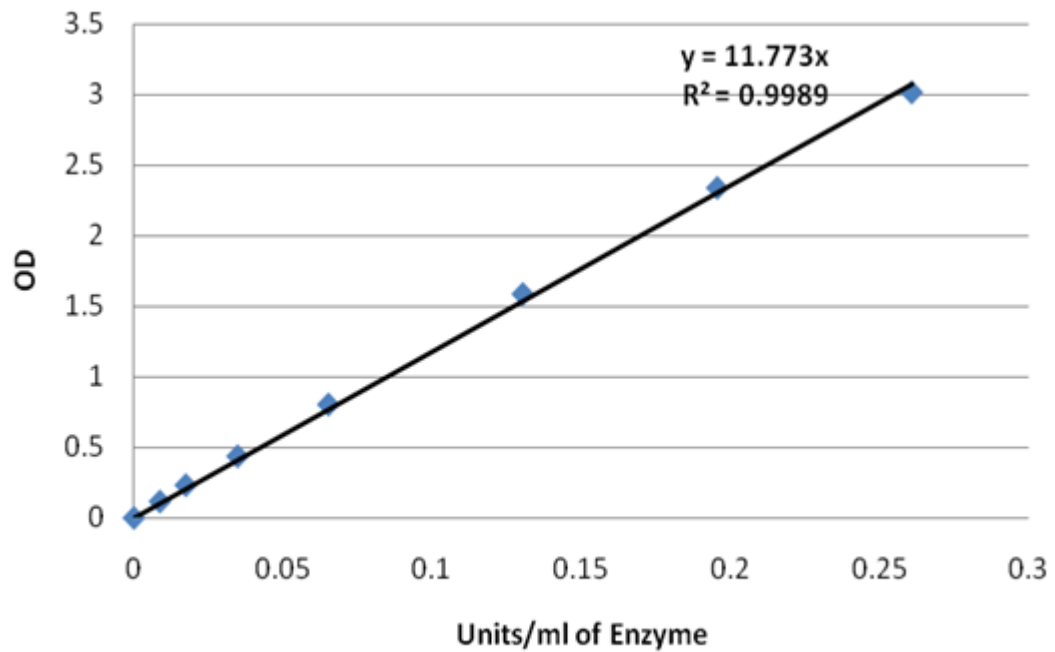


Figure A.4. L-methioninase enzymatic activity standard curve

Chromatograph from the Purification of Methioninase-Annexin V

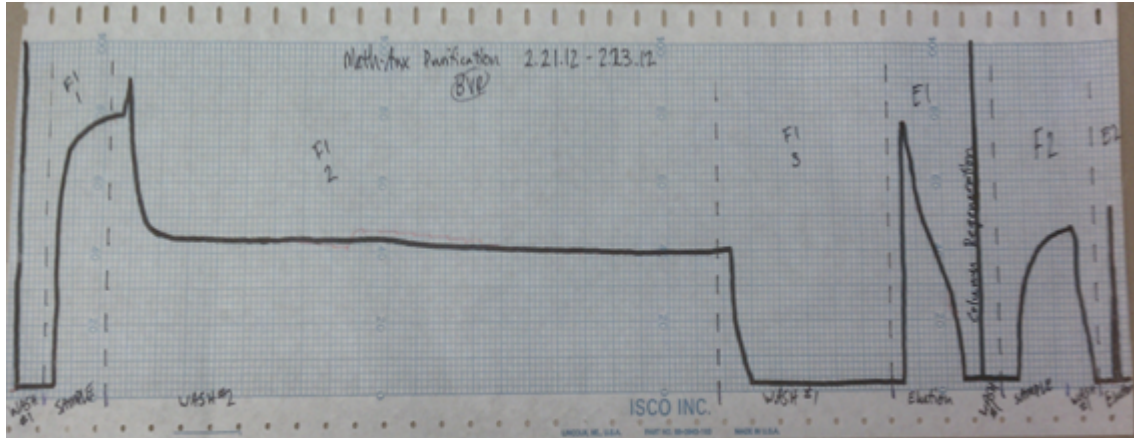


Figure A.5. Chromatograph from the purification of methioninase-annexin V.

Dissociation Constant for Methioninase-Annexin V Binding to Endothelial Cells

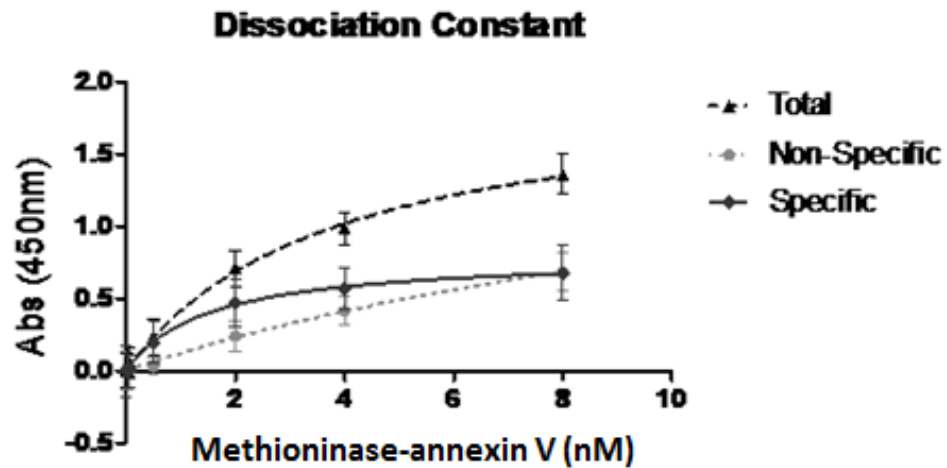


Figure A.6. Methioninase-annexin V binding to HAAE-1 endothelial cells.

Binding Stability of Cytosine Deaminase-Annexin V

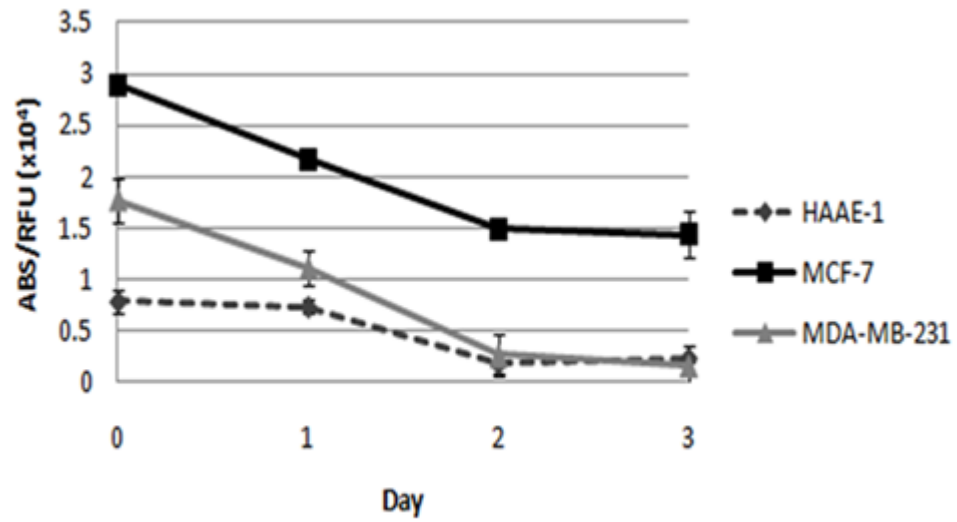


Figure A.7. Cytosine deaminase-annexin V binding stability.

Pathology Report of Treated MDA-MB-231 Breast Tumors in SCID Mice

Mice from each group were sent for analysis. Animals 234, 235, and 251 were untreated (saline only); animals 236, 240, and 241 received methioninase-annexin V; animals 244, 245, and 294 received selenomethionine; and animals 247, 250, 252, 932, 966, 973, and 988 received methioninase-annexin V and selenomethionine.

PATHOLOGY REPORT				
<i>OUHSC Comparative Medicine</i>				
DATE SUBMITTED: <u>05/07/2012</u>		ACCESSION NO: <u>183-12 through 198-12</u>		
INVESTIGATOR(s): <u>Dr. Harrison and Mr. Brent Van Rite</u>				
SPECIES: <u>Mice</u>		AGE: <u>About 11 weeks old</u>		SEX: <u>Females</u>
Accession No.	Animal No.	Lung Morphology	Liver Morphology	Transplanted tumor (% necrosis)
183-12	234	I observed <u>no</u> definitive evidence of metastasis.	I observed <u>no</u> definitive evidence of metastasis.	85%
184-12	235	I observed <u>no</u> definitive evidence of metastasis.	I observed <u>no</u> definitive evidence of metastasis.	30%
185-12	251	I observed <u>no</u> definitive evidence of metastasis.	I observed <u>no</u> definitive evidence of metastasis.	65%
186-12	236	I observed <u>no</u> definitive evidence of metastasis.	I observed <u>no</u> definitive evidence of metastasis.	65%
187-12	240	I observed <u>no</u> definitive evidence of metastasis.	I observed <u>no</u> definitive evidence of metastasis.	35%
188-12	241	I observed <u>no</u> definitive evidence of metastasis.	I observed <u>no</u> definitive evidence of metastasis.	70%
189-12	244	I observed <u>no</u> definitive evidence of metastasis.	I observed <u>no</u> definitive evidence of metastasis.	30%
190-12	245	I observed <u>no</u> definitive evidence of metastasis.	I observed <u>no</u> definitive evidence of metastasis.	20%
191-12	294	I observed <u>no</u> definitive evidence of metastasis.	I observed <u>no</u> definitive evidence of metastasis.	25%
192-12	247	I observed <u>no</u> definitive evidence of metastasis.	I observed <u>no</u> definitive evidence of metastasis.	35%
193-12	250	I observed <u>no</u> definitive evidence of metastasis.	I observed <u>no</u> definitive evidence of metastasis.	55%
194-12	252	I observed <u>no</u> definitive evidence of metastasis.	I observed <u>no</u> definitive evidence of metastasis.	45%
195-12	932	I observed <u>no</u> definitive evidence of metastasis.	I observed <u>no</u> definitive evidence of metastasis.	50%

M-183 thru 198-12 Page 1 of 2

Accession No.	Animal No.	Lung Morphology	Liver Morphology	Transplanted tumor (% necrosis)
196-12	966	I observed <u>no</u> definitive evidence of metastasis.	I observed <u>no</u> definitive evidence of metastasis.	30%
197-12	973	I observed <u>no</u> definitive evidence of metastasis.	I observed <u>no</u> definitive evidence of metastasis.	15%
198-12	988	I observed <u>no</u> definitive evidence of metastasis.	I observed <u>no</u> definitive evidence of metastasis.	55%

DIAGNOSIS:

There was no definitive gross or histologic evidence of metastasis within the lungs or liver sections evaluated. There is always the chance that a very small, early micrometastasis was overlooked. However, I evaluated the sections at both 10x and 20x. The severity of ischemic necrosis within the transplanted tumors ranged from about 15% to 85%.

Stanley D. Kesante
 SIGNATURE OF PATHOLOGIST

May 8, 2012
 DATE

Single-Walled Carbon Nanotube Standard Curve

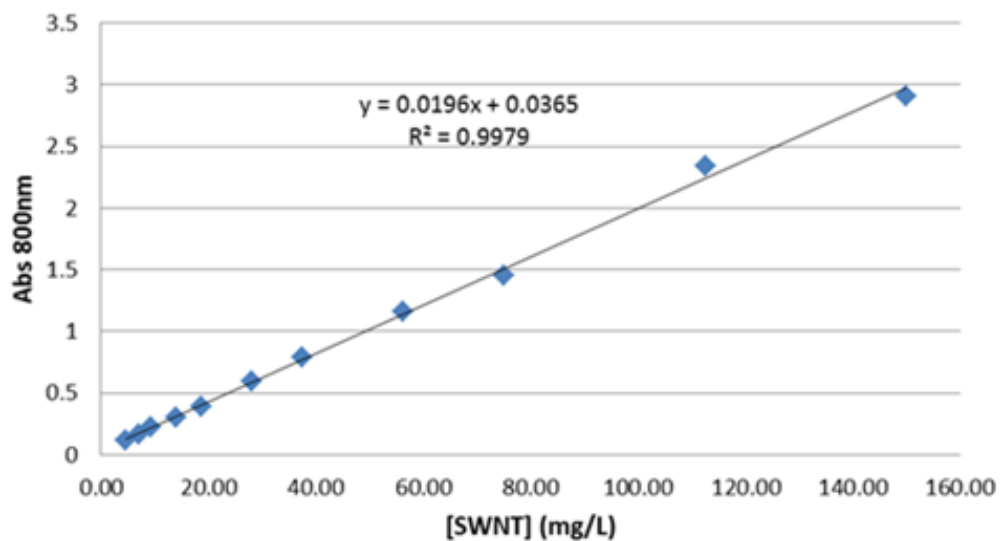


Figure A.8. Carbon nanotube standard curve in 1% sodium dodecyl sulfate.

Conjugation History of F3 Peptide to Carbon Nanotubes

SWNT Suspension History						SWNT-F3 Conjugation History				
Date	Initial SWNT (mg)	SDS (%)	Theoretical [SWNT] (mg/L)	[SWNT] (mg/L)	SWNT Recovery (%)	Date	F3 (mg)	Final [F3] (mg/L)	Final [SWNT] (mg/L)	SWNT Recovery (%)
5.18.11	3	1	600	-	-	5.18.11	1	74.2	89.5	-
5.25.11	3	1	600	496.2	82.7	5.25.11	1	-	121.9	24.6
5.25.11	3	1	600	348.1	58.0	5.25.11	1	-	110.9	31.9
6.5.11	3	1	600	413.6	68.9	6.4.11	1	103.2	68.3	16.5
6.5.11	3	1	600	309.5	51.6	6.4.11	1	138.5	60.1	19.4
6.6.11	3	1	600	403.4	67.2	6.6.11	1	-	145.4	36.0
6.6.11	6	1	1200	771.5	64.3	6.6.11	1	232.6	262.6	34.0
6.7.11	3	1	600	418.3	69.7	6.7.11	1	-	117.0	28.0
6.9.11	6	1	1200	627.2	52.3	6.8.11	1	-	283.0	45.1
6.20.11	6	1	1200	686.22	57.2	6.20.11	1	0	153.16	22.3
6.20.11	6	1	1200	663.98	55.3	6.20.11	1	34.4	206.22	31.1
6.28.11	6	1	1200	633.98	52.8	6.29.11	1	194.62	230.31	36.3
7.6.11	6	1	1200	683.57	57.0	7.6.11	1	229.93	209.69	30.7
7.12.11	6	1	1200	766.02	63.8	7.11.11	1	266.14	247.86	32.4
7.18.11	6	1	1200	602.76	50.2	7.18.11	1	266.14	198.27	32.9
7.28.11	6	1	1200	858.57	71.5	7.27.11	1	294.2	282.14	32.9
9.1.11	6	1	1200	674.59	56.2	9.15.11	1	348.51	233.16	34.6
1.13.12	6	1	1200	846.17	70.5	1.16.12	1	343.98	309.18	36.5
1.29.12	6	1	1200	849.74	70.8	1.29.12	1	378.38	311.22	36.6
1.29.12	6	1	1200	626.79	52.2	1.29.12	1	435.41	201.02	32.1
2.16.12	6	1	1200	778.83	64.9	2.19.12	1	671.68	236.12	30.3
2.16.12	6	1	1200	780.36	65.0	2.19.12	1	407.35	313.27	40.1
2.16.12	6	1	1200	805.36	67.1	2.19.12	1	532.27	341.02	42.3

Cytotoxicity of SWNT-F3 with NIR Laser to 4T1 Mammary Tumor Cells

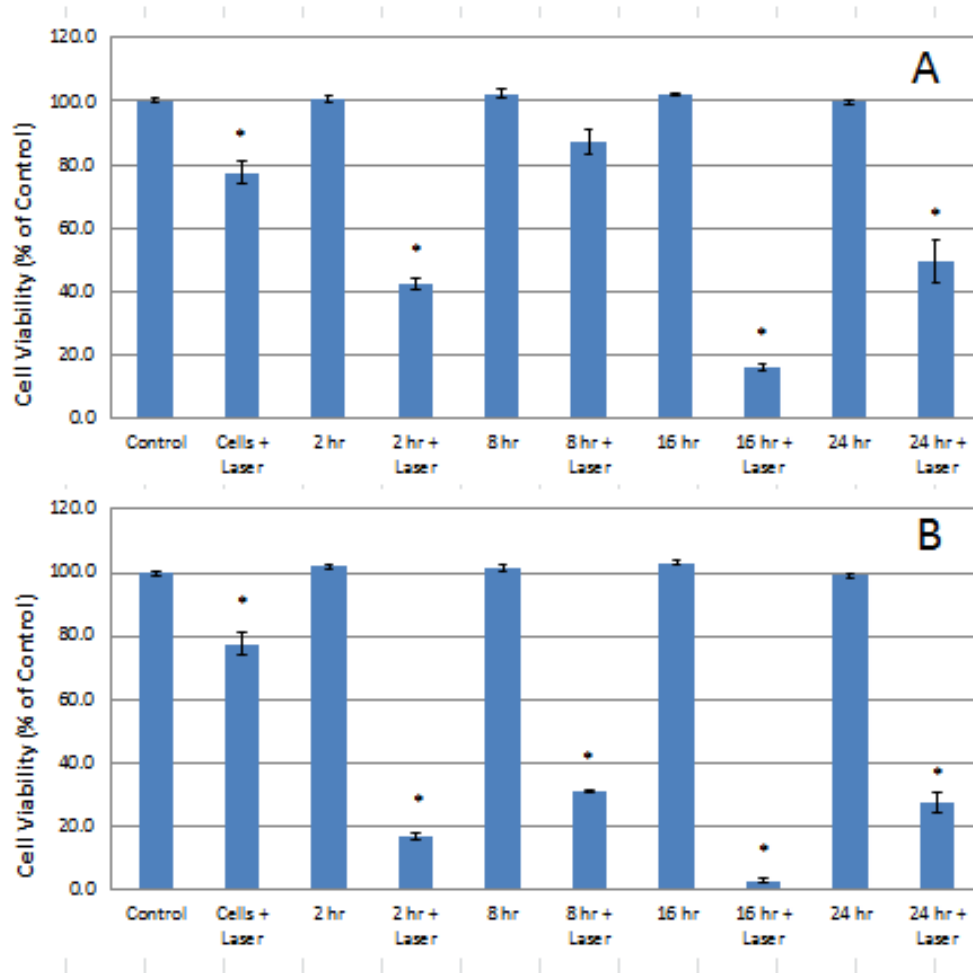


Figure A.10. Effect of SWNT-F3 with NIR laser 1 h (A, B) and 18 h (C, D) post-irradiation on 4T1 mouse mammary cancer cells using short (A, C) and very short (B, D) nanotubes.

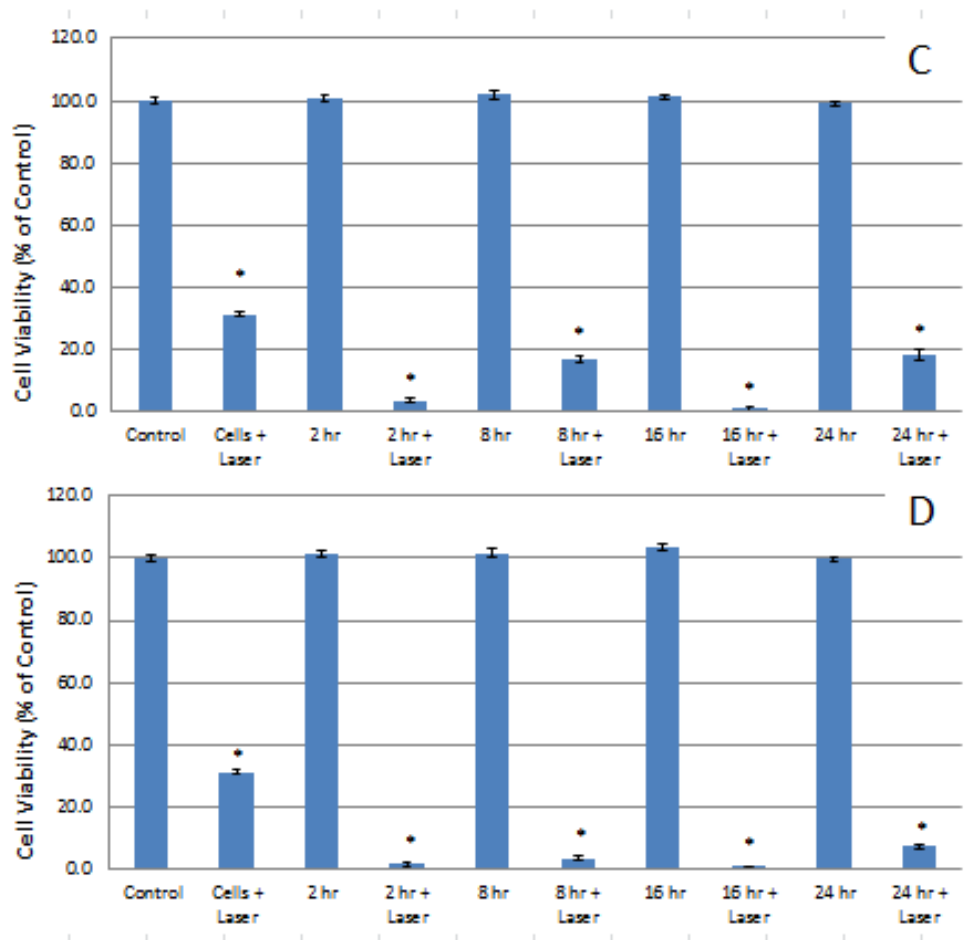


Figure A.10 (continued). Effect of SWNT-F3 with NIR laser 1 h (A, B) and 18 h (C, D) post-irradiation on 4T1 mouse mammary cancer cells using short (A, C) and very short (B, D) nanotubes.

Single-Walled Carbon Nanotube Absorption Spectra

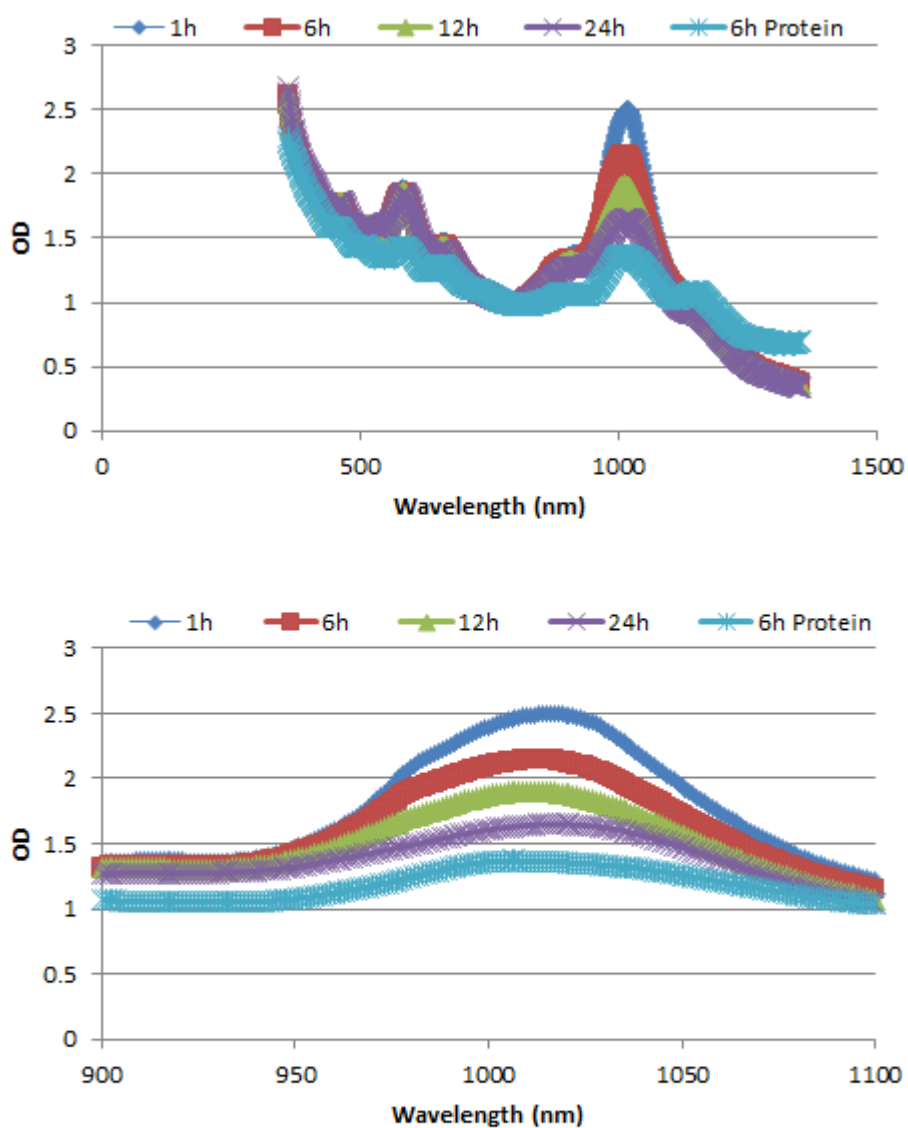


Figure A.10. Carbon nanotube absorption spectra after 1 h, 6 h, 12 h, and 24 h of sonication in 1% sodium dodecyl sulfate. The spectra for a sample of 6 h nanotubes with annexin V attached is shown in light blue. (A) Range: 360 – 1350 nm. (B) Range: 900 – 1100 nm.

APPENDIX B

Construction of Cytosine Deaminase – Annexin V Fusion Gene

1. Design primers for manufacturing by Integrated DNA Technologies (Coralville, IA).
 - a. CD primers: 5' LIC, **HRV 3C Protease site**; 3' *BamHI site*
 - i. **Sense primer:** 5'-gAC/ gAC/ gAC/ AAg/ ATg/ CTT/ gAA/ gTC/ CTC/ TTT/ CAg/ ggA/ CCC/ gTg/ ACA/ ggg/ ggA/ ATg/ gCA/ AgC -3'
 - ii. **Antisense primer:** 5'- gC/ CgC/ ATT/ ggA/ TCC/ AgA/ ACC/ gTC/ gCC/ CTC/ ACC/ AAT/ ATC/ TTC/ AAA/ CC -3'
 - b. Annexin V primers: 5' *BamHI site*; 3' LIC
 - i. **Sense primer:** 5'- Cg/ ATT/ CgC/ ggA/ TCC/ gCA/ CAg/ gTT/ CTC/ AgA/ ggC -3'
 - ii. **Antisense primer:** 5'-gA/ ggA/ gAA/ gCC/ Cgg/ TTA/ gTC/ ATC/ TTC/ TCC/ ACA/ gAg/ C -3'
2. Amplify yCD and annexin V genes using PCR (Expand High Fidelity PCR system purchased from Roche Applied Sciences; Madison, WI).

Step	# of Cycles	Temperature	Time
Initial Denaturation	1	94 °C	2 min
Amplification	31		
- Denaturation		94 °C	15 sec
- Annealing	(CD)	55 °C	30 sec
	(Annexin V)	55 °C	30 sec
- Elongation		72 °C	90 sec
Final Elongation	1	72 °C	7 min
Cooling	1	4 °C	∞

PCR Reaction Mixtures for Yeast Cytosine Deaminase (pQE30Xa + CD – 7/2009)			
Mix 1	Volume (µl)	Mix 2	Volume (µl)
PCR nucleotide mix	1	Enzyme mix	0.75
Sense primer	1.1	10X Buffer, w/ MgCl ₂	5
Antisense primer	1.4	ddH ₂ O, Sterile	19.25
Template DNA	1		
PCR grade water	20.5		
TOTAL	25		25
PCR Reaction Mixtures for Annexin V (pET 22b + STF-annexin -03/15/2006)			
Mix 1	Volume (µl)	Mix 2	Volume (µl)
PCR nucleotide mix	1	Enzyme mix	0.75
Sense primer	1.2	10X Buffer, w/ MgCl ₂	5
Antisense primer	1.2	ddH ₂ O, Sterile	19.25
Template DNA	2.5		
PCR grade water	19.1		
TOTAL	25		25

3. Purify PCR products using Qiaquick PCR purification kit protocol.
- To analyze purified DNA on a gel, add 1 volume of Loading Dye to 5 volumes of DNA. (Mix 1 µl loading dye with 5 µl DNA). Pipet up & down to mix before loading gel.
 - After the PCR products were purified, an agarose gel was run to check if the PCR worked. NO BANDS WERE DETECTED. After consulting Dr. Harrison, we decided the amount of primers added was insufficient, the annealing temperatures for both genes should be changed to 55°C, and the number of cycles during amplification should be 31. Steps 2 and 3 were repeated using 1 µl more than the value given in the above table. Below is a picture of the agarose gel obtained after the second PCR run. 4 µl of PCR product was mixed with 1 µl of loading buffer provided in the QIAquick PCR purification kit. 4 µl of 500 bp DNA ladder was also mixed with 1 µl of loading buffer to easily determine the amount of DNA present in the PCR reactions.

4. Digest CD and annexin V genes with BamHI restriction enzyme (separately) purchased from New England BioLabs (Beverly, MA).
 - One unit of enzyme will digest 1 μg of DNA in 1 hour @ 37 °C (in a total reaction volume of 50 μl).
 - Allow digestion to occur for 1 hour @ 37 °C using 20 U from a stock of 20,000 U/ml.
 - From the stock solution, I determined I would use 1 μl , corresponding to 20 Units of the enzyme per gene. 1 μl BamHI + 5 μl 1X buffer + 44 μl gene DNA.
5. Purify digested genes using Qiaquick PCR purification kit from Qiagen (Valencia, CA).
6. Ligate CD and annexin V genes using T4 DNA Ligase purchased from New England BioLabs.
 - Ligation should take place for 10 minutes @ RT using 1 μl of enzyme in 20 μl total reaction volume.
 - Three different tubes containing the same components were used for ligation.
7. Run agarose gel of ligated product using the following samples:
 - CD-annexin V
 - 500 bp DNA Marker
 - The band length that I was interested in was ~1500 bp (~1013 of annexin V + 500 of CD). Each tube sample contained either: a) CD + CD; b) CD + annexin V; or c) annexin V + annexin V.
 - The CD + annexin V sample was cut from the gel as follows.
8. Cut and agarose gel purify the appropriate gene fragments using Qiaquick gel extraction kit protocol from Qiagen (Valencia, CA).
 - Cut the appropriate fragment from gel with clean, sharp scalpel.
 - Weigh the gel slice in a colorless tube. (0.1451g = Gel weight)
 - Incubate at 50 °C for 10 minutes (or until gel slice is completely dissolved). To help dissolve, vortex the tube every 2-3 minutes during incubation.
9. Treat the ligated CD-annexin V gene with T4 DNA Polymerase (Novagen) to create sticky ends (LIC) on the gene.
 - Assemble the following components in a sterile 1.5 ml microcentrifuge tube on ice:

Component	Volume (µl)
0.2 pmol purified PCR product	4
10X T4 DNA Polymerase Buffer	2
25 mM dATP	2
100 mM DTT	1
Nuclease-free Water	10.6
2.5 U/µl T4 DNA Polymerase	0.4
TOTAL	20

- For 0.2 pmol PCR product, # of bp in insert * 650 = pg/pmol.
- Start reaction by adding enzyme. Stir with pipet tip to mix. Incubate at 22 °C for 30 minutes.
- Inactivate enzyme by incubating at 75 °C for 20 minutes.
- Store prepared Ek/LIC insert at -20 °C for use at a later time, or use immediately.
- From ligation gel, I estimated I had ~200 ng per 4 µl of DNA sample. I needed to have 0.2 pmol of DNA for polymerase reaction, and using the above equation for weight per # of bp in insert, I came up with needing 4.03 µl of DNA sample for reaction to occur – meaning 10.57 µl of nuclease-free water was needed. A positive control reaction was done using 2 µl of a provided insert. Also, a negative control was done by replacing the PCR product w/ an equal volume of nuclease-free water.

10. Anneal sticky end fusion gene to pET-30 Ek/LIC linear vector from Novagen (Madison, WI).

- Assemble the following components in a sterile 1.5 ml microcentrifuge tube:

Component	Volume (µl)
pET-30 Ek/LIC vector	1
Treated Ek/LIC insert (0.02 pmol)	2
Incubate for 5 minutes at 22 °C, than add:	
25 mM EDTA	1
TOTAL	4

- Mix by stirring with pipet tip. Incubate at 22 °C for 5 minutes.
- A positive control was done using the polymerase-treated control insert and a negative control was done using only water at the insert.

11. Transform annealed product into NovaBlue cells (GigaSingles).
 - LB + agar was made by combining 2g NaCl + 2g tryptone + 1g yeast extract + 3g agar (for 200 ml total volume) with pH 7.0 (one solution will have ampicillin and 1 will have kanamycin). Autoclave before using.
 - Have samples for positive control insert, test plasmid, negative control insert, and sample insert (CD-annexin V).

12. Extract plasmids containing fused gene insert using Qiaquick plasmid purification kit from Qiagen (Valencia, CA).
 - Pick a successfully transfected colony from the plates. Grow the bacterial cells for 16 hours in 5 ml of LB medium with kanamycin antibiotic.
 - Centrifuge the solution at 6,800xg & decant the supernatant.
 - Use gel extraction kit.

13. Run agarose gel to determine if the plasmid is correct size (should be ~7000 bp) and approximate concentration it is at.
 - Use 0.5% agarose gel to see the larger size samples.
 - Run each of the 4 samples of extracted plasmids (lanes 2-5)
 - 500 bp DNA Marker (lane 1 -> on right side)

14. Prepare extracted plasmid samples 2-4 for sequencing at Oklahoma Medical Research Foundation (OK City, OK).
 - Plasmid needs to be at ~ 100 ng/μl with at least 5 μl needed for each reaction.
 - OMRF provides the T7 promoter & terminator primers

15. Transform the plasmid containing the correct sequence into *E. coli* BL21(DE3) host for protein expression.

16. Inoculate *E. coli* BL21(DE3) cells that successfully grew on the agar plates in liquid LB medium for expression and purification.

QIAquick PCR Purification Kit Protocol

This protocol is designed to clean up DNA products from PCR reactions.

- Add ethanol (96–100%) to Buffer PE before use (see bottle label for volume).
 - All centrifuge steps are at 13,000 rpm (~17,900 x g) in a conventional tabletop microcentrifuge.
1. Add 5 volumes of Buffer PB to 1 volume of the PCR sample and mix. It is not necessary to remove mineral oil or kerosene. For example, add 500 µl of Buffer PB to 100 µl PCR sample (not including oil).
 2. Place a QIAquick spin column in a provided 2 ml collection tube.
 3. To bind DNA, apply the sample to the QIAquick column and centrifuge for 30–60 s.
 4. Discard flow-through. Place the QIAquick column back into the same tube. Collection tubes are re-used to reduce plastic waste.
 5. To wash, add 0.75 ml Buffer PE to the QIAquick column and centrifuge for 30–60 s.
 6. Discard flow-through and place the QIAquick column back in the same tube. Centrifuge the column for an additional 1 min.

IMPORTANT: Residual ethanol from Buffer PE will not be completely removed unless the flow-through is discarded before this additional centrifugation.

7. Place QIAquick column in a clean 1.5 ml microcentrifuge tube.
8. To elute DNA, add 50 µl Buffer EB (10 mM Tris·Cl, pH 8.5) or H₂O to the center of the QIAquick membrane and centrifuge the column for 1 min.

QIAquick Gel Extraction Kit Protocol

This protocol is designed to extract and purify DNA of 70 bp to 10 kb from standard or low-melt agarose gels in TAE or TBE buffer. Up to 400 mg agarose can be processed per spin column. For DNA cleanup from enzymatic reactions using this protocol, add 3 volumes of BufferQG and 1 volume of isopropanol to the reaction, mix, and proceed with step 6 of the protocol.

- The yellow color of Buffer QG indicates a pH ≤ 7.5 .
- Add ethanol (96–100%) to Buffer PE before use (see bottle label for volume).
- Isopropanol (100%) and a heating block or water bath at 50°C are required.
- All centrifugation steps are carried out at 13,000 rpm ($\sim 17,900 \times g$) in a microcentrifuge.
- 3 M sodium acetate, pH 5.0, may be necessary.

1. Excise the DNA fragment from the agarose gel with a clean, sharp scalpel. Minimize the size of the gel slice by removing extra agarose.

2. Weigh the gel slice in a colorless tube. Add 3 volumes of Buffer QG to 1 volume of gel (100 mg \sim 100 μ l). For example, add 300 μ l of Buffer QG to each 100 mg of gel. For $>2\%$ agarose gels, add 6 volumes of Buffer QG. The maximum amount of gel slice per QIAquick column is 400 mg; for gel slices >400 mg use more than one QIAquick column.

3. Incubate at 50°C for 10 min (or until the gel slice has completely dissolved). To help dissolve gel, mix by vortexing the tube every 2–3 min during the incubation.

IMPORTANT: Solubilize agarose completely. For $>2\%$ gels, increase incubation time.

4. After the gel slice has dissolved completely, check that the color of the mixture is yellow (similar to Buffer QG without dissolved agarose). If the color of the

mixture is orange or violet, add 10 µl of 3 M sodium acetate, pH 5.0, and mix. The color of the mixture will turn to yellow. The adsorption of DNA to the QIAquick membrane is efficient only at pH ≤ 7.5 . Buffer QG contains a pH indicator which is yellow at pH ≤ 7.5 and orange or violet at higher pH, allowing easy determination of the optimal pH for DNA binding. 5. Add 1 gel volume of isopropanol to the sample and mix. For example, if the agarose gel slice is 100 mg, add 100 µl isopropanol. This step increases the yield of DNA fragments < 500 bp and > 4 kb. For DNA fragments between 500 bp and 4 kb, addition of isopropanol has no effect on yield. Do not centrifuge the sample at this stage.

5. Place a QIAquick spin column in a provided 2 ml collection tube.

To bind DNA, apply the sample to the QIAquick column, and centrifuge for 1 min. The maximum volume of the column reservoir is 800 µl. For sample volumes of more than 800 µl, simply load and spin again.

6. Discard flow-through and place QIAquick column back in the same collection tube. Collection tubes are re-used to reduce plastic waste.
7. (Optional): Add 0.5 ml of Buffer QG to QIAquick column and centrifuge for 1 min. This step will remove all traces of agarose. It is only required when the DNA will subsequently be used for direct sequencing, in vitro transcription or microinjection.
8. To wash, add 0.75 ml of Buffer PE to QIAquick column and centrifuge for 1 min.

Note: If the DNA will be used for salt sensitive applications, such as blunt-end ligation and direct sequencing, let the column stand 2–5 min after addition of Buffer PE, before centrifuging.

9. Discard the flow-through and centrifuge the QIAquick column for an additional 1 min at 13,000 rpm (~17,900 x *g*).

IMPORTANT: Residual ethanol from Buffer PE will not be completely removed unless the flow-through is discarded before this additional centrifugation.

10. Place QIAquick column into a clean 1.5 ml microcentrifuge tube.

11. To elute DNA, add 50 µl of Buffer EB (10 mM Tris·Cl, pH 8.5) or H₂O to the center of the QIAquick membrane and centrifuge the column for 1 min.

QIAprep Spin Mini-prep Protocol

Use to extract plasmid from bacterial cells for applications such as plasmid DNA sequencing.

1. Begin a liquid culture of each colony selected from agar plates. Transfer 1 colony to a 1.5 ml microcentrifuge tube containing 1 ml of LB medium + kanamycin (or the appropriate antibiotic).
2. Incubate the microcentrifuge tubes at 37°C with shaking 220-250 rpm overnight (overnight but < 16 hours is best because cell lysis begins to occur at longer incubation times and reduces the amount of plasmid).
3. Centrifuge the tubes on the table-top microcentrifuge for 3 minutes at 10000 rpm.
Discard flow through.

4. Resuspend the bacterial cell pellet in 250 μ l Buffer P1 containing RNase A and LyseBlue reagent (in the brown 4°C fridge).
5. Add 250 μ l Buffer P2 to each tube and mix by inverting 4-6 times.
6. Add 350 μ l Buffer N3 to each tube and immediately mix by inverting 4-6 times (until blue color becomes white).
7. Centrifuge for 10 minutes at 13000 rpm using microcentrifuge.
8. Apply supernatant to a QIAprep spin column by decanting.
9. Centrifuge for 30-60 seconds. Discard flow through.
10. Recommended: Wash the column by adding 500 μ l Buffer PB to each and centrifuge for 30-60 seconds. Discard flow through.
11. Wash the column by adding 750 μ l Buffer PE to each and centrifuge for 30-60 seconds. Discard flow through.
12. Centrifuge for another 60 seconds to remove residual ethanol.
13. Transfer the QIAprep columns to new, sterile 1.5 ml microcentrifuge tubes. Elute DNA by adding 50 μ l Buffer EB to the center membrane of each column.
14. Let the columns sit for 60 seconds.
15. Centrifuge the columns for 60 seconds to collect the plasmid DNA.

Agarose Gel Electrophoresis

The following protocol is for making a 1% (w/v) agarose gel using SeaKem[®] LE agarose (Cambrex) using a BRL Life Technologies Horizon 58 electrophoretic cell with a total gel volume of 35 ml.

1. Assemble the electrophoretic cell.

2. Weigh out 0.50g agarose and dissolve in 50 ml of 1X TE buffer (40 mM Tris, 1 mM EDTA). Microwave 5 times in 30 second intervals on power level 5 with cap loosely on (cap will pop off and contents will spill out or glass will break otherwise).
3. Let the solution cool to 55°C and add 2.5 µl of 10 mg/ml of ethidium bromide stock to the 50 ml volume (mix the solution well to evenly distribute the ethidium bromide). Pour the gel into the cell (up to the blue line on the comb) and wait 30 min for solidification.
4. Once the gel has solidified pour the TE buffer over the gel until it covers the gel by about 1 mm. The gel is now ready to be loaded.
5. To each DNA sample to be loaded, add 2 µl of sample DNA to 1 µl loading dye (GelPilot DNA 5x Loading Dye, Qiagen #239901). The maximum volume of DNA sample is 20 µl for each well of the 8 comb gel which has a total volume of 25 µl.
 - Mixed 2 µl DNA from PCR + 1 µl loading dye with pipet, and then load into each well (for samples).
 - Mixed 2 µl blank from PCR + 1 µl loading dye with pipet, and then load into each well (for blanks).
6. For the marker lane, add 2 µl of 500 bp ladder (Bio-Rad #170-8203) to 1 µl loading dye.
7. Run the gel at 100 V (Low) until the first band gets $\frac{3}{4}$ of the way to the bottom of the gel.
8. View the gel using the UV box.

Note: 10X TE Buffer (per Liter): 1 mM EDTA (3.722g) and 40 mM Tris (48.456g) in DI Water.

Transformation Protocol for NovaBlue GigaSingles Competent Cells

1. Place the required number of 14 ml BD Falcon round-bottom polypropylene tubes on ice to pre-chill.
2. Thaw the required number of tubes of cells on ice and mix gently to ensure that the cells are evenly suspended and transfer the 50 μ l of cells to the round-bottom tubes.
3. Add 1 μ l of the DNA plasmid solution directly to the cells. Stir gently to mix.
4. Place the tubes on ice for 5 min.
5. Heat the tubes for exactly 30 s in a 42°C water bath; do not shake.
6. Place on ice for 2 min.
7. Add 250 μ l of room temperature SOC Medium to each tube.
8. Incubate at 37°C while shaking at 250 rpm for 60 min.
9. Plate 25 μ l of transformation solution on agar plates with the appropriate antibiotic.

Transformation Protocol for *E. coli* BL21(DE3) Cells

1. Thaw the required number of tubes of cells on ice and mix gently to ensure that the cells are evenly suspended.
2. Place the required number of 14 ml BD Falcon round-bottom polypropylene tubes on ice to pre-chill. Pipet 20 μ l aliquots of cells into the pre-chilled tubes.
3. Add 1 μ l of the DNA plasmid solution directly to the cells. Stir gently to mix.
4. Place the tubes on ice for 5 min.
5. Heat the tubes for exactly 30 s in a 42°C water bath; do not shake.
6. Place on ice for 2 min.

7. Add 80 μl of room temperature SOC Medium to each tube.
8. Incubate at 37°C while shaking at 250 rpm for 60 min prior to plating on selective medium.
9. Plate 25 or 50 μl of the transformation solution on LB agar plates containing the correct antibiotic (35 $\mu\text{g}/\text{ml}$ Kanamycin in this case).

Transformation of XL10-Gold Ultracompetent Cells for Quik Change XL Site-Directed Mutagenesis

1. Thaw 1 tube (135 μl) of XL10-Gold cells on ice. For each reaction to take place, pipet 45 μl of cells into pre-chilled 14 ml BD Falcon round-bottom polypropylene tubes. (3 tubes: mutagenesis control, sample, and transformation control)
2. Add 2 μl of the β -mercaptoethanol mix to the 45 μl of cells in each tube.
3. Swirl the tube gently and incubate on ice for 10 minutes, swirling gently every 2 minutes.
4. Transfer 2 μl of *Dpn I*-treated DNA from control and sample reaction to individual tubes of cells. Dilute the pUC18 control plasmid 1:10 in high-quality water and then add 1 μl to a third tube of cells. Swirl the transformation reactions gently to mix. Incubate the tubes on ice for 30 minutes.
5. Heat pulse the tubes for exactly 30 seconds at 42°C. (DO NOT EXCEED 42°C!). Preheat the NZY⁺ broth in the 42°C water bath for step 8.
6. Incubate the tubes on ice for 2 minutes.
7. Add 500 μl of NZY⁺ broth preheated to 42°C to each tube. Incubate the tubes at 37°C for 1 hour with shaking at 250 rpm.

8. Plate 250 μ l of the mutagenesis control transformation reaction on an Ampicillin + X-gal + IPTG plate. Plate 5 μ l of pUC18 transformation control reaction in 200 μ l of NZY⁺ broth on an Amp + X-gal + IPTG plate. Plate 250 μ l of mutagenesis sample transformation on two different Kanamycin + X-gal + IPTG plates.
9. Incubate the plates at 37°C for at least 16 hours.

QuikChange II XL Site-Directed Mutagenesis Protocol

1. Synthesize two complementary oligonucleotides containing the desired mutation, flanked by unmodified nucleotide sequence. Purify these oligonucleotide primers prior to use in the following steps (see Mutagenic Primer Design).

2. Prepare the control reaction as indicated below:

5 μ l of 10 \times reaction buffer
2 μ l (10 ng) of pWhitescript 4.5-kb control plasmid (5 ng/ μ l)
1.25 μ l (125 ng) of oligonucleotide control primer #1 [34-mer (100 ng/ μ l)]
1.25 μ l (125 ng) of oligonucleotide control primer #2 [34-mer (100 ng/ μ l)]
1 μ l of dNTP mix
3 μ l of QuikSolution reagent
36.5 μ l of double-distilled water (ddH₂O) to a final volume of 50 μ l

Then add

1 μ l of PfuUltra HF DNA polymerase (2.5 U/ μ l)

3. Prepare the sample reaction(s) as indicated below:

5 μ l of 10 \times reaction buffer
X μ l (10 ng) of dsDNA template
X μ l (125 ng) of oligonucleotide primer #1
X μ l (125 ng) of oligonucleotide primer #2
1 μ l of dNTP mix

3 μ l of QuikSolution

ddH₂O to a final volume of 50 μ l

Then add

1 μ l of PfuUltra HF DNA polymerase (2.5 U/ μ l)

4. If the thermal cycler to be used does not have a hot-top assembly, overlay each reaction with ~30 μ l of mineral oil.
5. Cycle each reaction using the cycling parameters outlined here. (For the control reaction, use a 5-minute extension time and run the reaction for 18 cycles.)

Note: It is important to adhere to the 18-cycle limit when cycling the mutagenesis reactions. More than 18 cycles can have deleterious effects on the reaction efficiency.

6. Following temperature cycling, place the reaction tubes on ice for 2 minutes to cool the reactions to $\leq 37^{\circ}\text{C}$.
7. Add 1 μ l of the *Dpn I* restriction enzyme (10 U/ μ l) directly to each amplification reaction below the mineral oil overlay using a small, pointed, pipet tip.
8. Gently and thoroughly mix each reaction mixture by pipetting the solution up and down several times. Spin down the reaction mixtures in a microcentrifuge for 1 minute, then immediately incubate the reactions at 37°C for 1 hour.
9. Transform *E. coli* XL10-Gold ultracompetent cells with the mutated L-methioninase-annexin V plasmid using above protocol.
10. Select several colonies with the blue phenotype and begin a 5 ml liquid culture containing kanamycin at 35 mg/L. Incubate the culture for ~16 hr at 37°C .
11. Centrifuge cultures for 10 min at 1000xg.

12. Extract plasmid from XL10-Gold cells using the QIAprep Spin Mini-prep protocol.
13. Deliver plasmid to OMRF DNA Sequencing Core Facility in Oklahoma City, OK for sequencing.
14. Compare sequencing results with the known correct nucleotide sequence for the L-methioninase-annexin V fusion gene.
15. With the correctly mutated plasmid, transform *E. coli* BL21(DE3) cells.

Fusion Protein Recombinant Protein Expression

NOTE: L-methioninase-annexin V production requires the addition of pyridoxal 5'-phosphate (an enzyme co-factor) to buffers.

1. Culture 5 µl of *E. coli* BL21(DE3) harboring pET- 30 Ek/LIC with the fusion gene L-methioninase-annexin V (or pET- 30 Ek/LIC with the fusion gene cytosine deaminase-annexin V) in 10 ml of LB medium containing 35 mg/L kanamycin in a 125 ml Erlenmeyer flask overnight at 37°C with shaking at 200 rpm.
 - LB medium: 1 liter DI H₂O + 10 g Tryptone + 5 g Yeast Extract + 10 g NaCl.
 - Add 35 mg Kanamycin to the 1 L of LB medium before taking out the 10 ml for the initial culture.
2. Add 10 ml of the cell culture to 1 liter of fresh culture medium + kanamycin and incubate at 37°C with shaking (200 rpm). Take 1 mL sample of medium before adding the bacteria, as a blank.
 - Label 1 ml tube 'LB.'
 - Transfer 250 ml of medium to each of 4 1L flasks.
 - Put in shaker at 37° C for 2 hr at 200 rpm.

- After 1.5 hr of shaking, measure optical density at 600 nm (absorbance) using a clear 96 well plate and microtiter plate reader of sample vs LB medium => using 250 μ l samples of each. When $OD_{600nm} \approx 0.5$, then proceed to next step.
3. Add isopropyl β -D-thiogalactopyranoside (IPTG - stored at -20°C) to a final concentration of 0.4 mM (24 mg IPTG per 1L flask) to each 250 ml solution in a 1L flask and incubate at 30°C with shaking (180 rpm) for 5 h to induce protein expression.
- Take 750 ml sample of solution before adding IPTG. Label it 'BI.'
 - Add total of 96 mg IPTG to flasks, put back in shaker at 30°C for 5 hours.
 - IPTG stimulates the production of fusion protein. (IPTG activates the promoter in the plasmid that will start the transcription of the gene that follows the promoter => methioninase-annexin V gene.)
4. Harvest the cells by centrifugation for 10 min at $1000 \times g$, at 4°C .
- Take 750 ml sample before centrifuge. Label sample 'BC.'
 - Centrifuge at $1000 \times g = \sim 3000$ rpm (centrifuge uses rpm – consult table on machine). Only 4 – 50 ml centrifuge tubes at a time, temp 4°C , 10 mins.
 - After first centrifuge, pour out supernatant, add more culture to same 4 tubes. Bacteria will be stuck to side of tubes; invert to pour out.
 - Can put the 4 tubes in -20°C freezer for overnight storage if desired.
5. Resuspend the cell pellet in 40 ml of sonication buffer.
- 0.05 mM N- p-tosyl-L-phenylalanine chloromethyl ketone (TPCK) - (stored at -20°C) => 0.704 mg.
 - 1 mM phenylmethylsulfonyl fluoride (PMSF) - (shelf) => 6.968 mg.
 - 1% HPLC ethanol - (flammables) => 400 μ l.
 - Note: Dissolve TPCK and PMSF in ethanol in microcentrifuge tube and then add to beaker.
 - 0.02 mM pyridoxal phosphate – (-20°C) => 400 μ l of 2 mM.
 - 0.01% β -mercaptoethanol – (bench top) => 4 μ l. .
 - 0.02 M sodium phosphate dibasic – (shelf) => 113.6 mg.

- Correct to pH 7.4 – using HCl.
 - Make this buffer in the 100 ml beaker.
 - Add ~10 ml to each of the 4 centrifuge tubes and vortex to resuspend cell pellets.
 - Pour contents of the 4 tubes back into the 100 ml beaker.
6. Lyse the cells by sonication at 4°C for 30 sec at 4.5 watts then allow it to cool for 30 sec on ice. This cycle was repeated for 4 times (= 5 times total) for a total sonication time of 2.5 min on power level 4.
- Clean sonicator tip with ethanol before and after use.
 - Put beaker in tub with an ice while sonicating.
7. Centrifuge the lysate obtained at 12,000 x g for 30 min to remove the cell debris and take the supernatant.
- Pour beaker contents into 1 50 ml centrifuge tube. Make a counterbalance for the centrifuge – volumes may be different because of weight of cells.
 - Centrifuge at 12000xg for 30 min => this equals ~10,000 rpm.
 - Take 750 µl sample after centrifuging. Label sample 'SS.' The proteins will be in the supernatant and the cell debris will be at bottom of tube.

Fusion Protein Recombinant Protein Purification

WASH BUFFER 1 (500 ml)

- 20 mM sodium phosphate dibasic => use 1.42 g
- 40 mM imidazole => use 1.362 g
- 500 mM NaCl => use 14.61 g
- 0.02 mM pyridoxal phosphate => use 2.5 ml of 2 mM
- Correct this to pH 7.4

WASH BUFFER 2 (400 ml)

- 20 mM sodium phosphate dibasic => use 0.8517 g
- 40 mM imidazole => use 0.817 g
- 500 mM NaCl => use 8.766 g

- 0.02 mM pyridoxal phosphate => use 2 ml of 2 mM
- 0.1% Triton X-114 => 3 ml
- Correct this to pH 7.4

ELUTION BUFFER (300 ml)

- 20 mM sodium phosphate dibasic => use 0.8517 g
- 500 mM imidazole => use 10.212 g
- 500 mM NaCl => 8.766 g
- 0.02 mM pyridoxal phosphate => use 2 ml of 2 mM
- Correct this to pH 7

8. After taking supernatant sample, add imidazole (40 mM) and NaCl (500 mM) to the lysate to reduce non-specific protein binding.
 - 40 mM imidazole => use 0.0817 g
 - 500 mM NaCl => use 1.168 g
9. Equilibrate a 5 ml HisTrap chromatography column with immobilized Ni⁺² using Wash Buffer 1 until the output reaches baseline at a flow rate of 1.6 ml/min.
10. Feed the soluble protein fraction into the column. Pool the drop-former fractions that collect while the soluble protein is being applied to the column. Take a 750 µl sample and label is "F1-1".
11. Wash the column with 70 column volumes of Wash Buffer 2 to remove unwanted proteins and endotoxin (350 ml). Pool the drop-former fractions that collect while Wash Buffer 2 is being applied to the column. Take a 750 µl sample and label is "F1-2".
12. Wash the column with 20 column volumes of Wash Buffer 1 to wash away remaining Triton X-114 detergent from the protein. The pen will reach baseline

(100 ml). Pool the drop-former fractions that collect while Wash Buffer 2 is being applied to the column. Take a 750 μ l sample and label is “F1-3”.

13. Elute the protein from the column using Elution Buffer. Begin collecting the fractions when the detector pen increases from baseline. Pool the drop-former fractions that collect while Elution Buffer is being applied to the column. Take a 750 μ l sample and label is “E1”.

14. Dialyze the eluted protein for 3 hours against 2 liters of dialysis buffer containing 20 mM sodium phosphate, 200 mM sodium chloride, and 0.02 mM pyridoxal phosphate at pH 7.4 to remove NaCl and imidazole from the protein solution and make it suitable for N-terminal His-tag cleavage. After dialysis is complete, take a 750 μ l sample and label is “AD1” (After Dialysis 1).

- 20 mM sodium phosphate dibasic => 5.678 g
- 200 mM sodium chloride => 23.376 g
- 0.02 mM pyridoxal phosphate => 20 ml of 2 mM
- Adjust to pH 7.4

15. Regenerate the column using this procedure:

- 25 ml of 1 M KCl => make 200 ml, use 14.91 g
- 25 ml of 1 M NaOH => make 200 ml, use 8.0 g
- 25 ml of DI Water
- 25 ml of 1 M HPLC grade ethanol => 1.5 ml ethanol + 23.5 ml DI Water

16. Measure the concentration of protein (BCA Protein assay or Bradford Protein Assay).

- Add 30 ml DI Water to tube w/ cell pellet. Take 750 μ l sample and label it ‘SP.’
- For each sample => SS, E1, F1, AD1
 - 30 μ l + 30 μ l DI water = 2x dilution
 - 30 μ l from 2x dilution + 30 μ l DI water = 4x dilution

- 30 μ l from 4x dilution + 30 μ l DI water = 8x dilution
- Use triplicates of each dilution for each sample
- From BCA Protein assay, sample AD1 tells us the protein concentration (~2 mg/ml this run). We have ~38 mg protein (19 ml after dialysis * 2 mg/ml = 38 mg).

17. Cleave the N-terminal His-tag by adding HRV 3C protease at 10 U/mg of protein with the recommended 10X buffer provided (stored @ -20°C). Incubate for 16 hr at 4°C with gentle shaking.

- We need to add 2 ml of 10x HRV 3C cleavage buffer to AD1.
- HRV 3C protease comes as 2 U/ μ l and we want to use it at 10 U/mg protein. We have ~38 mg protein
 - ~40 mg * 10 U/mg = 400 U
 - 400 U * 1 μ l/2U = 200 μ l HRV 3C protease. Add this to AD1.
- Take 750 μ l sample after cleavage is complete. Label it 'AC.'

18. Add imidazole (40 mM) and NaCl (500 mM) to the cleaved protein solution.

19. Equilibrate a 5 ml HisTrap chromatography column with immobilized Ni⁺² using Wash Buffer 1 until the output reaches baseline at a flow rate of 1.6 ml/min.

20. Feed the cleaved protein solution onto the HisTrap column.

- Collect first peak solution from the column (F2) for dialysis. This contains our protein.
- Take a 750 μ l sample of flow through #2 and label it 'F2.'

21. Elute uncleaved protein and HRV 3C protease with Elution Buffer.

- Collect elution. Take 750 μ l sample and label it 'E2.'

22. Dialyze purified protein for 3 hours against 2 liters of dialysis buffer containing 20 mM sodium phosphate, 100 mM NaCl and 0.02 mM pyridoxal phosphate

buffer at pH 7.4. After dialysis is complete, take a 750 µl sample and label it “AD2.”

- 20 mM sodium phosphate dibasic => use 5.5678 g
- 100 mM NaCl => use 11.688 g
- 0.02 mM pyridoxal phosphate => 10 mg
- Correct to pH 7.4
- Take 750 µl sample after dialysis.

23. Regenerate the column as above.

24. Pass the pure protein sample thru a 0.2 µm cellulose-acetate filter. Take 750 µl sample and label it ‘SF.’

25. Aliquot purified protein into cryovials and put in the liquid nitrogen tank prior to freeze-drying.

26. Do BCA Protein Assay or Bradford Protein Assay on all samples..

27. Perform L-methioninase enzyme activity assay on samples all samples with dilutions of 1x, 5x, 10x, 15x.

28. Perform an SDS-PAGE on samples BI, SS, F1, E1, AD1, AC, F1, SF, Marker

- Suspend 50 µl of sample + 50 µl loading buffer (95% Laemmli sample buffer + 5% β-mercaptoethanol).
- For BI, centrifuge and resuspend in 100 µl of loading buffer.

BCA Protein Assay Protocol

Reagent Preparation:

- Dilute the Reconstitution Buffer 1:1 with autoclaved DI water => Working Reconstitution Buffer (WRB).
 - Example: 100 µl DI water + 100 µl Reconstitution Buffer.
- Add 100 µl of WRB to Compatibility Reagent tube. Stir and pipet up and down 20 times to mix. NOTE: each well assayed requires 4 µl of Compatibility Reagent.
- Determine amount of BCA Working Reagent required knowing each well needs 260 µl. To prepare BCA Working Reagent, mix BCA Reagent A (clear) with BCA Reagent B (blue) 50:1. After addition, the solution will turn bright green.

- Example: 10 ml Reagent A + 200 μ l Reagent B.

Assay Procedure:

1. In a 96-well plate, add 9 μ l of protein sample to well (run in triplicates).
2. Add 4 μ l of Compatibility Reagent solution to the sample in each well.
3. Tap side of plate to facilitate mixing. Incubate at 37°C for 15 minutes.
4. Add 260 μ l of BCA Working Reagent to each well. Tap side of plate to facilitate mixing. Incubate at 37°C for 30 minutes.
5. Cool the plate at room temperature for 3 minutes.
6. Measure the absorbance at 562 nm versus no protein sample (DI water only).
7. Compare with a standard to calculate the protein concentration.

How to make standard curve using BSA:

[BSA] (mg/ml)	BSA (μ l)	Water (μ l)	[BSA] (μ g/ml)	A _{562 nm}	Std Dev
2	100	0	2000	1.066	0.035
1.5	75	25	1500	0.796	0.052
1	50	50	1000	0.54	0.006
0.75	37.5	62.5	750	0.427	0.014
0.5	25	75	500	0.289	0.013
0.25	12.5	87.5	250	0.151	0.015
0.125	50 of the 0.25 mg/ml solution	50	125	0.089	0.009
0	0	100	0	0	0.004

Bradford Protein Assay

1. In a 96 well micro plate, mix 5 μ l of enzyme sample with 250 μ l of 1x Bio-Rad reagent.
2. Incubate at room temperature for 10 min.
3. Measure the absorbance at 595 nm.

4. Compare with a standard to calculate the protein concentration.

How to make Standard curve:

1. Prepare a solution of BSA at 2 mg/ml.
2. Do a serial dilution of the BSA according to the following table:

[Protein] (mg/ml)	BSA (μ l)	Water (μ l)
2	100	0
1.5	75	25
1	50	50
0.75	37.5	62.5
0.5	25	75
0.25	12.5	87.5
0.125	50 of the 0.25 mg/ml solution	50
0	0	100

Bradford Protein Microassay

1. In a 96 well micro plate, mix 10 μ l of enzyme sample with 200 μ l of 1x Bio-Rad reagent.
2. Incubate at room temperature for 10 min.
3. Measure the absorbance at 595 nm.
4. Compare with a standard to calculate the protein concentration.

SDS-PAGE Analysis of Proteins

Components	Stacking gel 4%	Separating gel 12%	Separating gel 10%	Separating gel 8%
dH ₂ O	1.82 ml(2*910 μ l)	1.67 ml (2*835 μ l)	1.70 ml (2*850 μ l)	1.74 ml (2*870 μ l)
1.5 M Tris-HCL pH 8.8	-	1.25 ml (2*625 μ l)	1.25 ml (2*625 μ l)	1.25 ml (2*625 μ l)
1 M Tris-HCL pH	312.5 μ l	-	-	-

6.8				
10 % (w/v) SDS	25 µl	50 µl	50 µl	50 µl
Acrylamide (29%) Bis (1%)	333 µl	2 ml (2*1000µl)	1.97 ml (2*985µl)	1.93 ml (2*965µl)
Ammonium persulfate 10%	12.5 µl	25 µl	25 µl	25 µl
TEMED	2.5 µl	5 µl	5 µl	5 µl
Total	2.5 ml	5 ml	5 ml	5 ml

THESE VOLUMES ARE FOR 1 GEL

Ammonium Persulfate – make 10 mg for 100 µl

1. Assemble the glass plates on the gel casting stand and fill with water to ensure that they are sealed.
2. Mix the components of separating gel (use an 8% separating gel for Meth-Anx), adding the TEMED last. Mix well and immediately fill the glass plates, leaving a 1.5 cm gap at the top (for the stacking gel).
3. Immediately add 1 ml of isopropanol on top of the gel to prevent oxygen from inhibiting the polymerization. Wait 20 min for solidification.
4. Pour off the isopropanol and rinse with dH₂O to remove any residual isopropanol. Mix the components for the 4% stacking gel and pour on top of the separating gel. Insert the well-comb and wait 20 min for solidification.
5. Preheat a water bath to 100°C.
6. Prepare the SDS-PAGE loading buffer by diluting β-mercaptoethanol 20 X (1:20) with the SDS-blue buffer (prepare stock of loading buffer to add to each sample – Example: for 3 ml total volume, add 2.85 ml of Laemmli buffer to 0.15 ml of β-mercaptoethanol).
7. Mix 75 µl of each protein sample with 25 µl of SDS-PAGE loading buffer.

8. Immediately heat the samples to 100°C for 2 min.
9. Allow the samples to cool down for at least one min before loading the gel.
Assemble the solidified gels in the buffer chamber. Fill the chamber with running buffer (144 g Glycine, 30.3 g Tris base, and 10 g SDS to 1 L of dH₂O -> THIS IS 10X BUFFER!).
10. Load 10 µl of each protein sample into the wells. Run the gel at a constant voltage of 100 V for about 1.5 hours, or until the dye front reaches the bottom of the gel. Cut off the stacking gel and discard it.
11. Stain the separating gel with a staining solution containing 45 % (w/v) dH₂O, 45% (w/v) methanol, 10 % (v/v) acetic acid, and 0.25 % (w/v) Coomassie Brilliant Blue R250. To stain, microwave the box containing the gel and stain solution in 10-15s bursts on high power (be sure there is enough stain to cover the gel). Just before the solution starts to boil, remove from microwave and place on shaker at RT for 5 minutes.
12. To destain the gel, pour the stain back into its container (it can be re-used several times) and rinse the tray with dH₂O. Repeat washing with dH₂O until the discard is clear. To remove the extra stain on the gel, use a destain solution (same as the staining solution, but without the Coomassie Blue). Put the tray on the shaker at RT. Changing the destain may be necessary. Protein bands will be visible immediately on a light table.

NOTES:

- SDS – in reagents – denatures protein to monomeric form
- Ammonium Persulfate 10% (0.01g for 0.1 ml) – polymerization
- TEMED – initiation booster for polymerization
- Acrylamide (29%) Bis (1%) – polymer

2 Buffers – (1.5 M Tris-HCL: 23.65g for 100ml; 1 M Tris-HCL: 15.764g for 100ml)

Destain (4 Liters) - 1.8 L dH₂O, 1.8 L methanol, 0.4 L acetic acid

L-Methioninase Enzyme Activity Assay

L-methioninase will convert L-methionine to α -ketobutyrate and be developed by MBTH.

1. Mix for following and incubate at 37°C for 10 min.
 - 100 μ L of potassium phosphate buffer 0.5 M at pH 8 (to a final concentration of 0.05 M) (for 10ml use 0.87g of potassium phosphate dibasic (MW= 174.18))
 - 125 μ L of L-methionine 0.1 M (for 3ml use 0.04476g)
 - 50 μ L of pyridoxal phosphate 0.2 mM
 - 225 μ L of enzyme sample (for the blank, replace by potassium phosphate buffer)
2. Add 62.5 μ L of 50 % (w/v) trichloro-acetic acid to terminate the reaction (for 15 ml use 7.5g).
3. Centrifuge at maximum speed for 2 min.
4. Mix the following and incubate 50°C for 30 min:
 - 250 μ L of the supernatant from reaction above
 - 500 μ L of sodium acetate buffer 1 M at pH 5 (for 20 ml use 1.6406g (MW=82.03))
 - 200 μ L of MBTH 0.1% (= 1 mg/ml MBTH: 3-Methyl-2-benzo-thiazolinone hydrazone hydrochloride hydrate.) MBTH reacts with the α -ketobutyrate to produce the color change that we measure.
5. Transfer 250 μ l of sample to transparent 96-well plate.
6. Measure the absorbance at 320 nm against the blank using a microtiter plate reader.

Cytosine Deaminase Enzyme Activity Assay

Cytosine deaminase will convert 5-FC to 5-FU; spectrophotometric properties will be monitored at 255 and 290 nm.

1. Prepare stock of 0.5 mg/ml of 5-FC diluted in PBS.
2. Add 775 μ l of PBS to the appropriate number of microcentrifuge tubes where reaction will take place.
3. Add 225 μ l of enzyme sample to the tubes. (The following dilution example can be done for a 4.5x dilution: add 50 μ l enzyme sample + 175 μ l PBS. When doing a dilution, add the PBS prior to enzyme sample).
4. Incubate the reaction at 37°C for 30 minutes.
5. Remove 50 μ l of sample and quench it in 1 ml of 0.1 N HCl.
6. Transfer 250 μ l to a clear 96-well plate.
7. Read absorbance at 255 & 290 nm using a microtiter plate reader.

QCL-1000 Endpoint Chromogenic Limulus Amebocyte Lysate Endotoxin Assay

The principle used to determine endotoxin quantities is the following: Step 1: a proenzyme is converted to an enzyme by the endotoxin. Step 2: the enzyme converts a substrate + water to a peptide and p-nitroaniline. The p-nitroaniline is then measured at 405 nm, and an endotoxin concentration can be calculated from a standard curve made using known amounts of *E. coli* endotoxin.

1. Reconstitute 1 vial containing lyophilized Limulus Amebocyte Lysate using 1.4 ml/vial of lysate. Once reconstituted, it is stable up to 1 week when stored at -20°C immediately following reconstitution. Thaw and use only once. Keep in a dark place.

2. Reconstitute the *E. coli* endotoxin vial using 1.0 ml of LAL Reagent Water warmed to room temperature. Prior to use, vigorously mix for 15 minutes because the endotoxin tends to attach to glass. Our kit contained 28 EU of lyophilized endotoxin. Once reconstituted, it is stable for 4 weeks when stored at 4°C. Keep in a dark place.
3. Reconstitute the chromogenic substrate by adding 6.5 ml of LAL Reagent Water to obtain a final concentration of roughly 2 mM. Once reconstituted, it is stable for 4 weeks when stored at 4°C. Keep in a dark place.
4. Prepare the stop reagent => 10 g Sodium Dodecyl Sulfate (SDS) in 100 ml of DI Water.
5. Prepare the endotoxin sample dilutions that will be used to construct the standard curve. Make dilutions in 15 ml centrifuge tubes.

[Endotoxin] (EU/ml)	Endotoxin Stock Solution	Endotoxin Standard (1 EU/ml)	LAL Reagent Water
1.0	0.1 ml	-	$(28-1)/10 \text{ ml} = 2.7 \text{ ml}$
0.5	-	0.5 ml	0.5 ml
0.25	-	0.5 ml	1.5 ml
0.1	-	0.1 ml	0.9 ml

* NOTE: the bottom 3 standards are made from the 1.0 EU/ml solution made first. Vigorously vortex each dilution for at least 1 minute before proceeding to the next dilution. Also 28 is variable depending on the kit received – check literature with product for proper value to use.

6. Using a clear 96-well plate, add 50 µl of each standard and sample into appropriate wells (running all samples in triplicate). The BLANK wells should receive 50 µl of LAL Reagent Water in place of sample. When adding to wells, use the same pattern of addition throughout the assay to be consistent.

7. Add 50 μl of LAL to each well and then tap on the side of the plate to facilitate mixing.
8. Incubate for 10 minutes at 37°C.
9. Add 100 μl of substrate solution (pre-warmed to 37°C) to each well. Tap the side of the plate to facilitate mixing.
10. Incubate for 6 minutes at 37°C.
11. Add 50 μl of stop reagent (SDS). Tap the side of the plate to facilitate mixing.
12. Read absorbance at 405 nm.

Biotinylation of Fusion Proteins Protocol

It is necessary to use a protein concentration in the range of 0.2-5 mg/ml for labeling.

We will use 5.32 ml (5320 μl) of protein at 0.94 mg/ml (which gives a total of 5 mg of protein).

1. Buffer should be Dialysis #2 buffer or 100 mM sodium phosphate, 150 mM sodium chloride, and 0.02 mM pyridoxal phosphate, pH 7.4 -> use 12,000 – 14,000 MWCO dialysis tubing for 3 hours.
2. Dissolve SureLINK Chromophoric Biotin at 0.5 mg per 25 μL anhydrous DMF immediately prior to use.
3. Using a 20-fold excess of biotin for conjugation, add the appropriate volume of 20 mg/ml (or 25 ng/ μl) SureLINK Chromophoric Biotin to the protein solution.
4. Volume (μL) of 20 mg/mL biotin for conjugation reaction =

$$\frac{5320 \mu\text{l} \times (0.94 \text{ mg protein}) \times (20 \text{ molar excess})}{(316 \text{ kDa}) \times (25 \text{ nmole}/\mu\text{L})} = 12.66 \mu\text{L}$$

$$\% \text{ DMF} = \text{Vol. of biotin stock} \div \text{Vol. of protein to be biotinylated}$$

$$= 12.66 \mu\text{L} \div 5333 \mu\text{L}$$

= 0.24 % DMF

4. Incubate at 4°C for 4 hours with gentle agitation.
5. Remove the unconjugated chromophoric biotin by dialysis using a 12-14k MW membrane in 2L of 1X modification buffer (100 mM sodium phosphate, 150 mM sodium chloride, and 0.02 mM pyridoxal phosphate at pH 7.4) for 3 hours. Change dialysate and run for 3 hours. Change dialysate and run a final dialysis overnight. All dialysis is done at 4°C with gentle stir.

Labeling of Fusion Proteins with FITC

Label the FP in order to visualize FP binding to cells under a fluorescence microscope.

1. Weigh out FITC (stored at -20°C in foil packet to protect it from light with dessicant). Ex: 0.7 mg
2. Dissolve FITC completely in PBS to make approximately a 1 mg/ml solution of FITC (for all steps using FITC, use containers wrapped in foil to protect the FITC from light). Ex: 0.7 ml
3. Remove vial of lyophilized FP from -80°C freezer.
4. Make a solution of 50 mM borate buffer by diluting the 20x borate buffer (on shelf) in nanopure water.
5. Reconstitute the lyophilized FP in 500 µl of 50 mM borate buffer.
6. Add 100 µl of the FITC solution to the FP solution. Briefly spin down the vial to collect FP and FITC at the bottom of the vial.
7. Incubate at room temperature for 1 hr.
8. Make (2) 2-liter dialysis buffers of 20 mM sodium phosphate dibasic.

Ex: 5.678 g / 2 L DI H₂O, pH 7.4

9. Add the labeling solution to a dialysis cassette (slide-a-lyzer 3.5k MWCO, Fisher Scientific) and begin a 3.5 hr dialysis at 4°C (wrap beaker in foil).
10. Transfer the dialysis cassette to new dialysis buffer and allow 3.5 hr dialysis at 4°C (wrap beaker in foil).
11. Remove labeled protein sample from dialysis cassette. Store at 4°C, protected from light.

Labeling of L-Methioninase-Annexin V with DyLight 680

1. To protect reagents from moisture, allow DyLight NHS Esters and DMF to equilibrate to room temperature before opening the vials.
2. Add 100 µL of DMF to the DyLight NHS Ester. Pipette up and down or vortex until it is completely dissolved.

Note: Allow the dye to completely dissolve for 5 minutes and then vortex again.

3. Suspend Meth-Anx in 0.05 M sodium borate buffer, pH 8.5 (or 0.1 M sodium phosphate, 0.15 M NaCl, pH 7.2-7.5) to be in the range of 1-10 mg/ml.
4. Transfer the appropriate amount of reagent (based on calculations) to the reaction tube containing the protein. Mix well and incubate at room temperature for 1 hour.

Calculate the amount (mg) of DyLight NHS Ester Dye to be added to the labeling reaction:

$$\frac{\text{total amount of protein (mg)}}{\text{MW of protein}} \times 10 \text{ molar excess} \times \text{MW of DyLight 680}$$

= ___ mg of DyLight 680

Calculate the microliters of NHS-ester dye solution to add to the reaction:

$$\text{___ mg of DyLight 680 (from previous calculation)} \times \frac{100 \mu\text{l}}{1 \text{ mg}} =$$
$$= \text{___ } \mu\text{l of DyLight 680 NHS-ester solution at 10 mg/ml}$$

5. Remove non-reacted reagent from the protein by dialysis against 2 L of 20 mM sodium phosphate dibasic pH 7.4, using a 12-14k MWCO dialysis membrane for 4 hr at 4°C. 5.678 g for 2 L DI H₂O.

Note: Wrap the beakers being used for dialysis to protect the DyLight 680 from the light.

6. Transfer the dialysis cassette to new dialysis buffer and allow 4 hr dialysis at 4°C.
7. Transfer the dialysis cassette to new dialysis buffer and allow overnight dialysis at 4°C.
8. Remove labeled protein sample from dialysis cassette. Store at 4°C protected from light or lyophilize to powder and store at -80°C.

Binding Assays for Fusion Proteins to Endothelial and Cancer Cells

1. Grow endothelial cells in 6 T-75 flasks using F12K medium containing 10% FBS, ECGS, heparin, and penicillin/streptomycin until they reach 80-85% confluence.
2. Transfer 5×10^4 cells/well to 48 wells on (2) 24-well plates.
3. Expose phosphatidylserine (PS) on surface of endothelial cells by adding 1 mM H₂O₂. Treat the cells in all wells with 100 μl of F12K medium with 1mM H₂O₂ for 1 hour at 37°C and 5% CO₂. Remove after incubation period.

4. Fix the cells in all 48 wells by adding 100 μ l/well PBS buffer containing 0.25% glutaraldehyde. Remove before proceeding.
5. Quench excess aldehyde groups by incubating with 100 μ l/well of 50 mM NH_4Cl , diluted in PBS buffer, for 5 min. Remove after incubation period.

Note: For cancer cells, perform a 1 hr pre-treatment with 0.5% BSA diluted in PBS at 37°C.

6. Dilute biotinylated fusion protein in 0.5% BSA diluted in PBS buffer, with concentrations of 20 nM, 12 nM, 8 nM, 4 nM, 2 nM, 0.5 nM, and 0.05 nM. Add 300 μ l to wells in Sets 1 and 2, using triplicates of each concentration. The blank for each set will receive no FP.
 - a. Set 2 (21 wells) gets PBS + BSA + 2 mM Ca^{+2} + FP
 - b. Blank (3 wells) gets PBS + BSA + 2 mM Ca^{+2}
 - c. Set 1 (21 wells) gets PBS + BSA + 5 mM EDTA + FP
 - d. Blank (3 wells) gets PBS + BSA + 5 mM EDTA
7. Incubate for 2 hours at 37°C, 5% CO_2 .
8. Wash 4 times with 300 μ l of 0.5% BSA diluted in PBS buffer.
9. Add 300 μ l of Streptavidin-HRP (2 μ g/ml) and incubate for 1 hour at room temperature. (Streptavidin-HRP is in 4°C glass fridge)
10. Wash 4 times with 300 μ l of PBS buffer.
11. Add 300 μ l of the chromogenic substrate O-phenylenediamine (OPD) to each well. (OPD is in -20°C freezer). The OPD solution is made with phosphate citrate buffer (1 capsule in 100 ml DI water). Prior to use, add 40 μ l of 30% H_2O_2 . Weigh out the desired amount of OPD with a concentration of 0.4 mg/ml.
12. Incubate for 30 minutes at room temperature and in the dark to minimize OPD color change.
13. Transfer 100 μ l of the supernatant to 96-well plates.

14. Measure absorbance at 450 nm.

Visualization of L-Methioninase-Annexin V for Endothelial and Cancer Cells

1. Grow 1 flask of HAAE-1 cells in F12K medium + FBS + ECGS + heparin + pen/strep.
2. Place autoclaved 22x22 (mm) cover glass in a 35 mm petri dish.
3. Coat the cover glass with 0.1% porcine gelatin.
4. Add 250 μ l of cell suspension to the cover glass. (Use 2 petri dishes – 1 for full visualization; 1 for negative control -> leave out FP)
5. Let the cells adhere for 4 hr at 37°C, 5% CO₂.
6. Add 2 ml of F12K medium to the petri dish. Incubate overnight at 37°C, 5% CO₂.
7. Add FP (that has been labeled with FITC) diluted to 100 nM in F12K medium + 2 mM Ca²⁺. Incubate for 2 hr at 37°C, 5% CO₂. *For the control plate, add only medium + 2 mM Ca²⁺ (no FP).*
8. Wash the petri dishes 4 times using medium + 2 mM Ca²⁺ to remove any unbound CD-Anx.
9. Remove the cover glass from the petri dish, touch the side of it to a piece of paper towel to remove excess liquid, and apply a drop of Fluor-gel drop (Fisher Scientific #NC9703847) to a glass microscope slide. Place the cover glass with cells upside down on top of the Fluor-gel.
10. Visualize the cells using fluorescence microscopy.

Binding Stability Assay for Fusion Proteins to Endothelial and Cancer Cells

In this assay we will be using, at the beginning, “growth medium” (F-12K + 10% FBS + pen/strep + ECGS + heparin) and, later on, “FP suitable medium” which is

composed of the “growth medium” with 2 mM Ca^{2+} , 0.02 mM pyridoxal phosphate, and 1000 μM methionine (because annexin V binding is Ca^{2+} dependant, pyridoxal phosphate is a cofactor for the methioninase, and higher methionine to eliminate methionine depletion effect).

1. Seed 5×10^4 cells in 6 wells on each of 4 plates and grow them until they reach 70% confluence using growth medium (24 wells total). Let the cells grow overnight.
2. Add 300 μl of growth medium containing 1 mM H_2O_2 to expose phosphatidylserine.
3. Wash 3 times (using 250 μl of FP suitable medium each time).
4. Add 300 μl of FP suitable medium containing 100 nM FP that has previously been biotinylated.
5. Incubate for 2 h at 37 °C.
6. Wash 3 times (using 250 μl of FP suitable medium each time).
7. Add 1 ml of FP suitable medium.
8. Each day (0, 1, 2, & 3), take one plate (6 wells). Remove the medium and replace with 300 μl of FP suitable medium. Perform an Alamar Blue assay to determine cell viability.
 - a. Add 10% (30 μl) of Alamar Blue
 - b. Incubate for 4 hours at 37°C.
 - c. Transfer 250 μl to an opaque 96-well plate
 - d. Measure fluorescence: excitation – 530 nm; emission – 590 nm.
9. Wash 2 times using FP suitable medium (using 250 μl each time).

10. Fix the cells by adding 100 μ l/well of FP suitable medium containing 0.25% glutaraldehyde. Incubate for 5 min at room temperature. Remove after incubation period.
11. Quench excess aldehyde groups by incubating with 100 μ l/well of FP suitable medium containing 50 mM ammonium chloride (NH_4Cl) for 5 minutes at room temperature. Remove after incubation period.
12. Wash 3 times using FP suitable medium (using 250 μ l each time).
13. Add 300 μ l of Streptavidin-HRP.
14. Incubate for 1 hour at room temperature.
15. Wash 3 times using FP suitable medium (using 250 μ l each time).
16. Add 300 μ l of the chromogenic substrate O-phenylenediamine (OPD) to each well. The OPD solution is made with phosphate citrate buffer (1 capsule in 100 ml DI water). Prior to use, add 40 μ l of 30% H_2O_2 . Weigh out the desired amount of OPD with a concentration of 0.4 mg/ml.
17. Incubate for 30 minutes at room temperature and in the dark to minimize OPD color change.
18. Transfer 100 μ l of the supernatant to 96-well plates.
19. Measure absorbance at 450 nm.

Methioninase-Annexin V Cytotoxicity Assay for Endothelial and Cancer Cells

This assay we will be using “growth medium” (F12K medium + 10% FBS + pen/strep + heparin + ECGS) and later on “FP suitable medium” which is composed of the “growth medium” with 2 mM Ca^{2+} (because annexin V binding is Ca^{2+}

dependent), 0.02 mM pyridoxal 5'-phosphate (co-factor), and L-methionine adjusted to 1000 μ M (to mask the methionine depletion effect).

1. Seed cells in 42 wells on (7) 24-well in growth medium. Plate #1 will receive Meth-Anx in only 3 wells, and the rest will have no Meth-Anx with varying prodrug concentrations (24 wells). Plates #2-7 will receive Meth-Anx and the prodrug (18 wells). Begin the experiment the day after plating cells.
2. Add 300 μ l of growth medium containing 1 mM H_2O_2 to expose phosphatidylserine. Note: For cancer cells, skip this step.
3. Wash 2 times using 250 μ l of growth medium.
4. Add 300 μ l of FP suitable media containing 500 μ M L-methionine and 100 nM Methioninase-Annexin V FP to appropriate wells (21 wells). Add 300 μ l of FP suitable media only to those wells with no Meth-Anx (21 wells).
5. Incubate for 2 hr at 37°C, 5% CO_2 .
6. Wash 4 times using 250 μ l of FP suitable medium.
7. Add 300 μ l of FP suitable medium containing varying concentrations of the prodrug Selenomethionine to all plates => 5000 μ M, 1000 μ M, 500 μ M, 100 μ M, 50 μ M, 10 μ M. For the BLANK (0 μ M), only add FP suitable medium to the cells.
8. Incubate at 37°C, 5% CO_2 .
9. On Day 1, remove medium and replace with 300 μ l of FP suitable medium.
Perform the Alamar Blue assay to determine cell viability.
 - e. Add 10% (30 μ l) of Alamar Blue.
 - f. Incubate for 4 hours at 37°C, 5% CO_2 .
 - g. Transfer 250 μ l to an opaque 96-well plate
 - h. Read fluorescence: excitation – 530 nm; emission – 590 nm.

10. Wash using 250 μ l FP suitable medium.
11. Add 300 μ l of FP suitable medium containing varying concentrations of the prodrug Selenomethionine to all plates => 5000 μ M, 1000 μ M, 500 μ M, 100 μ M, 50 μ M, 10 μ M. For the BLANK (0 μ M), only add FP suitable medium to the cells.
12. Incubate at 37°C, 5% CO₂.
13. Repeat steps 9-12 for Day 2 and Day 3.

Cytosine Deaminase-Annexin V Cytotoxicity Assay for Endothelial and Cancer Cells

In this assay we will be using, at the beginning, “growth medium” (F12K medium + 10% FBS + 1% Pen/Strep + Heparin + ECGS) and, later on, “FP suitable medium” which is composed of the “growth medium” with 2mM Ca²⁺ (because annexin V binding is Ca²⁺ dependant).

1. Seed cells in 63 wells on (3) 24-well. Begin the experiment (Day 0) the day after plating.
2. Add 300 μ l of FP suitable media containing 1 mM H₂O₂ to all wells. For cancer cells, skip this step.
3. Incubate for 1 hr at 37°C, 5% CO₂.
4. Wash using 250 μ l of FP suitable medium.
5. Add 300 μ l of FP suitable media containing 100 nM yCD-Annexin V (FP) to plate #1 (21 wells). Plates #2 and #3 will receive FP suitable medium only.
6. Incubate for 2 hr at 37°C, 5% CO₂.
7. Wash 4 times using 250 μ l of FP suitable medium.
8. For plates #1 and #2, add 1000 μ l/well of FP suitable medium containing varying concentrations of the prodrug 5-fluorocytosine (5-FC) => 2000 μ M,

1000 μM , 750 μM , 500 μM , 250 μM , 125 μM . For the BLANK (0 μM), only add FP suitable medium to the cells. For plate #3, add 1000 μl /well of FP suitable medium containing 5-fluorouracil (5-FU) at the same concentrations as the 5-FC. Leave 3 wells on each plate for the Alamar Blue blank (medium + 10% Alamar Blue reagent).

9. Incubate for 72 hr at 37°C, 5% CO₂. Replace FP suitable medium containing the correct prodrug/drug concentration each day to produce new 5-FC.
10. On Day 3, remove plates from incubator; remove the medium and replace with 300 μl of FP suitable medium containing the correct 5-FC concentration. Perform an Alamar Blue assay to determine cell viability.
 - a. Add 10% (30 μl) of Alamar Blue.
 - b. Incubate for 4 hours at 37°C, 5% CO₂.
 - c. Transfer 250 μl to an opaque 96-well plate
 - d. Read fluorescence: excitation – 530 nm; emission – 590 nm.
11. Wash using 250 μl FP suitable medium.
12. Repeat steps 2 - 9.
13. On Day 6, remove plates from incubator; remove the medium and replace with 300 μl of FP suitable medium containing the correct 5-FC or 5-FU concentration. Perform an Alamar Blue assay to determine cell viability, as above.
14. Wash using 250 μl FP suitable medium.
15. Repeat steps 2 – 9.
16. On Day 9, remove plates from incubator; remove the medium and replace with 300 μl of FP suitable medium containing the correct 5-FC or 5-FU concentration. Perform an Alamar Blue assay to determine cell viability.

- a. Add 10% (30µl) of Alamar Blue.
- b. Incubate for 4 hours at 37°C, 5% CO₂.
- c. Transfer 250 µl to an opaque 96-well plate
- d. Read fluorescence: excitation – 530 nm; emission – 590 nm.

ELISA for L-Methioninase-Annexin V Detection in Mouse Serum

Biotinylated methioninase–annexin V fusion protein clearance time determination.

1. Use streptavidin-coated 96 well plates from Thermo Fisher Scientific.
2. Add 50 µl of each serum sample to wells (2 dosage levels – 10 mg/kg and 1 mg/kg; 4 time points per dosage level – 1 hr, 4 hr, 8 hr, and 24 hr post-injection; 4 samples with no injection as the blank).
3. Cover the plate with adhesive cover and incubate for 60 min at 37°C.
4. Shake out the plates into a sink. Wash the plates with *Wash buffer* 4 times by adding 200 µl and shaking out the *Wash buffer* into a sink. Pat plates dry by inverting on paper towel.
5. Add 50 µl of Annexin V polyclonal antibody (rabbit) diluted to 1.25 µg/ml (recommended by Abcam) in *Diluting Buffer* to each well.
6. Cover the plate with adhesive cover and incubate for 60 min at 37°C.
7. Shake out the plates into a sink. Wash the plates with *Wash buffer* 4 times by adding 200 µl and shaking out the *Wash buffer* into a sink. Pat plates dry by inverting on paper towel.
8. Add 50 µl of anti-rabbit IgG-HRP conjugate (secondary antibody) diluted to 1:1,000 (initially at about 1 mg/ml) using *Diluting Buffer* to each well.
9. Cover the plate with adhesive cover and incubate for 60 min at 37°C.

10. Shake out the plates into a sink. Wash the plates with *Wash buffer* 4 times by adding 200 μ l and shaking out the *Wash buffer* into a sink. Pat plates dry by inverting on paper towel.
11. Add 50 μ l of OPD solution to each well.
12. Cover the plate with adhesive cover and incubate for 30 minutes at room temperature in the dark.
13. Read absorbance at 450 nm.

Reagent List:

1. Diluting Buffer
 - 0.5 g Tween 20
 - 2.5 g BSA (0.25%)
 - Add PBS to 1 L.

NOTE: Do not add sodium azide with HRP-IgG method.

2. Wash Buffer
 - 5 g Tween 20 (0.05%)
 - Add PBS to 1 L.
3. OPD Solution
 - 1 phosphate-citrate capsule in 100 ml of DI H₂O
 - Weigh out OPD powder at 0.4 mg/ml and put in centrifuge tube wrapped in aluminum foil
 - Immediately before use, add 40 μ l of 30% H₂O₂ to initiate the reaction
 - Add necessary amount of buffer solution to tube and use ASAP

Injection of MDA-MB-231/GFP Cancer Cells into Flank of Mice

1. Grow MDA-MB-231/GFP cells to inject 3 T-75 cm² culture flasks of cells per mouse. Split the cells from 1 => 3 flasks about every 3 days.
2. Lift and plate the cells in three 150 cm² culture dishes.

3. On the day prior to lifting and injecting the cells, replace the medium with penicillin/streptomycin-free medium. Use this medium until the injections. (Advised by colleague at HSC).
4. On the day prior to injections, place a vial of BD Matrigel Basement Membrane Matrix in a beaker with water and place at 4°C overnight to thaw.
5. On the day of injections, lift the cells as usual using 6 ml of PBS and Trypsin-EDTA followed by 12 ml of medium.
6. Transfer 3 plates to each 50 ml centrifuge tube.
7. Centrifuge all tubes to combine them into one 50 ml centrifuge tube and remove supernatant.
8. Add 0.1 ml * # of mice to inject = _____ ml of medium to the total cell pellet and resuspend.
9. Assemble 2 sterilized 1.5 ml microcentrifuge tubes for each mouse to be injected in an ice/ice water bath to cool cells for transport to animal facility.
10. Add 100 µl of BD Matrigel Basement Membrane Matrix to one 1.5 ml microcentrifuge tube for each mouse.
11. Mix cell suspension and add 100 µl to the other 1.5 ml microcentrifuge tube for each mouse.
12. Bring samples and 100 µl pipet with tips to animal facility.
13. Sedate the mice using ketamine/xylazine or isoflurane. If the mice have hair, shave the flank area that will receive the injection.

14. Combine the BD Matrigel Matrix with the cell suspension and mix. Draw the suspension into a 1 ml Tuberculin Syringe with detachable 25G 5/8" slip tip needle.
15. Insert needle beneath the skin of the flank and inject the cell-matrix suspension.
16. Allow the needle to stay in place for 1-2 minutes to help the matrix solidify to keep the cells in place.
17. Remove needle and place mouse back in cage and observe as directed in IACUC regulations.

Detection of PS Exposed in Mice Tumors using Cryosectioning and Immunohistochemistry Staining

To detect PS that was translocated to the outer leaflet of the plasma membrane of tumor vascular endothelial cells and tumor cells using biotinylated Meth-Anx.

1. Using an orthotopic model, inject 6 female SCID mice with $\sim 7-8 \times 10^6$ cancer cells, using a 1:1 mixture of growth medium to matrigel and a total injection volume of 200 μ l.
2. Allow the tumors sufficient time to grow to a diameter above 3 mm, in which the tumors will require the development of tumor vasculature to supply nutrients for continued growth, using the equation: $\text{Volume} = (\text{width})^2 \times \text{length}/2$
[Measurement of dimensions is done using a digital caliper (mm).]
3. Inject 220 μ l of biotinylated Meth-Anx (which corresponds to 100 μ g of annexin V) i.p.
4. Under isoflurane anesthetic, open the chest cavity to expose the heart.

5. Insert a 27G butterfly needle into the left ventricle and hook up a pump to deliver 10 ml of heparinized saline + 2 mM Ca^{+2} . The heparin is used to prevent coagulation of any remaining blood in circulation.
6. Cut the ascending vena cava to allow the circulation to be emptied.
7. Pump the heparinized saline + 2 mM Ca^{+2} solution at ~1.3 ml/min.
8. Fix the tissue by pumping 0.25% glutaraldehyde + 2 mM Ca^{+2} .
9. Immediately resect the tumor area and soak the tissue in 20% sucrose + 2 mM Ca^{+2} .
10. Bring the mouse samples to the Imaging Core at OMRF in Oklahoma City to have cryoembedding and cryosectioning done. Request 1 slide to be stained with H&E and 2 unstained slides.
11. Store slides at -80°C until staining can be done.
12. Prior to staining, remove slides from the freezer and allow them to reach RT.
13. Rinse the slides with PBS + 2 mM Ca^{2+} .
14. Block the slides with PBS containing 0.5% BSA and 2 mM Ca^{2+} for 30 min at RT.
15. Rinse the slides with PBS + 2 mM Ca^{2+} .
16. Incubate the slides with streptavidin-HRP for 30 min at RT.
17. Rinse the slides with PBS + 2 mM Ca^{2+} and shake off excess.
18. Incubate the slides with the activated DAB solution for 10 min at RT.
19. Rinse the slides with reagent water for 3 min to remove excess DAB.
20. Counterstain the slides with hematoxylin for 4 min at RT.
21. Rinse the slides with the following to remove excess hematoxylin:

- a. Tap water
- b. DI water
- c. Ammonia water (50 ml DI water + 0.1 ml ammonia hydroxide) – 10 slow dips
- d. DI water

22. Air dry and mount the slides with of ImmuniHistoMount (Santa Cruz Biotechnology # sc-45086). Do not apply a coverslip.

Tissue Biodistribution of L-Methioninase-Annexin V in SCID Mice with Tumor

To determine the quantity of Meth-Anx that binds to vasculature in individual organs.

1. Using an orthotopic model, inject 6 female SCID mice with as close to $7-8 \times 10^6$ cancer cells as possible, using a 1:1 mixture of growth medium to matrigel and a total injection volume of 200 μ l.
2. Allow the tumors sufficient time to grow to a diameter above 3 mm, in which the tumors will require the development of tumor vasculature to supply nutrients for continued growth, using the equation: $\text{Volume} = (\text{width})^2 \times \text{length}/2$
[Measurement of dimensions is done using a digital caliper (mm).]
3. When the appropriate sized tumors are present, perform an i.p. injection of 3 mice with 10 mg/kg dose of Meth-Anx tagged with DyLight 680 fluorescent dye.
4. Using the IVIS imaging system, take whole-animal images to capture the tumor (GFP) and Meth-Anx (DyLight 680) at 1, 12, and 24 h post-injection to determine location of Meth-Anx in relation to the tumor.
5. Sacrifice the 3 mice, remove a blood sample to obtain serum, and resect out the major organs (tumor, lung, liver, heart, spleen, kidneys, stomach).

6. Image the organs of each mouse all together to see the intensity of the DyLight 680 signal. Present the data as photons per second/g of tissue.

Treatment of Breast Tumors on SCID Mice with L-Methioninase-Annexin V

This protocol is for the mouse on a normal diet. For the methionine-deficient experiment, start the mice on the diet the day before the first FP injection and use a Selenomethionine at 5 mg/kg.

1. Inject 7 female SCID mice per group with $\sim 7-8 \times 10^6$ cancer cells using a 1:1 mixture of growth medium to matrigel and a total injection volume of 200 μ l.
2. Allow the tumors sufficient time to grow to a diameter above 3 mm³, in which the tumors will require the development of tumor vasculature to supply nutrients for continued growth, using the equation [Volume = (width)² x length/2]. Measurement of tumor dimensions is done every 3-4 days using a digital caliper (mm).
3. When the tumors begin to grow by average tumor volume, random mice were selected to be viewed with the IVIS imaging system. A GFP signal in the flank region provides evidence that the MDA-MB-231/GFP tumor cells are alive.
4. Randomize the mice into 4 groups.
5. Begin the treatment period (Day 0) by performing intraperitoneal injections of all mice as shown (~5:00 pm injections):
 - a. Control Group 1 – saline
 - b. FP Group 2 – L-methioninase-annexin V at 10 mg/kg
 - c. SeMet Group 3 – saline
 - d. Treatment Group 4 – L-methioninase-annexin V at 10 mg/kg
6. On days 1-3, performing intraperitoneal injections of all mice as shown (~7:00 am injections):

- a. Control Group 1 – saline
 - b. FP Group 2 – saline
 - c. SeMet Group 3 – Selenomethionine at 10 mg/kg
 - d. Treatment Group 4 – Selenomethionine at 10 mg/kg
7. Repeat steps 4 and 5 for 2 additional treatment cycles
 8. Measure the tumor dimensions and body weight of each mouse every 3-4 days.
 9. Observe the tumor growth for up to 4 weeks or until tumor size mandates termination.
 10. When tumor weight reaches ~10% of body weight, sacrifice the mouse by CO₂ overdose and cervical dislocation.
 11. Dissect out the lungs, liver, and tumor and image them in a 6-well plate using the IVIS imaging system in the Rodent Barrier to detect any GFP signal that would represent tumor metastases.
 12. Place all mouse parts in formaldehyde to fix the tissue for 2-3 days at room temperature.
 13. Deliver samples to Dr. Stanley Kosanke, OU HSC Pathology, to have paraffin blocks made. Precision Histology, Inc will section and mount on slides and perform hematoxylin & eosin staining. Dr. Kosanke will view slides and provide a pathology report for each mouse requested.

Determination of Blood Flow through MDA-MB-231/GFP Tumors

The purpose of this test is to demonstrate that there is less blood flow going through tumors that have been treated with methioninase-annexin V fusion protein and selenomethionine compared to untreated tumors. The methioninase-annexin V + SeMet treatment is hypothesized to damage microvessels, causing clotting and reducing the amount of blood flow through the tumor.

1. Using an orthotopic model, inject 6 female SCID mice with as close to 6×10^6 cancer cells as possible, using a 1:1 mixture of growth medium to matrigel and a total injection volume of 200 μ l.
2. Allow the tumors sufficient time to grow to a volume above 3 mm³, in which the tumors will require the development of tumor vasculature to supply nutrients for continued growth, using the equation: $\text{Volume} = (\text{width})^2 \times \text{length}/2$
[Measurement of dimensions is done using a digital caliper (mm).]
3. When the appropriate sized tumors are present, treat 3 mice with Meth-Anx at 10 mg/kg and 10 mg/kg SeMet. Use 3 mice as an untreated control. (3 cycles of treatment = 12 days)
4. Inject the DyLight 680 fluorescent dye at 1 mg/kg via i.p. injection.
5. Allow the dye to circulate for 30-60 min.
6. Using the IVIS imaging system, capture images of the blood flow in the region of the tumor. Use 3D reconstruction of the mouse if necessary to determine dye intensity in treated vs untreated mice.
7. After all of the images are taken, open the chest cavity to expose the heart under isoflurane anesthetic
8. Insert a 27G butterfly needle into the left ventricle and hook up a pump to deliver 10 ml of heparinized saline + 2 mM Ca⁺². The heparin is used to prevent coagulation of any remaining blood in circulation.
9. Cut the ascending vena cava to allow the circulation to be emptied.
10. Pump the heparinized saline + 2 mM Ca⁺² solution at ~1.3 ml/min.
11. Fix the tissue by pumping 10 ml of 10% formalin.

12. Immediately resect the tumor area and soak the tissue in formaldehyde.
13. Bring the mouse samples to Dr. Stan Kosanke (OUHSC – Pathology) to have paraffin embedding done and send samples for sectioning to Precision Histology.

Carbon Nanotube Standard Curve

1. Sonicate 6 mg of SWNTs in 5 ml of 1% SDS for 1 hr.
2. Immediately, without centrifuging, make dilutions using deionized water and transfer 250 μ l to a 96-well plate.
3. Measure the absorbance at 800 nm using a microtiter plate reader to make a curve of SWNT concentration versus absorbance.

Conjugation of F3 Peptide to SWNTs

1. Add 6 mg of SWNTs to 5 ml of 1% SDS solution (500 mg for 50 ml).
2. Sonicate the SWNT suspension for 1 hr at 22% power (7 watts) – put glass vial into beaker with cold water to dissipate heat.
3. Centrifuge the SWNT suspension for 30 minutes at 15,700 x g (13,000 rpm microcentrifuge)
4. Measure the concentration of SWNT in suspension.
5. Set out DSPE-PEG-Maleimide linker and to warm up to room temperature (15-20 min). Store linker in nitrogen atmosphere.
 - When putting linker vial away, put in nitrogen glass w/ cap slightly off, turn on nitrogen for 1 min, and quickly close cap, turn off nitrogen.
6. Dissolve DSPE-PEG-Maleimide linker at 2 mg/ml in warm DI water.
 - NOTE: If linker does not dissolve easily, incubate at 37°C or warm water bath for 15 minutes and then pipet up and down to dissolve.

7. Reconstitute 1 mg of F3 peptide in 2 ml of PBS (pH 7.4). (The F3 is in 1 mg aliquots)
8. Mix 1 ml of the linker solution with the 2 ml peptide solution to create a suspension with a 1:2 ratio of peptide to linker. (Use an extra 1 ml PBS to wash out all of the F3 solution from the vials – total of 3 ml for peptide + 1 ml of linker solution)
9. Stir gently for 15 hr at room temperature. (Use large shaker at 50 rpm)
10. Treat F3-linker reaction mixture with 40 μ l of L-cysteine dissolved in DI water at 5 mg/ml for 1 hr with gentle shaking, to block unreacted maleimide groups.
11. Add the 4 ml F3-linker solution to the 5 ml of the SWNT suspension.
12. Mix at room temperature and 50 rpm shaking for 30 min.
13. Dialyze for 8 hr. Change the buffer after 4 hr.
 - 2L of DI Water with a 50k MW dialysis membrane
 - Note 1: Be very specific on the time of this dialysis because the nanotubes will aggregate if left longer than the 8 hours.
 - Note 2: You can take the sample out of the dialysis membrane and put it into a foiled 15-ml centrifuge tube and into the 4^o fridge overnight and then continue in the morning, but a better suspension results from immediate centrifugation.
14. Centrifuge for 1 hr at 15,700 x g to remove any SWNT aggregates.
15. Determine the final SWNT concentration.
16. Determine the final concentration of F3 using the Bradford Protein Microassay.

Visualization of SWNT-F3 by Fluorescence and Confocal Microscopy

1. Plate cells in chambered slides or in 35 mm petri dishes on 22 mm cover glasses to achieve ~80% confluence.
2. Incubate for 24 hr at 37°C, 5% CO₂.

3. Incubate the cells with SWNT-F3 at 60 mg/L (SWNT) for 2, 8, 16 or 24 hr at 37°C, 5% CO₂.
4. Wash the cells with medium 4 times.
5. Stain the cells with CellMask plasma membrane stain for 30 min at 37°C @ 7.5 µg/ml in warm medium.
6. Wash the cells with medium 4 times.
7. Fix the cells with 10% buffered formalin for 10 min at 37°C.
8. Wash the cells with medium 4 times.
9. Mount on a slide with 1 drop of Fluoro-Gel to preserve fluorescence.
10. View under fluorescence or confocal microscopy.

NIR Laser Setup and Configuration

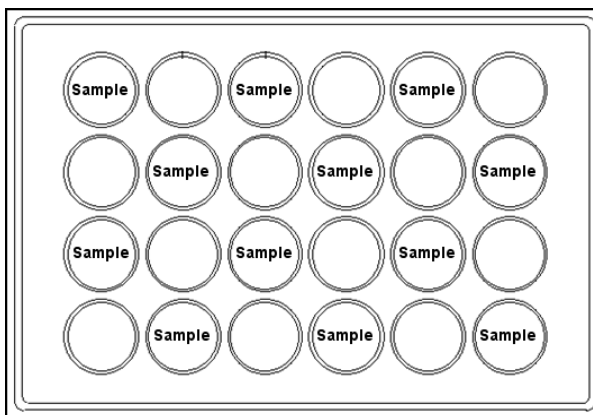
It is important to wear protective eyewear during all laser experiments while the laser is on. Protective glasses can be found in D201. You must also put laser test warning signs on the door to the lab before beginning this experiment.

1. Turn on laser and fix laser beam size to cover one well on a 24 well plate (1.8 cm diameter) as follows:
 - Turn the key to the “On” position. (O = off, I = on)
 - Place black laser test paper with black side down above laser (it may be necessary to place an empty 24 well plate on top of the paper to hold it in place).
 - Press “Standby” on the screen and hold down the foot pedal to emit the laser for 30 seconds.
 - Lift foot off of pedal and press the “Standby” button again to stop the laser.
 - Hold the black laser test paper up behind an empty 24 well plate to determine if the laser beam diameter is large enough to cover an entire well.

- If the beam is not the right size, move the laser fiber either up or down to decrease/enlarge the beam diameter and repeat the above steps until an acceptable beam diameter is obtained.
2. Adjust the power level as follows:
 - Turn on NOVA II laser measurement device and place black box above laser.
 - Adjust the power on the laser using the up and down arrows on the screen.
 - Press “Standby” and hold down the foot pedal to emit the laser.
 - Read the equivalent power on the NOVA II device (this is the power actually felt).
 - Adjust the power level on the screen until the desired power is read by the NOVA II device.
 - Once the NOVA II device shows that the desired power level has been reached, remove the black box and turn off the NOVA II device; this is the power setting to be used.
 3. Irradiate each of the wells designated to receive laser treatment with a beam diameter of 1.6 cm and a local power of 5.86 W for 120 seconds to achieve an energy density of 350 J/cm².

SWNT-F3 + NIR Laser Test Protocol

1. Seed 5x10⁴ cells in each of 30 wells on a total of 3 plates and grow them until they reach 70% confluence using appropriate growth medium. Wells intended to receive NIR treatment should be placed on the plate as pictured below.



2. Incubate the cells with SWNT-F3 at 60 mg/L in medium for 2, 8, 16, and 24 hr at 37°C, 5% CO₂. Laser only samples receive medium only.
3. Wash 4 times using 250 µl of medium.
4. Add 300 µl of appropriate cell medium.
5. Setup the laser for irradiation using the appropriate power level to achieve the desired total energy density for each cell line.

NOTE: It is important to wear protective eyewear during all laser experiments while the laser is on. Protective glasses can be found in D201. You must also put laser test warning signs on the door to the lab before beginning this experiment.

4. Irradiate each of the wells designated to receive laser treatment
5. Once irradiated, incubate the plates at 37°C, 5% CO₂ for 1 hr.
6. Evaluate cell viability using the Alamar Blue Assay:
 - Add 10% (30µl) of Alamar Blue.
 - Incubate for 4 hr at 37°C, 5% CO₂.
 - Transfer 250 µl to an opaque 96-well plate
 - Read fluorescence: excitation – 530 nm; emission – 590 nm
7. Replace medium and incubate the plates at 37°C, 5% CO₂ for 14 hr.
8. Evaluate cell viability using the Alamar Blue Assay.